

Winter 2007

Chitosan paste from crawfish shells as a synthetic bone graft material: Preparation, characterization and animal study

Jerome G. Saltarrelli Jr.
Louisiana Tech University

Follow this and additional works at: <https://digitalcommons.latech.edu/dissertations>



Part of the [Biomedical Engineering and Bioengineering Commons](#)

Recommended Citation

Saltarrelli, Jerome G. Jr., "" (2007). *Dissertation*. 550.
<https://digitalcommons.latech.edu/dissertations/550>

This Dissertation is brought to you for free and open access by the Graduate School at Louisiana Tech Digital Commons. It has been accepted for inclusion in Doctoral Dissertations by an authorized administrator of Louisiana Tech Digital Commons. For more information, please contact digitalcommons@latech.edu.

**CHITOSAN PASTE FROM CRAWFISH SHELLS AS A SYNTHETIC
BONE GRAFT MATERIAL – PREPARATION,
CHARACTERIZATION AND
ANIMAL STUDY**

by

Jerome G. Saltarrelli Jr., B.S.

**A Dissertation Presented in Partial Fulfillment
of the Requirements for the Degree
Doctor of Philosophy**

**COLLEGE OF ENGINEERING AND SCIENCE
LOUISIANA TECH UNIVERSITY**

March 2007

UMI Number: 3264697

INFORMATION TO USERS

The quality of this reproduction is dependent upon the quality of the copy submitted. Broken or indistinct print, colored or poor quality illustrations and photographs, print bleed-through, substandard margins, and improper alignment can adversely affect reproduction.

In the unlikely event that the author did not send a complete manuscript and there are missing pages, these will be noted. Also, if unauthorized copyright material had to be removed, a note will indicate the deletion.

UMI[®]

UMI Microform 3264697

Copyright 2007 by ProQuest Information and Learning Company.

All rights reserved. This microform edition is protected against unauthorized copying under Title 17, United States Code.

ProQuest Information and Learning Company
300 North Zeeb Road
P.O. Box 1346
Ann Arbor, MI 48106-1346

LOUISIANA TECH UNIVERSITY

THE GRADUATE SCHOOL

March 3, 2007

Date

We hereby recommend that the dissertation prepared under our supervision by Jerome G. Saltarrelli Jr., B.S.

entitled CHITOSAN PASTE FROM CRAWFISH SHELLS AS A SYNTHETIC BONE
GRAFT MATERIAL - PREPARATION, CHARACTERIZATION AND ANIMAL
STUDY

be accepted in partial fulfillment of the requirements for the Degree of Doctor of Philosophy

Deh P. Murkhego
Supervisor of Dissertation Research
Steve J.
Head of Department
Biomedical Engineering
Department

Recommendation concurred in:

Steve J.
Daniel Mills
P. DeLuca
P. Schroyer

Advisory Committee

Approved: Paul Paruchandran
Director of Graduate Studies

Approved: Timothy M. McLooney
Dean of the Graduate School

Stan Noyen
Dean of the College

ABSTRACT

Bone loss associated with musculoskeletal trauma or metabolic diseases often requires bone grafts. Autograft or allograft bones are limited in supply. Therefore, development of synthetic bone graft materials is an active area of research. For several years the biomaterials group at LSUHSC-Shreveport has been investigating the use of chitosan purified from crawfish shells using a process patented by my research advisor, Dr. Debi Mukherjee.

Chitin is a polysaccharide that exists in fungi, exoskeleton of insects and outer shell of crustaceans. It is biocompatible, osteoconductive, antimicrobial, biodegradable, non-toxic, haemostatic, fungicidal, and the second most abundant natural polysaccharide on earth. Removal of the acetyl group from chitin forms chitosan. Chitosan is more useful due to the presence of amino groups that impart a positive charge to the molecule. This positive charge interacts with cells or can act as a binding site for other functional groups thereby expanding the role of chitosan molecules.

The objectives of this study are:

1. Test for the presence of bone in grafted and ungrafted defects and compare the results among the different groups.
2. Test and compare the differences in stiffnesses and fracture loads among the different groups.

3. Test, via microcomputed tomography, defect reduction in samples treated with the graft.
4. Test for the amorphous nature of crawfish chitosan.
5. Compare the purity of crawfish chitosan extracted using Dr. Debi Mukherjee's procedure with commercially available chitosan.

The first portion of this experiment was characterization of crawfish chitosan, extracted using a method patented by Dr. Debi Mukherjee, to determine the individual chemical "fingerprint" of crawfish chitosan. Tests established that crawfish chitosan contains identical functional groups as chitosan monomer and chitosan glutamate and possessing an amorphous structure.

In the second portion of this study, purified chitosan was mixed with cultured osteoblasts and compounded with a calcium salt creating a bone graft paste. Eighteen male Lewis rats underwent the surgical procedure. A critical size defect was created in rat femurs following a published protocol and repaired through use of a metal plate with and without crawfish chitosan bone graft paste. Histological examination and bone graft analysis of defected areas demonstrated the presence of bone in defect areas that were filled with experimental paste material and reduced or no bone growth on control femurs.

Chitosan possesses the necessary properties, when combined with plaster of Paris and osteoblasts, to create a bone graft that is osteoconductive, osteoinductive and osteogenic.

APPROVAL FOR SCHOLARLY DISSEMINATION

The author grants to the Prescott Memorial Library of Louisiana Tech University the right to reproduce, by appropriate methods, upon request, any or all portions of this Dissertation. It is understood that "proper request" consists of the agreement, on the part of the requesting party, that said reproduction is for his personal use and that subsequent reproduction will not occur without written approval of the author of this Dissertation. Further, any portions of the Dissertation used in books, papers, and other works must be appropriately referenced to this Dissertation.

Finally, the author of this Dissertation reserves the right to publish freely, in the literature, at any time, any or all portions of this Dissertation.

Author Jerome G. Satt

Date 03/03/2007

DEDICATION

In memory of my father, Jerome G. Saltarrelli.

TABLE OF CONTENTS

ABSTRACT	iii
DEDICATION	vi
LIST OF TABLES.....	xiii
LIST OF FIGURES	xiv
ACKNOWLEDGMENTS	xviii
CHAPTER 1 - Introduction.....	1
Bone Grafts	1
Autograft	1
Allograft.....	2
Demineralized Bone Matrix	4
Bone Morphogenic Protein	4
Xenograft	5
Synthetic Bone Graft.....	6
Hydroxyapatite	7
Calcium Phosphate Cement	8
Calcium Sulfate Salt (Plaster of Paris).....	8
Chitosan	9
Extraction from Crawfish Shells (<i>Procambarus clarkii</i>).....	11

Chitosan Characterization	12
Fourier Transform Infrared Spectroscopy	13
¹ H Nuclear Magnetic Resonance Spectroscopy	13
Differential Scanning Calorimetry	13
Chitosan Properties	15
Biocompatibility	15
Antibacterial Properties	15
Haemostatic and Anticoagulant Properties	16
Wound Healing	17
Drug Delivery	19
Anti-Tumor and Anti-Viral Characteristics	19
Nerve Cell Regeneration	20
Dietary and Hypocholesterolemic Properties	20
Tissue Engineering	21
Cartilage Tissue Engineering	21
Bone Tissue Engineering	22
Scaffolds for Tissue Engineering	24
Commercial Products	25
Bone Biology	26
Ossification	27
Intramembranous Ossification	27
Endochondral Ossification	29
Bone Resorption	31

Bone Repair.....	32
Graft Incorporation	34
Discussion of the Literature.....	35
Hypothesis.....	37
CHAPTER 2 – Materials and Methods	40
Crawfish Chitosan Characterization.....	40
Fourier Transform Infrared Spectroscopy	40
¹H Nuclear Magnetic Resonance Spectroscopy	40
Differential Scanning Calorimetry	40
Surgical Materials and Methods.....	41
Surgical Materials	41
Osteoblast Cell Culture.....	41
Crawfish Chitosan Extraction	41
Crawfish Chitosan Bone Graft Preparation	42
Critical Size Defect Model	43
Surgical Procedure.....	43
Sacrifice.....	45
Harvest	45
Histological Sectioning	45
Undecalcified Sectioning	45
Undecalcified Materials.....	45

Undecalcified Histological Embedding.....	46
Undecalcified Histological Staining Materials	49
Decalcified Histology Materials.....	50
1X Phosphate Buffered Saline.....	51
Decalcified Histological Procedure	52
Histological Analysis.....	53
Post Harvest Analysis	53
Microcomputed Tomography.....	53
Mechanical Testing.....	54
CHAPTER 3 - Results.....	55
Chitosan Characterization.....	55
Fourier Transform Infrared Spectroscopy	55
¹ H Nuclear Magnetic Resonance Spectroscopy	57
Differential Scanning Calorimetry	59
Gross Anatomy.....	61
Six Month	61
Nine Month	62
Undecalcified Histological Sectioning	63
Six Month.....	63
Nine Month	65
Histological Data	69
Decalcified Histological Sectioning	70

Post Harvest Analysis	79
Microcomputed Tomography	79
Six month	79
Nine month.....	83
Mechanical Testing.....	88
Six month	88
Nine month.....	90
CHAPTER 4 - Discussion	92
Characterization	92
Fourier Transform Infrared Spectroscopy	92
Nuclear Magnetic Resonance	93
Differential Scanning Calorimetry	94
Experimental Design	95
Gross Anatomy.....	96
Undecalcified Histological Sectioning	99
Six Month.....	100
Nine Month	100
Decalcified Histological Sectioning	101
Post Harvest Analysis	102
Four-Point Bending.....	102
Microcomputed Tomography.....	103
Conclusion.....	103

Future Work.....	105
APPENDIX A – Nuclear Magnetic Resonance Spectroscopy Protocol	109
APPENDIX B – Cell Culture Protocol	111
APPENDIX C – Graft Components.....	114
APPENDIX D – Sacrifice Time Table	116
APPENDIX E – Additional Animal Samples	118
APPENDIX F – Animal Care and Use IRB Form from LSU-Shreveport	120
REFERENCES	123

LIST OF TABLES

Table 1. Chitosan extraction from crawfish.	42
Table 2. Sacrifice schedule (number of animals).	45
Table 3. Undecalcified histological embedding procedure.	47
Table 4. Undecalcified histological staining procedure.	50
Table 5. Decalcified histological embedding procedure.	52
Table 6. Common FTIR peak locations.	57
Table 7. Stiffness, bending moment and displacement.	91
Table 8. Experimental design for a future study.	107

LIST OF FIGURES

Figure 1. Chitin molecule	10
Figure 2. Chitosan molecule.....	10
Figure 3. Structure of cortical and cancellous bone [58].	27
Figure 4. Intramembranous ossification [54].	29
Figure 5. Endochondral ossification [54].	31
Figure 6. Scanning electron micrograph, osteoclast (Univ. of Oulu).....	32
Figure 7. Rat in surgical frame.....	44
Figure 8. Exakt cutter.....	48
Figure 9. Exakt grinder.....	49
Figure 10. Miles Tissue Tek II.....	53
Figure 11. Mechanical testing apparatus.....	54
Figure 12. Crawfish chitosan and chitosan glutamate – FTIR.	55
Figure 13. Crawfish chitosan and chitosan monomer – FTIR.	56
Figure 14. Comparison of NMR spectra.	58
Figure 15. Crawfish chitosan – DSC.....	60
Figure 16. Industrial chitosan – DSC.....	60
Figure 17. Six mo. Rat 6 left operated control – gross.	61
Figure 18. Six mo. Rat 13 left experimental – gross.	62
Figure 19. Six mo. Rat 14 left experimental – gross.	62

Figure 20. Nine mo. Rat 19 left operated control – gross.....	63
Figure 21. Nine mo. Rat 18 left experimental – gross.	63
Figure 22. Six mo. operated control (Goldner's, undecal., 5L-WW).....	64
Figure 23. Six mo. experimental (Goldner's, undecal., 13L-SS).	64
Figure 24. Six mo. unoperated control (Goldner's, undecal., 25L-MM).	65
Figure 25. Nine mo. operated control (Goldner's, undecal., 7R-69).	66
Figure 26. Nine mo. operated control (Goldner's, undecal., 7R-69).	66
Figure 27. Nine mo. operated control (Goldner's, undecal., 7R-76).	67
Figure 28. Nine mo. operated control (Goldner's, undecal., 7R-81).	67
Figure 29. Nine mo. experimental (Goldner's, undecal., 17L-62).	68
Figure 30. Nine mo. experimental (Goldner's, undecal., 17L-64).	68
Figure 31. Nine mo. unoperated control (Goldner's, undecal., 27R-59).	69
Figure 32. Histological data - percent bone growth.	70
Figure 33. Three mo. operated control (H&E, decal., 8L-1).	71
Figure 34. Three mo. experimental (H&E, decal., 11L-1).....	72
Figure 35. Three mo. unoperated control (H&E, decal., 3L-1).	72
Figure 36. Three mo. operated control (Safranin O, decal., 1L-2).	73
Figure 37. Three mo. experimental (Safranin O, decal., 10R-3).	73
Figure 38. Three mo. unoperated control (Safranin O, decal., 3L-2).	74
Figure 39. Six mo. operated control (H&E, decal., 6L-1).....	74
Figure 40. Six mo. experimental (H&E, decal., 14L-2).....	75
Figure 41. Six mo. operated control (Safranin O, decal., 4R-2).	75
Figure 42. Six mo. experimental (Safranin O, decal., 14L-1).	76

Figure 43. Nine mo. operated control (H&E, decal., 20L-1).	76
Figure 44. Nine mo. experimental (H&E, decal., 18L-2).....	77
Figure 45. Nine mo. unoperated control (H&E, decal., 20R-2).....	77
Figure 46. Nine mo. operated control (Safranin O, decal., 20L-3).	78
Figure 47. Nine mo. experimental (Safranin O, decal., 18L-3).....	78
Figure 48. Nine mo. unoperated control (Safranin O, decal., 29L-2).	79
Figure 49. Six mo. Rat 6 operated control (single slice) - μ CT.	80
Figure 50. Six mo. Rat 6 operated control (single slice) - μ CT.	81
Figure 51. Six mo. Rat 14 experimental (single slice) - μ CT.....	81
Figure 52. Six mo. Rat 14 experimental (single slice) - μ CT.....	82
Figure 53. Six mo. Rat 14 experimental (3-D) - μ CT.....	82
Figure 54. Six mo. Rat 24 unoperated control (single slice) - μ CT.	83
Figure 55. Nine mo. Rat 19 operated control (single slice) - μ CT.	84
Figure 56. Nine mo. Rat 19 operated control (3-D) - μ CT.....	84
Figure 57. Nine mo. Rat 19 operated control (3-D) - μ CT.....	85
Figure 58. Nine mo. Rat 18 experimental (single slice) - μ CT.	85
Figure 59. Nine mo. Rat 18 experimental (3-D) - μ CT.	86
Figure 60. Nine mo. Rat 18 experimental (3-D) - μ CT.	86
Figure 61. Nine mo. Rat 28 unoperated control (3-D) - μ CT.....	87
Figure 62. Nine mo. Rat 28 unoperated control (single slice) - μ CT.....	87
Figure 63. Six mo. Rat 04 right operated control - 4-point bending.	88
Figure 64. Six mo. Rat 14 left experimental - 4-point bending.	89
Figure 65. Six mo. Rat 15 left experimental - 4-point bending.	89

Figure 66. Nine mo. Rat 16 left experimental - 4-point bending.....	90
Figure 67. Mechanical data - bending moments at failure.	91
Figure 68. Deformed femur, six month operated control group (5L).....	97
Figure 69. Lewis rat skeleton.....	98
Figure 70. Rat housing.....	99

ACKNOWLEDGMENTS

I would like to thank everyone who assisted with this project. My committee: Dr. Steven Jones, Dr. Debi Mukherjee, Dr. David Mills, Dr. Sidney Sit and Dr. Mark DeCoster, for their support and guidance, Errin Robinson and Al Ogden for assisting with animal surgeries and mechanical testing, Tracee Terry for μ CT testing, Dr. Ernie Blakeney for DSC and NMR testing, Dr. Mike McShane for FTIR testing, everyone in the animal care facility at LSUHSC-Shreveport, Sheila Rodgers for direction with the histological sectioning and chitosan extraction, and Dollie Smith for osteoblast cell culturing.

My wife, Michelle, provided invaluable support, inspiration, love, patience and understanding. Without her this project would not have been possible. I would like to thank my parents and in-laws for continued support and motivation. Last, but not least, I would like to thank my employer, Dr. Howard Gebel and Anthony Roggero for their patience, understanding and support.

CHAPTER 1

INTRODUCTION

Bone loss associated with musculoskeletal trauma or metabolic diseases often require bone grafting. Ideal bone grafts possess osteoinductive, osteogenic, and osteoconductive characteristics. Osteoinductivity is the ability to cause undifferentiated mesenchymal cells to differentiate into chondrocytes and osteoblasts leading to bone formation [9,15,16,53,55,63,87,103]. Osteogenicity is the ability to form new bone with only components contained in the graft, living cells that are capable of differentiation into bone [9,53,55,87,103]. Osteoconductivity is the ability to support vascular and bone ingrowth from the recipient bed into the graft site [9,15,53,55,87,103]. There are four types of bone grafts: autograft, allograft, synthetic graft and xenograft.

Bone Grafts

Autograft

Autografts have long been considered the gold standard and the only type of bone graft that is osteoconductive, osteogenic and osteoinductive [94]. Autografts contain all the proteins, growth hormones and structural integrity of innate bone and are traditionally harvested from the iliac crest, ribs, proximal tibia and distal femur, although harvesting from the iliac crest is preferred

[86,87,94,123]. Cancellous grafts are revascularized faster than cortical grafts and are repaired completely [15]. Cancellous bone grafts are repaired by creeping substitution which initially involves appositional bone growth, cortical bone grafts are repaired through a reverse creeping substitution [15,55]. Cortical bone is primarily used in load bearing situations. Burchardt reported cortical grafts remain as necrotic and viable bone, whereas cancellous bone grafts are completely incorporated [15]. Bauer and Muschler reported optimum skeletal incorporation with vascularized cancellous autografts [9]. Non-vascularized cortical autografts demonstrated superior strength and provided an osteoconductive substrate for bone formation [9]. Autografts possess no risk of viral transmission. While autografts have many positive attributes, a few serious side effects can occur. Autograft harvesting causes additional pain through a secondary surgical site [32,94], in addition to increased costs. Pain can be minor, post-operatively, or chronic, lasting several months (15% of patients report pain lasting more than three months [103]). Level of pain is associated with amount of bone dissected for grafting [103]. Risk of infection is increased due to a second surgical site [32,94]. Since bone for the graft is harvested from the patient, autografts elicit no immunological response, but are in limited supply.

Allograft

An allograft is a bone graft composed of bone harvested from a cadaveric donor. Allografts are osteoinductive and osteoconductive, they contain some proteins necessary for bone formation, but most osteoinductive components are destroyed during sterilization. Allografts have a higher absorption rate and lower

percentage of revascularization compared to autografts [32], probably due to protein conformational changes which occur during sterilization. Allografts contain no viable cells therefore osteogenic potential is non-existent [32]. The lack of viable cells is caused by methods used to sterilize, in an effort to prevent viral transmission. Even though donated bone is treated to prevent viral transmission, viral transmission is still a possibility [86]. The risk of contracting HIV from allografts has been reported as <1 per 1,000,000, only two allografts have been linked to transmission of the AIDS virus out of 3,000,000 recorded transplants [53,55,86,103,147]. These treatments, freezing and irradiation, alter not only incorporation of the graft, they alter structural characteristics [55,86,87], probably by changing protein confirmation. Differences are seen between osteoinductivity, osteoconductivity and method of sterilization [9,32]. Since bone is harvested from a donor, allogenic bone grafts elicit a larger immune response [9,32,53]; they cause less pain due to presence of only a primary surgical site and decrease risk of infection. Burchardt describes three types bone repair with allografts [15]. Type I bone repair is normal repair along a clinically acceptable course without any fatigue failures. Type II bone repair occurs when significant genetic differences exist between the donor and recipient, chronic repair. The exact mechanisms of genetic acceptance or rejection is unknown, but Bauer and Muschler report no clear link between the extent of graft incorporation and degree of human leukocyte antigen (HLA) matching [9]. HLA is a group of genes that encode for cell surface antigen presenting proteins that are responsible for

immunological transplant related reactions. Type III bone repair is quickly and completely resorbed with no sign of initial defect.

Demineralized Bone Matrix

Demineralized bone matrix is processed allograft bone [8,32], cortical bone is the preferred source as it possesses a lower potential for immunological reaction and is more osteoinductive than cancellous bone [16]. Demineralized bone matrix is composed of allograft bone that has been treated with acid to remove mineral components [123] but leave behind necessary growth factors and other proteins that facilitate bone growth [32,54,85,89,125,147]. Since demineralized bone matrix is a derivative of natural bone, it is biocompatible and allows for complete healing of critical defects [28]. Demineralized bone matrix is osteoconductive [9] and due to acid extraction, has little risk of viral transmission [147]. Due to the presence of collagen, growth factors and proteins (bone morphogenic proteins), demineralized bone matrix is osteoinductive [25,32]. While demineralized bone matrix offers osteoconductivity and osteoinductivity, demineralized bone matrix offers no structural support [54,125,147], therefore any use of demineralized bone matrix must be augmented with other fixation.

Bone Morphogenic Protein

Bone morphogenic proteins (BMP) are low molecular weight non-collagenous proteins naturally present that induce bone formation. During mechanostimulation, bone stress causes a release of alkaline phosphatase, which raises pH of surrounding tissue [99]. Increase in pH causes recruitment of macrophages and fibroblasts which secrete growth factors and cytokines. A

portion of released growth factors are bone morphogenic proteins. BMP2, BMP4 and BMP7 activate Cbfa1 (core bonding factor alpha 1) gene which encodes Cbfa1 transcription factor. Cbfa1 directly regulates the amount of matrix deposited [5,54]. Due to BMP's important role in ossification, recombinant human BMPs (rhBMP) have been developed [53,58,123,143]. RhBMPs possess the ability to speed healing by inducing endochondral ossification [53], and since BMPs are naturally derived, they initiate no immunological reactions [147]. Nanograms of naturally occurring BMP initiate healing, where micrograms of rhBMP are necessary to perform identical tasks [58,143]. Research has yet to be completed on the long term effects of increased levels of rhBMPs on other tissues. Burg, Porter and Kellum reported the effectiveness of rhBMP2 and rhBMP7 in inducting bone formation [16].

Xenograft

A xenograft is a graft containing components from other species. These grafts fail due to severe immunogenic responses. However, derivatives from tissues of other species have shown promising results. Several groups have reported processed bovine collagen from skin and bone demonstrates biocompatibility [9,123]. Components from skin or bone from other species is preferred over using whole tissue, as whole bovine tissue can transmit disease causing prions. Prions, proteins that function as viruses, cause diseases such as Bovine Spongiform Encephalopathy (BSE) or Mad Cow Disease [154], Creutzfeldt-Jakob disease in humans.

Synthetic Bone Graft

A synthetic bone graft is primarily formulated from materials that do not contain organic components of bone. Synthetic bone grafts avoid many problems caused by use of natural bone in bone grafts. Viral transmission, additional surgical site and immunological reaction are all factors that can be avoided or reduced through use of a synthetic bone graft. Viral transmission is not a concern since natural components can be sterilized or otherwise treated to remove viral contaminants present. Individual components of a synthetic bone graft can be treated to remove any harmful contaminants prior to addition to the graft, without affecting other more sensitive components. The second harvesting site is not needed; this reduces secondary site morbidity and decreases surgical costs. Components used in synthetic bone grafts are tested for biocompatibility prior to addition to the graft; this reduces or eliminates any immunological reactions. Most synthetic bone grafts are soluble in acidic pH, Bauer and Muschler report that due to solubility of synthetic bone grafts in acidic pH, macrophages will digest graft particles without initiation of an inflammatory response [9]. In addition to osteoconductivity, osteoinductivity and osteogenicity, porosity and interconnectivity are important in bone grafting. Natural bone has a pore diameter of 200-900 microns [94,137], synthetic bone graft pore size of 100 to several hundred microns is necessary for bone ingrowth [10,161]. Porosity is important for angiogenesis and calcification. Blood vessel formation dictates the ossification process. Small pores limit angiogenesis, therefore limiting oxygen transport, leading to local hypoxic conditions which favor endochondral

ossification [137]. Larger pore sizes, 100 μ m and up, prevent hindrance of angiogenesis, thereby allowing oxygen transport and promoting intramembranous ossification [137]. Porosity also affects bone ingrowth. As the degree of porosity increases, the speed and amount of ingrowth increases [58,123,154]. Beppu and Santana report increased porosity, as well as higher contact area which offer improved anchorage conditions for mineralization deposits [10]. Hing et al. reported porosity as a major contributor to osseointegration. Increased levels of microporosity promoted ingrowth of dense new bone earlier than bone grafts with less microporosity [59]. Microporosity was found to alter the dynamics and pattern of osseointegration [59].

Hydroxyapatite. Hydroxyapatite, $\text{Ca}_{10}(\text{PO}_4)_6(\text{OH})_2$ with a Ca:P ratio of 5:3 (1.66), is hydrated calcium phosphate cement most often mistaken for the inorganic phase of bone [58]. Hydroxyapatite has a similar, but not identical, crystallographic structure to natural bone mineral [58]. Due to structural similarities, hydroxyapatite has been used as a synthetic bone graft [13,26,28,32,58,68,76]. Hydroxyapatite is biocompatible [32], osteoconductive [32], non-toxic [32], elicits no immune response [32], and provides structural support under compression [53]. Hydroxyapatite is not osteoinductive [32], it contains no proteins, and possesses negligible pores [32], which indirectly inhibits angiogenesis. When used as a bone graft, hydroxyapatite particles migrated and settled [32,68,76], which led to a lack in significant resorption [26,32]. Gazdag et al. reported that due to lack of resorption and particle migration, large segments will remain at the repair site for up to ten years [53].

Calcium Phosphate Cement. Calcium phosphate cement is a bone substitute material that crystallizes resulting in resorbable microporous hydroxyapatite [28,103]. Calcium phosphate cement bonds to bone [28], provides structural support under compression [28,103], is biodegradable [28], and will restore bone contour [28]. Several different varieties of calcium phosphate salts are available ranging from tricalcium phosphate (TCP) to bioglass. Each is biodegradable, osteoconductive and chemically able to bond to bone. They are either non-porous (bioglass) [103] or microporous (TCP) [123] (which indirectly inhibits angiogenesis) and non-osteoinductive [103,123].

Calcium Sulfate Salt (Plaster of Paris). Plaster of Paris, $\text{CaSO}_4 \cdot \frac{1}{2}\text{H}_2\text{O}$, was first used in 1892 by Dreesman to treat osteomyelitis [32,126,137]. The function of plaster of Paris was to occupy the infrabony environment, acting as a scaffolding device and preventing epithelial invagination until resorption takes place [3,32], it can be used in the presence of infection with no ill effects [123,126]. Plaster of Paris is biologically inert [32,125,126], has a resorption rate similar to the growth rate of new bone [26] and is completely resorbed [26,125,126], however high turnover and high resorption rate has also been reported [8,28]. This difference in results can be attributed to the form of plaster of Paris tested, defect size, defect location (loaded or unloaded) and quality of plaster of Paris used. Damien and Parsons reported the use of plaster of Paris as a good drug delivery system especially for antibiotics [32]. Indirectly, plaster of Paris promotes bone formation. Osteoblasts adhere to plaster of Paris and osteoclasts absorb the calcium sulfate, absorption is associated with a large

number of osteoclasts [125]. The adhering of osteoblasts and absorbing of osteoclasts, facilitates bone formation [13,26]. Plaster of Paris does not stimulate osteogenesis [32,136] nor does it inhibit bone formation [126]. Strocchi et al. reported improved angiogenesis. Calcium sulfate increased the growth of microvessels in the defect site compared to unfilled defects [151]. Plaster of Paris usage can lead to a slight elevation in serum calcium and alkaline phosphate levels [32], which can be overcome with extra water consumption. Rush, Laurencin and Khan reported calcium sulfate as brittle and unable to resist compressive loads [86,137]. To overcome this, defects filled with plaster of Paris must have internal or external fixation.

Chitosan. Chitin is a naturally occurring linear polysaccharide found in fungi, yeast, invertebrates, shellfish and crustaceans [90,111,114,135,146]. Chitin, composed predominately of poly [β -(1 \rightarrow 4)-2-acetamido-2-deoxy-D-glucopyranose] [40,56,97,135], is the second most abundant natural polysaccharide, following cellulose and annual production is estimated to be 10^{10} - 10^{11} tons [45]. Chitosan, composed of β (1 \rightarrow 4) linked 2-acetamido-2-deoxy- β -D-glucose (N-acetylglucosamine), is a derivative of chitin, first discovered by Rouget in 1859 [90,135], formed by removal of an acetyl group. Deacetylation is accomplished by either enzymatic or alkaline hydrolysis. Chitin with a degree of deacetylation of 75% or higher is considered chitosan [83,143]. Deacetylation creates chemically active amine groups which give chitosan a positive charge. This positive charge allows chitosan to possess functional properties [20,24,40,56,90,97,128,129,146]. Functional characteristics range

from biocompatibility to hypercholesterolemia to anti-tumor properties. The positive charge is due to protonation, addition of a H^+ which occurs below pH 5 [49], of a NH_2^+ group located at the C2 position on the chitin molecule [40], therefore charge density is pH dependent [49]. The degree of functional properties is dependent on level of deacetylation (charge percentage) [158]. Chitin contains two hydroxyl groups while chitosan contains one amino group and two hydroxyl groups in a repeating hexoamine residue [84]. The structures of chitin and chitosan are shown in Figures 1 and 2.

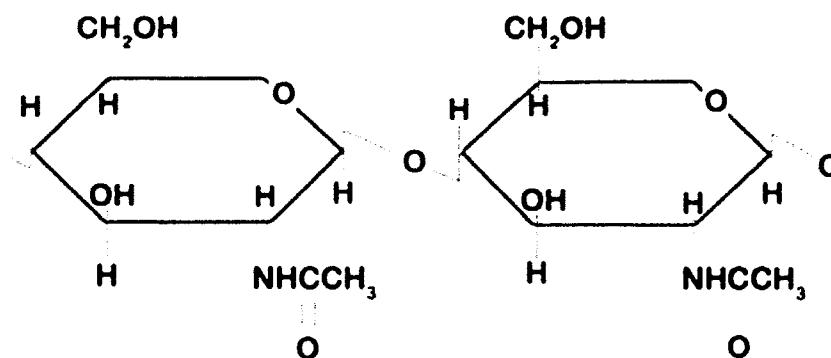


Figure 1. Chitin molecule.

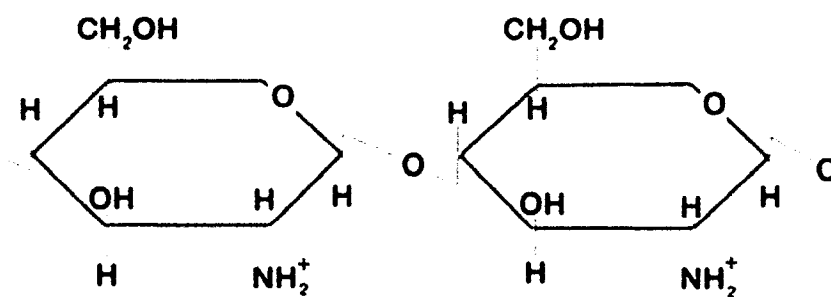


Figure 2. Chitosan molecule.

In addition to chemically active amine groups, chitosan is more readily soluble in dilute acids. Chitin is insoluble in water, dilute aqueous salt solutions and most organic solvents [111]. Chitosan's increased solubility, along with reactivity, causes chitosan to have more functionality in biomedical applications.

Chitin is found in three forms: α -chitin, β -chitin, and γ -chitin. α -chitin consists of anti-parallel chains ($\uparrow\downarrow\uparrow$) [85,135,152] and is found primarily in arthropods and crustaceans [152]. β -chitin is comprised of parallel chains ($\uparrow\uparrow\uparrow$) [85,135,152] and is found in marine diatoms and squid pens [152]. γ -chitin consists of two parallel chains and one anti-parallel chain ($\uparrow\uparrow\downarrow$) [135,152] and has been reported in the past, but its existence is controversial [152]. Chitin is present in highest concentrations in the shell of crustaceans. Crustacean shells consist mainly of 30–40% protein, 30–50% minerals (mostly in the form of calcium carbonate), and 20–30% α -chitin [46]. Chitosan is an excellent source of nitrogen, containing approximately 6.89% [84], in the form of primary aliphatic amino groups [84]. According to No and Meyers, crawfish chitin contains 7.01% nitrogen on a moisture-free, ash-free basis [111]. Chitin is a major source of surface pollution [41,42,48,56,85] therefore recycling is environmentally beneficial.

Extraction from Crawfish Shells (*Procambarus clarkii*)

Chitosan is the deacetylated derivative of chitin. General extraction process for chitin is removal of proteins and minerals from crawfish shells. Deproteinization, removal of proteins, is accomplished by treating ground crawfish shells in a dilute sodium hydroxide solution, 3.5% w/v, at an elevated

temperature, 65-100°C. All proteins are removed in a two hour time period [29,46,56,111,113,114]. Demineralization, removal of minerals, is accomplished by submerging deproteinated shells in a dilute solution of 1N hydrochloric acid, at room temperature for 2-3 hours with agitation [46,111,113,114]. Following deproteinization and demineralization, the extracted product is chitin. Chitin is converted into chitosan by removal of acetyl groups; this is accomplished by submerging chitin in a concentrated sodium hydroxide or potassium hydroxide solution, 50% w/v, at elevated temperature, ~100°C. Degree of deacetylation increased rapidly during the first hour and slowed afterward [46,159]. Treatment beyond two hours does not deacetylate significantly and has been found to cause polymer degradation [100,111,114,144,152]. It should be noted that a small amount of deacetylation occurs during chitin extraction [111]. Rinaudo, Milas and Desbrieres reported a convenient way to achieve a high level of deacetylation as 5% w/v of sodium hydroxide at 100°C for three hours [134]. The volume of chitosan extracted varies according to order of steps, Fernandez-Kim reported high yield with demineralization, deproteinization and deacetylation [46].

Chitosan Characterization

Functional properties of chitosan are due to polycationic nature, charge density, which is directly proportional to degree of deacetylation (i.e. the higher degree of deacetylation, the more free amine groups and higher the charge density) and degradation. Chitosan is degraded by enzymatic hydrolysis resulting in oligosaccharides of variable lengths [18,20,35,40,49,83,106,152,162]. Highly deacetylated forms of chitosan exhibit the lowest degradation rates [49].

Since level of deacetylation is important in defining chitosan's functional properties, it is essential to have the ability to measure the level of deacetylation. Several different methods have been employed.

Fourier Transform Infrared Spectroscopy

Fourier transform infrared spectroscopy (FTIR) passes a known wavelength of infrared light through a sample and records the amount of energy absorbed by the molecule. FTIR has been used to determine level of deacetylation [38,92] of chitosan, weakening of spectra occurring at 1665 cm^{-1} (amide I) is associated with deacetylation [21,34,127].

^1H Nuclear Magnetic Resonance Spectroscopy

^1H nuclear magnetic resonance spectroscopy (NMR) aligns protons with intrinsic magnetic moments with a very powerful external magnetic field and perturbs the alignment using an electromagnetic field. The perturbations are measured and recorded. All nuclei with odd numbers of protons and some with even number of protons have intrinsic magnetic moments, ^1H and ^{13}C are most widely used. ^1H NMR has been used to determine the degree of deacetylation of chitosan [47,57,60,67,88,132] as part of chemical characterization [134]. Although, Domard and Rinaudo reported that ^1H NMR may not be sensitive for low acetyl concentration [34].

Differential Scanning Calorimetry

In differential scanning calorimetry (DSC), differences in amount of heat required to increase the temperature of a sample and a reference are measured as a function of temperature. During melting, more heat is flowing to the sample,

this is an endothermic reaction. During crystallization, less heat is required to raise the temperature (less heat is flowing to the sample), this is an exothermic reaction. DSC measures the amount of energy absorbed or released. DSC has been used to characterize chitosan [79,81]. Different values have been reported for the location of endothermic peaks. Agnihotri and Aminabhavi reported pure chitosan having an endothermic peak at 53°C [2], while Dong et al. reported a single endothermic peak occurring at 100°C [36]. A range of endothermic peak locations, ~35°C-160°C, reported by Cervera et al. and Ratto and Hatakeyama [19,131], was attributed to water loss. In addition to water loss, different reported temperatures can be attributed to different chitosan extraction techniques, different chitosan sources, level of deacetylation and purity. Chitosan is amorphous, it lacks crystalline form, when only one peak between 35°C - 160°C is present [19]. Exothermic peaks were seen between 280°C and 300°C [19]. Cardenas and Miranda reported that as the level of deacetylation increases, the decomposition temperature decreases [17]. The samples with high degrees of deacetylation will have decomposition temperature approaching 313°C, based on 92% deacetylated chitosan. Dong et al. reported chitosan having a glass transition (T_g) temperature between 140°C-150°C [36]. Glass transition temperature is the temperature at which molecules have little or no mobility, below the T_g the material is in "glassy" state and above T_g the material is in "rubbery" state. In "glassy" state the material is brittle and hard, and in "rubbery" state the material is soft and flexible.

Chitosan Properties

Biocompatibility

Chitosan has demonstrated biocompatibility in multiple studies. *In vivo*, chitosan has elicited no pathological inflammatory responses [120], no abnormalities were seen in radiographs where chitosan was incorporated as a bone graft component [76] and chitosan elicited no signs of necrosis or degeneration [76] when used as part of a bone graft. Chitosan demonstrated a very low incidence of chitosan-specific reactions [120]. Rao and Hatakeyama reported the non-toxic nature of chitosan, acute systemic toxicity tests with chitosan in mice did not demonstrate any toxic effects [130]. Chitosan has been used to reduce toxicity of positively charged liposomes [45].

Antibacterial Properties

Chitosan possesses antibacterial and antimycotic properties. Interactions between positive charge of the chitosan molecule and negative charge of a bacterial cell wall lead to altered cell permeability. This altered permeability prevents transport of essential nutrients into the cell and results in leakage of proteinaceous and other intracellular components [22,24,145,146]. Chitosan inhibits bacterial proliferation independent of the bacterial charge, both gram-negative and gram-positive bacteria are inhibited [112,115,129] although the antibacterial effect was greater with gram negative bacteria [22,33]. Antibacterial efficacy is dictated by degree of deacetylation, pH and temperature. As degree of deacetylation increases, antibacterial effect increases [22,33,44,144]. The same correlation is observed with temperature. As temperature increases, the antibacterial efficiency increases [24]. An inverse relation is observed with pH,

antimicrobial efficiency increases as pH decreases [74,112]. Chitosan in media with a pH of 7.0 or greater demonstrated no antimicrobial activity [44,162]. Only small amounts of chitosan were required to inhibit bacterial growth. Kumar determined growth of *Escherichia coli* was inhibited in a solution with as little as 0.025% chitosan [84]. Jumma reported lipid emulsion prepared with chitosan demonstrated antimycotic properties [74].

Haemostatic and Anticoagulant Properties

Chitosan has demonstrated haemostatic and anticoagulant properties [18,84,106]. Native chitosan promotes haemostasis while chitosan coupled with sulfur acts as an anticoagulant [90]. Okamoto et al. worked on haemostatic properties of chitosan, determining that blood coagulation time varied significantly in a dose-dependent manner [118] and chitosan was found to be a superior haemostatic agent compared to chitin [118]. Chitosan causes blood coagulation by influencing platelets to form a clot [83,118], and significantly increases platelet adhesion [27]. Chitosan promotes blood coagulation in very low concentrations [130]. Fradet et al. reported the effective use of chitosan as a haemostatic agent under severe anticoagulation conditions [48], however Kind reported the ineffective use of chitosan as a topically applied haemostatic agent for liver laceration compared to pressure alone [80]. Difference in chitosan functionality is possibly due to the level of deacetylation, chitosan source, preparation procedure and interactions with medicinal compounds; none of which were discussed.

Wound Healing

Chitosan has been shown to possess wound healing properties [83] that accelerate healing by approximately 75% [41,42]. Chitosan treated wounds generated normal tissue elements, no visible scarring was observed at the wound surface [96]. This is due to chitosan's ability to inhibit fibroplasia [20,40,41,82,84,96,157]. Attempts to grow fibroblasts in media containing chitosan resulted in rounding up of cells, extension of short processes, inability to lay down and eventually cell death [96]. In addition to fibroplasia inhibition, chitosan and chitin have been shown to cause release of type I collagenase from fibroblasts [119]. During the final stages of wound healing, granulation tissue is degraded by enzymes, such as type I collagenase, and remodeled [119]. Early release of type I collagenase results in early degradation of granulation tissue and remodeling leading to decreased scar formation. In addition to inhibiting fibroplasia, chitosan accelerates wound healing by accelerating the infiltration of inflammatory cells and migration of polymorphonuclear cells [157]. Based on chitosan's superior ability to accelerate wound healing, several wound dressing materials are being tested. Chitosan wound dressings have been shown to possess the ability to control bacterial growth [40,75,78,102], perform haemostatic functions [144] and increase the proliferation of human F1000 fibroblasts [45]. Chitosan possesses natural anti-bacterial, haemostatic and analgesic properties. Chitosan bandages were shown to stop bleeding at a rate of 600 milliliters per minute [144]. The difference in ability of chitosan to inhibit fibroplasia or promote fibroblast proliferation can be attributed to several factors,

such as: degree of deacetylation, chitosan source, molecular weight and method of production. These factors are omitted in the literature and lead to differences in reported results, which has resulted in chitosan's slow progression as a biomaterial. On skin, chitosan was reported to promote production of keratin [83] resulting in decreased scar formation. A chitosan conjugate, N-carboxybutyl chitosan, was shown to favor formation of loose connective tissue rather than dense fiber bundles [11]. Angiogenesis plays an important role in wound healing by re-supplying blood to affected areas. Re-vascularization allows cells to proliferate and repair to continue. Chitosan has demonstrated angiogenesis promotion during wound healing [83]. Okamoto et al. demonstrated the ability of chitosan to reduce inflammatory pain [117]. Chitosan's wound healing ability, angiogenic, analgesic and antibacterial capabilities make it suitable for artificial skin. Kumar et al. demonstrated superior healing with artificial skin composed of chitosan [83] and wound healing is accelerated by chitosan oligomers released upon degradation [84]. Chandy reported accelerated healing and healed skin surface with chitosan artificial skin [20]. Chitosan films have been developed into artificial kidney membranes [39]. Due to charge on the chitosan molecule, artificial kidney membranes containing chitosan demonstrated high tensile strength and suitable permeability [40,41,106]. Orally administered chitosan has been shown as a treatment for renal failure. Taken orally, chitosan significantly reduces creatinine and serum urea levels [146]. Chitosan films were shown to turn more hydrophobic when sterilization was accomplished through autoclaving [130]. Increased hydrophobicity improves chitosan's film and gel forming

capabilities. Gel modification with alginate resulted in increased hydrophilicity, increase in hydrophilicity is proportional to the volume of alginate added [65].

Drug Delivery

Chitosan has demonstrated drug delivery capabilities. Gupta and Kumar reported the use of chitosan as part of a transdermal drug delivery system [56,83,84]. Oral [77,83], nasal [83] and ophthalmic preparations [83] of chitosan have been prepared for drug delivery. Formulations containing chitosan have been used for control release [39,40,41,45,75,84,146] and as a hydrophilic drug absorption enhancer across intestinal and nasal mucosa [146]. Microspheres and nanoparticles have been developed with chitosan for mucosal drug delivery [163] and as hydrophobic drug carriers [2,78]. Degradation rate of chitosan has important implications on drug delivery capabilities, the larger the particle size and the higher the degree of deacetylation, the longer the degradation rate [51,68,78,162]. Particle size can be controlled by varying amounts of chitosan within the particle [72].

Anti-Tumor and Anti-Viral Characteristics

Chitosan, along with chitosan conjugates, have demonstrated anti-tumor and anti-viral properties. Chitosan inhibits viral infection in animal cells [128] and stimulates immune response to viral antigens [129]. Shahidi reported chitosan's role as an inhibitor of tumor cell growth [144]. Several chitosan conjugates have been reported as demonstrating anti-tumor properties. Water-soluble N-succinyl-chitosan-mitomycin C conjugates [75], 6-O-carboxymethyl-chitin [138] and chitosan conjugates of 5-fluoro uracil [45] have demonstrated anti-tumor activity.

Anti-tumor activity can be attributed to malignant cells possessing a net electronegative surface charge that interacts with chitosan's polycationic surface charge [106]. Kato et al. reported use of chitosan nanoparticles as part of gadopentetic neutron capture therapy for cancer treatment [75]. Concentration of gadolinium in melanoma tissue in mice was approximately 74% of the original dose contained in an intratumoral injection of gadolinium-chitosan nanoparticles, compared to only 0.7% of the original dose when administered in a dimeglumine gadopentetate solution.

Nerve Cell Regeneration

Chitosan possesses possible nerve cell regeneration properties. Patel et al. reported on chitosan's ability to accelerate nerve growth and repair [124]. Researchers reported chitosan's high affinity for nerve cells [69,165], this is due to the polycationic nature of chitosan. Kumar et al. reported on the ability of chitosan to cause PC12 cells to extend neurites upon exposure to nerve growth factor [83]. PC12 cells are from a well characterized cell line derived from transplantable rat adrenal pheochromocytoma. PC12 cells respond reversibly to nerve growth factors. Freier et al. developed chitin-based tubes for neuronal support [50]. Chitosan-based tubes were compared to chitin-based tubes and found to have higher mechanical strength and higher nerve cell affinity than chitin-based tubes.

Dietary and Hypocholesterolemic Properties

Chitosan has been shown to possess dietary and hypocholesterolemic properties. This is an area of controversy as opposing results have been

reported. NiMhurchu et al. reported marginally greater weight loss with chitosan treatment combined with lifestyle and dietary change in 250 patients [110] while Kumar reports no change in body weight with chitosan treatment, unspecified number of patients [83]. These differences can be attributed to molecular weight, production method, degree of deacetylation, chitosan source and sample size. Chitosan binds to fat in the stomach before digestion trapping the fat and preventing absorption in the digestive tract [39,84,144,146]. Binding is due to the polycationic nature of chitosan and anionic nature of fat molecules. Since fat is not absorbed, chitosan intake increases fecal fat excretion and significantly decreases total serum cholesterol [83,146].

Tissue Engineering

Cartilage Tissue Engineering. Chitosan demonstrated superior performance in cartilage tissue engineering. Iwasaki et al. reported alginate-chitosan scaffolds enhanced biological responses of seeded chondrocytes *in vitro*, including enhanced cell attachment and cellular proliferation [70]. Chitosan concentration was found to smooth scaffold surface. Increasing chitosan concentration resulted in smoothing of the alginate-chitosan scaffold surface [70]. DiMartino and Risbud described chondrocytes cultured on chitosan sulfate scaffolds as maintaining round morphology and exhibiting preserved synthesis of extracellular matrix [1]. Chitosan sulfate hybrid polymer fibers exhibited increased cellular attachment and proliferation *in vitro* compared to alginate [1]. Kumar reported chitosan promotion of chondrocyte attachment and extracellular matrix synthesis [83]. Hoemann et al. measured PCNA (proliferating cell nuclear

antigen) expression and increased cell density to determine increased proliferation of chondrocytes due to chitosan exposure [61]. A combination of chitosan/GP (disodium β -glycerol phosphate) blood solution improved quantity and quality of cartilage repair [62].

Bone Tissue Engineering. Chitosan demonstrated potential in bone tissue engineering. Chitosan demonstrated osteoconductive properties [72]. In culture, chitosan sulfate promoted mineral deposition and growth by osteoblasts [1]. Borah, Scott and Wortham reported induction of bone growth in chitosan treated defects [12]. Calcification was observed on chitosan membranes after seven days [10], this calcification was the same observed with apatites [10], the major mineral in bone being hydroxyapatite. Bone defects treated with chitosan demonstrated increased calcification at increasing time intervals [12]. Chitosan sponges seeded with osteoblasts produced mineralized tissues [142]. Chitosan supported initial attachment and spreading of osteoblasts [43] and had an inhibitory effect on fibroblast cell attachment [82], this inhibitory effect leads to decreased scar formation. In addition to an inhibitory effect on fibroblasts, Fakhry et al. reported preferential initial attachment and spreading of osteoblasts over fibroblasts [43]. The characteristic of chitosan to promote adhesion of osteoblasts is governed by the degree of deacetylation. Cellular adhesion increases as level of deacetylation increases [14,40,51,65,128]. Hu et al. tested nanocomposite rods composed of chitosan and hydroxyapatite for internal fixation of bone [66]. Chitosan/HA nanocomposite rods were found to possess high bending strength and high modulus of elasticity. Addition of hydroxyapatite

increased bending strength, compared to chitosan, but lowered the elastic modulus [66]. Increased elasticity is due to water absorbed by the chitosan component of the nanocomposite rods. A chitosan/hydroxyapatite paste was tested by several groups and reported to be osteoconductive [68,78] as well as a suitable osteoblast cell delivery system [105]. McCord, Spence and Hudson reported on chitosan/hydroxyapatite paste as having superior tensile modulus and comparable tensile strength to bone, along with the ability to self-harden. However, chitosan/hydroxyapatite paste demonstrated inferior shear strength [101]. Cho et al. reported on the use of a chitosan/calcium sulfate composite as a bone graft and observed significant bone formation in defect, compared to a control group [25]. This combination was found to promote early bone formation and decrease the period of bony consolidation [26], activate macrophages and mononuclear cells and induce production of fibroblast growth factor and platelet derived growth factor [26]. After six weeks, histological examination showed nearly normal cortical bone [25]. Mallette, Quigley and Adickes reported defects treated with chitosan formed cortical bone, while control defects exhibited classic osteoblastic-osteoclastic sequence [96]. Klokkevold et al. demonstrated chitosan's ability to enhance osteogenesis. Chitosan doubled the number of osteoblast colonies *in vitro* [82]. DiMartino and Risbud reported on chitosan's ability to bind with growth factors, making chitosan suitable for bone engineering [1]. Incorporation of chitosan nanoparticles into bone cements provides effective antibacterial action [145]. Cell proliferation and tissue organization is strengthened and accelerated by presence of host stromal matrix along with the

chitosan macromolecule [107]. As a potential treatment of osteoporosis, Li et al. demonstrated that low molecular weight chitosan inhibits formation of osteoclast-like multinucleated cells and inhibits bone resorbing activity *in vitro* [89]. Osteoporosis occurs when bone absorption exceeds formation.

Scaffolds for Tissue Engineering. Scaffolds composed of chitosan have been tested for several different applications. Pan et al. reported using chitosan scaffolding as a support for hepatocytes [122]. Chitosan scaffolds have been developed as blood vessel supports due to chitosan's ability to form scaffolds with pore sizes approximately 50 to 150 micrometers, its ability to withstand maximum pressures of 4300 mmHg and enable rapid proliferation of blood vessel epithelial cells [164]. Properties of tubular blood vessel scaffold varied according to the temperature under which the film was formed [164]. A scaffolding sponge containing chitosan suitable for bone tissue engineering was reported on by Seol et al. [142]. The chitosan bone sponge possesses a pore size of approximately 100 to 200 micrometers and demonstrated accelerated osteoblast proliferation. Pore sizes of approximately 100 micrometers are necessary for bone growth. Li et al. tested collagen based scaffolds reinforced with chitosan for bone tissue engineering [91]. The pore sizes in the collagen-chitosan scaffold were approximately 100 to 200 micrometers, ideal for proliferation of bone tissue. By increasing the volume of chitosan fibers, Li et al. demonstrated an increased compressive strength, but an increase in fiber length caused a decrease in scaffold porosity [91]. Tan and associates developed 3-D gel scaffolding composed of collagen and chitosan. Chitosan concentration

greatly influenced pore size [153] and gel viscosity [153], the viscosity increased proportionally to chitosan concentration. Tan et al. reported chitosan affects cell proliferation but does not significantly affect cell viability [153].

Commercial Products

Therapeutic contact lenses [45] containing chitosan were reported by Felse. Chitosan contact lenses demonstrated a higher permeability to oxygen compared to conventional lenses [39,40,41]. Felse and Panda reported the use of chitosan as supporting material for implantable glucose biosensors [45]. Chitin has been used in the production of sutures due to its ability to resist degradation in bile, urine and pancreatic fluids [41,84]. Romoren et al. reported on the long term storage of chitosan. Chitosan maintains *in vitro* transfection efficiency and physiochemical properties for over a year when stored at 4°C [136]. Chitosan has been successfully used in cosmetics [39,40,56,75,85]. Along with chitosan's natural antimicrobial properties, chitosan's polycationic nature naturally attracts to skin and hair. In wastewater industry, chitosan has demonstrated metal chelating properties by binding various metal ions [39,45,56,84,92,129], it has been used to collect and remove trace amounts of metal ions in river water samples [39]. In photography, chitosan has been found to be a suitable fixing agent [39,40,41,56,84]. In paint manufacturing, chitosan is used as a thickening agent [39]. In the paper industry, chitosan is used in paper finishing and as a surface treatment on photographic and carbonless copy paper [39,40,56,84,90]. In textile industry, chitosan is used in dye chelation, removing dyes from dye processing effluents [39,45,84] and to impart antistatic and soil repellent

characteristics to textiles [40]. In agriculture, chitosan was found to have growth accelerating and growth enhancing effects on wheat seeds [40]. Chitosan has good emulsifying properties, it is used in the food industry [40,56,84,90] for thickening and gel-forming [39].

Bone Biology

Bone is composed of two types of tissue: cortical and cancellous. Cortical bone is dense and surrounds cancellous bone, thickness varies by location, thicker layers are found surrounding bones under stress (load bearing), such as a femur or humerus. Cancellous bone is internal, to cortical, and contains trabeculae with void (empty space), with much higher surface area than cortical. All bones are composed of cells and a complex matrix consisting of organic and inorganic components. Three types of cells are present in bone: osteoblasts, osteocytes and osteoclasts. These cells are responsible for bone production, maintenance and resorption, respectively. Bone matrix is composed of organic and inorganic components. The organic component consists of 95% collagen, mainly Type I with some Type V, with the remainder being non-collagenous proteins; osteocalcin, bone sialoprotein, osteopontin and osteonectin. The inorganic portion of the matrix is composed of calcium and phosphate salts. The location of cortical and cancellous bone in the femoral head is in Figure 3.

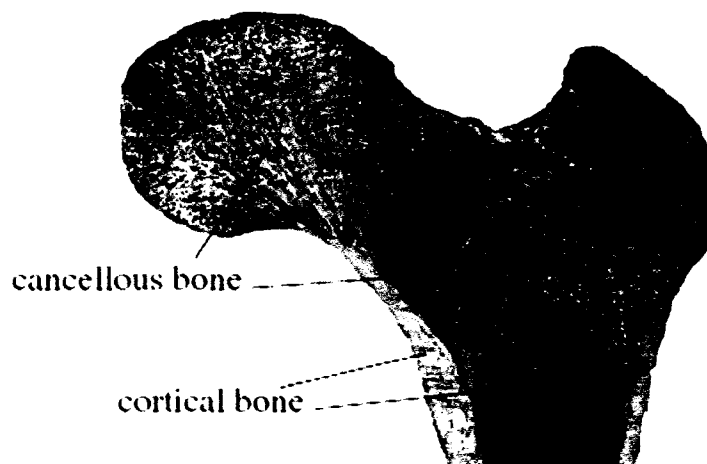


Figure 3. Structure of cortical and cancellous bone [58].

Ossification

Bone formation occurs following two different pathways: intramembranous and endochondral. Intramembranous ossification is direct differentiation of mesenchymal cells into osteoblasts and is responsible for development of flat bones (i.e. skull). Endochondral ossification is differentiation of mesenchymal cells into chondrocytes, which are replaced by osteoblasts and is responsible for most skeletal development, especially long bones.

Intramembranous Ossification. During intramembranous ossification cells derived in the neural crest proliferate and condense into nodules. Some of these cells differentiate into osteoblasts, while others form capillaries. Osteoblasts secrete a matrix, osteoid, that is capable of mineralization through binding of calcium salts. As osteoid is secreted, osteoblasts retreat. Occasionally, an osteoblast is trapped in mineralizing osteoid. When this occurs, the osteoblast differentiates into an osteocyte. As the osteoid calcifies, spicules are formed that radiate out from the point of ossification. These spicules connect and become

trabeculae of cancellous bone. The surface of the entire area of calcified spicule is surrounded by compact mesenchymal cells that develop into periosteum, a vascularized membrane that surrounds bone. Cells on the inner surface of the periosteum continue to produce matrix. This matrix becomes dense and upon calcification forms cortical bone. Bone morphogenic proteins (BMP) are thought to orchestrate direct differentiation of mesenchymal cells into osteoblasts. BMPs (BMP2, BMP4 and BMP7) activate core binding factor alpha one (Cbfa1) gene which encodes for Cbfa1 transcription factor. Cbfa1 transcription factor activates the genes for osteocalcin, osteopontin and other matrix proteins thereby causing direct transformation of mesenchymal cells into bone forming cells. Sources for mesenchymal cells are the periosteum, intracortical zone, endosteum and bone marrow; however hemopoietic cells of the bone marrow make no significant contribution to bone formation [15]. Figure 4 shows intramembranous ossification diagrammatically.

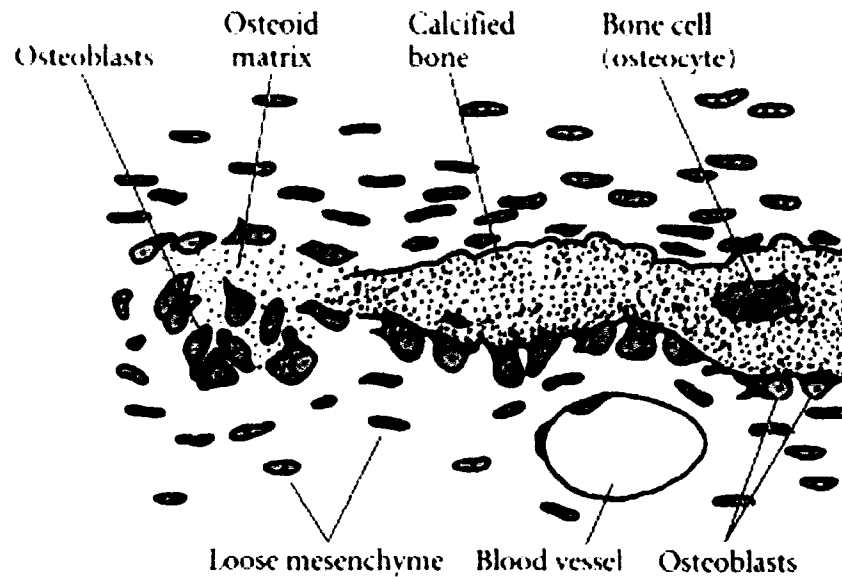


Figure 4. Intramembranous ossification [54].

Endochondral Ossification. Endochondral ossification consists of five steps (Figure 5):

1. Mesenchymal cells commit to differentiate into chondrocytes. Commitment is dictated by paracrine factors that cause nearby mesodermal cells to express two transcription factors, Pax1 and Scleraxis. Pax1 and Scleraxis are thought to activate cartilage specific genes.
2. Condensation of committed mesenchymal cells into nodules. Two factors are critical for initiation and maintenance of the nodules, neural cell adhesion molecule (N-CAM) and neural cadherin (N-cadherin). N-CAM is crucial for initiation of committed mesenchymal cellular condensation and N-cadherin is essential for nodule maintenance.

3. Chondrocyte proliferate and form a scaffolding model for bone growth. During proliferation, chondrocytes secrete cartilage-specific matrix.
4. After cells form the shape of the bone, proliferation ceases and chondrocytes undergo hypertrophy. In hypertrophy, chondrocytes stop dividing and increase volume. The hypertrophic chondrocytes secrete collagen type X and fibronectin, which allows the matrix to bind calcium carbonate and become mineralized.
5. Angiogenesis (blood vessel growth and invasion) occurs within the cartilage model and hypertrophic chondrocytes undergo apoptosis. New bone formation or repair must always be preceded by formation of a vascular network. As apoptosis occurs, cells surrounding the cartilage model will differentiate into osteoblasts. These osteoblasts will secrete a bone specific matrix directly on the cartilaginous matrix.

Endochondral ossification begins in the future location of the middle of the bone and spreads outward.

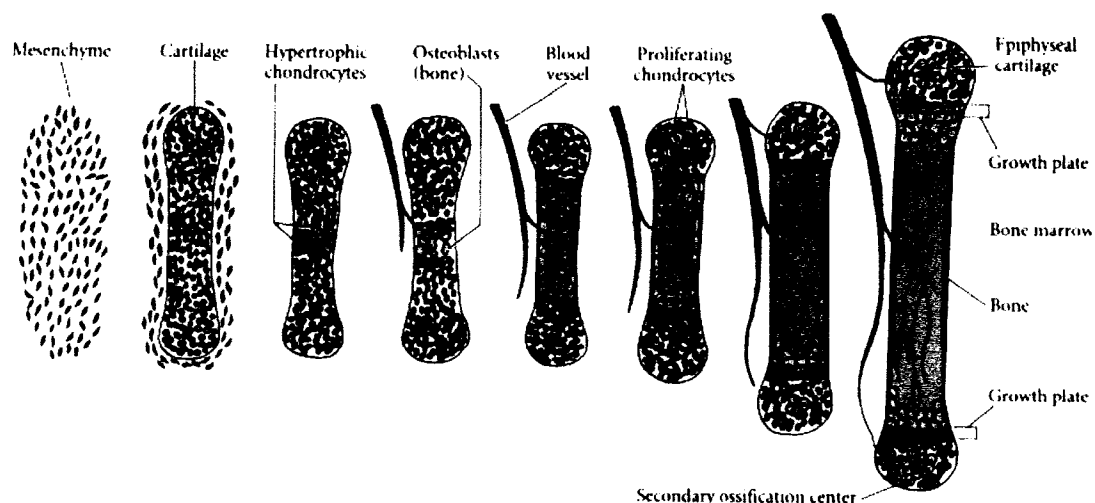


Figure 5. Endochondral ossification [54].

Bone Resorption

Bone resorption is performed by specialized cells called osteoclasts. Osteoclasts are specialized multinucleated macrophages [58,155] that dissolve bone into constituent components. Resorption occurs naturally as a mechanism of maintenance, whereby stress fractures cause release of alkaline phosphatase leading to a change in pH. The change in pH recruits macrophages (osteoclasts) to the site to remove debris. Osteoclasts, Figure 6, possess a specialized cytoskeleton that permit establishment of an isolated microenvironment between itself and debris (bone). Bone matrix is demineralized by a process involving proton transport which causes acidification of the isolated microenvironment [155]. The quantity of bone resorbed is dictated by expression of osteoclastogenesis stimulator (RANK) and an inhibitor (OPG) [155].



Figure 6. Scanning electron micrograph, osteoclast (Univ. of Oulu).

Bone Repair

Bone repair occurs through endochondral ossification. Bone is the only tissue that is repaired with formation of new bone; all other tissue is repaired with connective tissue [58]. Repair endochondral ossification is similar to molecular and cellular patterns seen in embryonic endochondral ossification. Local method of repair is dependent on blood supply. Complete repair is by endochondral ossification but local osteoprogenitor cells that are in contact with a good blood supply differentiate directly into osteoblasts. Angiogenesis plays a major role in the method of repair.

Bone repair occurs following the events [54] listed:

1. A haematoma forms due to damage to the periosteum (a nutrient-supplying vascularized membrane surrounding bone) and local tissue.
2. The interruption of blood supply causes local tissue necrosis, due to hypoxic conditions.

3. Macrophages and fibroblasts are recruited to the area. The macrophages remove debris and the fibroblasts secrete extracellular matrix. Mauney et al. proposed the recruitment of macrophages and fibroblasts are caused by a local change in pH due to release of alkaline phosphatase caused by mechanostimulation [99]. Macrophages and fibroblasts release growth factors and cytokines which recruit mesenchymal cells from the periosteum and bone marrow. Mesenchymal cells proliferate and differentiate into osteoprogenitor cells (precursors to osteoblasts).
4. Cellular proliferation causes the periosteum to thicken and formation of fracture callus around fracture site. Osteoprogenitor cells that are close to undamaged bone, good blood supply, directly differentiate into osteoblasts. These osteoblasts quickly form osteoid which is mineralized into bone. Cells farther away from a vessel, hypoxic conditions, differentiate into chondrocytes and form cartilage, which stabilizes the fracture and allows angiogenesis to occur. In mechanically stable bone, bone formation occurs by intramembranous ossification. In mechanically unstable bone, angiogenesis cannot take place and avascular tissue, cartilage, is laid down to stabilize the fracture. Once the fracture is stabilized, cartilage is replaced by bone [5,54].
5. Following angiogenesis, new bone is deposited on the cartilaginous matrix.

Graft Incorporation

Following graft implantation, normal processes immediately initiate incorporation by endochondral ossification. While specific details differ between different grafting materials, general principles are the same. The graft is used as scaffolding, osteoconduction, whereby chondrocytes lay down cartilage which undergo hypertrophy and are invaded by osteoblasts. Osteoblasts lay down bone and are followed by osteoclasts which remodel bone and remove the graft.

Graft incorporation begins with formation of a haematoma at implantation site [9,133]. The haematoma releases cytokines and growth factors which begin the ossification cascade [9]. Within minutes of graft implantation, platelets are released [133]. The release of platelets, leads to recruitment of polymorphonuclear leukocytes (PMN) by chemotaxis, this takes approximately one hour post-implantation [133]. Over the next three to eighteen hours, PMNs accumulate and adhere together [133]. Adhesion of PMNs cause recruitment of fibroblasts, by chemotaxis, and fibroblast attachment to the implanted graft, this occurs approximately one day post-implantation [133]. For the next day, day two, chemotaxis for fibroblasts and attachment of fibroblasts to the graft continues [133], this is osteoconduction. On the third day, cells on the implanted matrix proliferate and signal transduction occurs from the implanted matrix to fibroblast cell surface [133]. Signal transduction causes differentiation of chondroblasts into chondrocytes during the fourth and fifth days, this is osteoinduction. Chondroblasts are mesenchymal stem cells recruited from periosteum, intracortical zone, endosteum and/or bone marrow that are

committed to differentiating into chondrocytes. During the next two days, day six and seven, chondrocytes synthesize and secrete cartilage specific extracellular matrix [133]. Following differentiation, chondrocytes undergo hypertrophy, cartilage matrix mineralizes and angiogenesis takes place [133], day nine. Angiogenesis occurs via existing Haversian and Volkmann canals [9]. During days ten and twelve, mesenchymal stem cells surrounding the graft differentiate into osteoblasts, which synthesize and secrete bone matrix [133]. Following secretion of bone matrix, local macrophages differentiate into a multinucleated osteoclast. During days twelve through eighteen, osteoclasts remodel and dissolve the implanted bone graft [133]. Following remodeling, bone marrow differentiates and the graft is completely dissolved [133].

Discussion of the Literature

Chitosan is biocompatible, antibacterial, antifungal, haemostatic, antiviral, non-toxic and osteoconductive. It has demonstrated scar reduction properties. The degradation rate can be manipulated and it can be used as a drug delivery vehicle as well as a delivery vehicle for growth factors. Chitosan has demonstrated wound healing abilities and analgesic properties along with promoting osteogenesis. Chitosan is not structurally supportive, grafted bone must be stabilized with internal or external fixation, and will only dissolve in an acidic solution, will not form a paste singularly in a neutral pH solution. Chitosan has many characteristics that make it a favorable polymer for a bone graft, including osteoconduction, drug delivery capabilities, anti-bacterial and anti-fungal characteristics and haemostatic properties. In addition, chitosan

possesses a positive charge that enables it to bind with other functional compounds thereby expanding its functionality.

Calcium sulfate, plaster of Paris, is biocompatible, able to dissolve in neutral pH, non-toxic, and inert. It has successfully been used as filler in boney voids for more than one hundred years. It is resorbed quickly and completely and can be used as a drug delivery vehicle. Calcium sulfate can be used in the presence of osteomyelitis and absorption is associated with large numbers of osteoclasts, which indirectly promotes bone formation. Calcium sulfate has been proposed to promote angiogenesis. Calcium sulfate is not structurally supportive, grafted bone must be supported with either internal or external fixation, nor will it promote osteogenesis.

Bone grafting is the traditional treatment for bone loss due to musculoskeletal trauma or metabolic diseases. Autografts are in limited supply and subject the patient to additional risks of infection and pain. Allografts are also limited in supply and subject the patient to increased risks of immune reaction and disease. Therefore, development of synthetic bone graft materials is an active area of research. Ideally a bone graft should be osteoconductive, osteoinductive and osteogenic. Currently available bone grafts possess one or two of these characteristics but none possess all three. By combining crawfish chitosan, plaster of Paris and osteoblasts this study aims to develop a bone graft that possesses all three characteristics.

Hypothesis

Ideally a bone graft is osteoconductive, osteoinductive and osteogenic. It should be able to repair a defect with its constituent components as well as support osteoblast proliferation and recruit mesenchymal cells from the surrounding tissue to continue the reparative process. Synthetic bone grafts currently available perform one or two of these functions.

The long-term purpose of this study is development of a synthetic bone graft which is osteoconductive, osteoinductive and osteogenic. The general hypothesis is that a combination of crawfish chitosan, plaster of Paris and cultured osteoblasts will have all three of these properties. The graft would be osteoconductive, as chitosan and plaster of Paris have demonstrated osteoconductive properties [3, 32, 72]. Osteoblasts would provide the cellular basis for matrix deposition [15], and plaster of Paris would promote angiogenesis [151], which in turn would facilitate bone repair. In addition, plaster of Paris indirectly recruits macrophages (osteoclasts) [125]. Absorption of plaster of Paris is associated with a large number of osteoclasts which release growth factors and cytokines, recruiting mesenchymal cells. The graft function can be detected through decalcified histology sections, undecalcified histology sections, mechanical testing and microcomputed tomography. Specific hypotheses will be based on a comparison of experiments on two sets of defected bones, one containing the crawfish chitosan bone graft and the other containing no graft. Bone is composed of organic and inorganic components, 95% of the dry weight of bone is due to collagen fibers (organic) and bone mineral crystals (inorganic).

Decalcified histology sections will be stained with Hematoxylin and Eosin. Hematoxylin is a basophilic dye and Eosin is an acidophilic dye. Eosin will bind to collagen because of its acidic nature. Undecalcified histology sections will be stained with a Goldners' Trichrome. Light green stain is a component of Goldners' Trichrome stain that dyes collagen fibers due to collagens' acidic nature. The first hypothesis is that the presence of the graft material will promote the growth of bone, as measured by microcomputed tomography, decalcified histology sectioning and undecalcified histology sectioning. The second hypothesis is that bone with and without the graft material will have different stiffnesses and different fracture loads, as measured with a mechanical loading device. The third hypothesis is that the appearance of the defect in three-dimensional microcomputed tomography images of the bone will be smaller, both internally and externally, for defects that have been treated with the graft material. Microcomputed tomography will be used to produce single slice X-ray images as well as three dimensional rendered images. This initial investigation was designed to evaluate the promise of the material for bone grafts and to direct the research toward more definitive tests in the future if such promise is demonstrated. Therefore, the testing methodologies were chosen not only for their appropriateness to the study of bone grafting, but also for their availability.

Further hypotheses will relate to the properties of the chitosan being used, as opposed to the effect of the material on bone growth. Currently available commercial grade chitosan contains amorphous and crystalline structures. The combination of amorphous and crystalline structures makes

degradation unpredictable as crystals degrade at a different rate than amorphous structures. The crawfish chitosan used in this project was heated then cooled rapidly in liquid nitrogen, which is a common practice in creating amorphous structures, therefore a fourth hypothesis is that the crawfish chitosan is amorphous following heating and rapid cooling. The amorphous nature of the material will be characterized with a differential scanning calorimetry, which measures the differences in amount of heat required to increase the temperature of a sample and a reference.

A fifth hypothesis is that the procedure being used in this study to extract crawfish chitosan, which was patented by Dr. Debi Mukherjee, Louisiana Health Sciences Center, Shreveport, Louisiana yields a chitosan with a purity similar to commercially available medical grade chitosan. Spectra from the extracted crawfish chitosan and commercially available chitosan will be compared with two techniques, Fourier transform infrared spectroscopy (FTIS) and nuclear magnetic resonance spectroscopy (NMRS). Spectral similarities for the two materials will be characterized, and characteristic spectra or “fingerprints” of crawfish chitosan extracted using Dr. Debi Mukherjee’s procedure will be delineated. Such spectra will be useful in later studies, both for quality control and for characterizing the relationship between the structure and properties of the extracted chitosan.

CHAPTER 2

MATERIALS AND METHODS

Crawfish Chitosan Characterization

Fourier Transform Infrared Spectroscopy

Fourier transform infrared spectroscopy (courtesy of Louisiana Tech University, Ruston, Louisiana) was performed on solid samples using a Nicolet Nexus 470 spectroscope with 512 scans per sample and a resolution of 1.

¹H Nuclear Magnetic Resonance Spectroscopy

Nuclear magnetic resonance spectroscopy (courtesy of Centenary College, Shreveport, Louisiana) was performed on a Bruker Avance 300. Sample was prepared for ¹H nuclear magnetic resonance spectroscopy per published ASTM protocol with 16 scans at 90°C. The nuclear magnetic resonance spectroscopy protocol is listed in Appendix A.

Differential Scanning Calorimetry

Differential scanning calorimetry (courtesy of Centenary College, Shreveport, Louisiana) was performed on a Perkin Elmer DSC 6 with solid samples. The isothermal temperature was 25°C for 3 minutes and the dynamic range was 25-400°C at a rate of 10°C/minute with a sample weight of 25 milligrams.

Surgical Materials and Methods

Surgical Materials

Isoflurane USD (Halocarbon Laboratories), Sunbeam electric shaver (model 059750-070-000), 70% ethyl alcohol (Fisher Healthcare), Betadine (Purdue Pharma L.P.), four hole titanium plate (cut from a twelve hole oral-maxillofacial plate, Synthes Corporation), Dremel tool (Ryobi Corporation, model HT20VS), 3.0 absorbable coated vicryl suture (Ethicon), calcium sulfate hemihydrate 98% (Aldrich Chemical Company, Inc.), and Polysporin (Pfizer Consumer Healthcare).

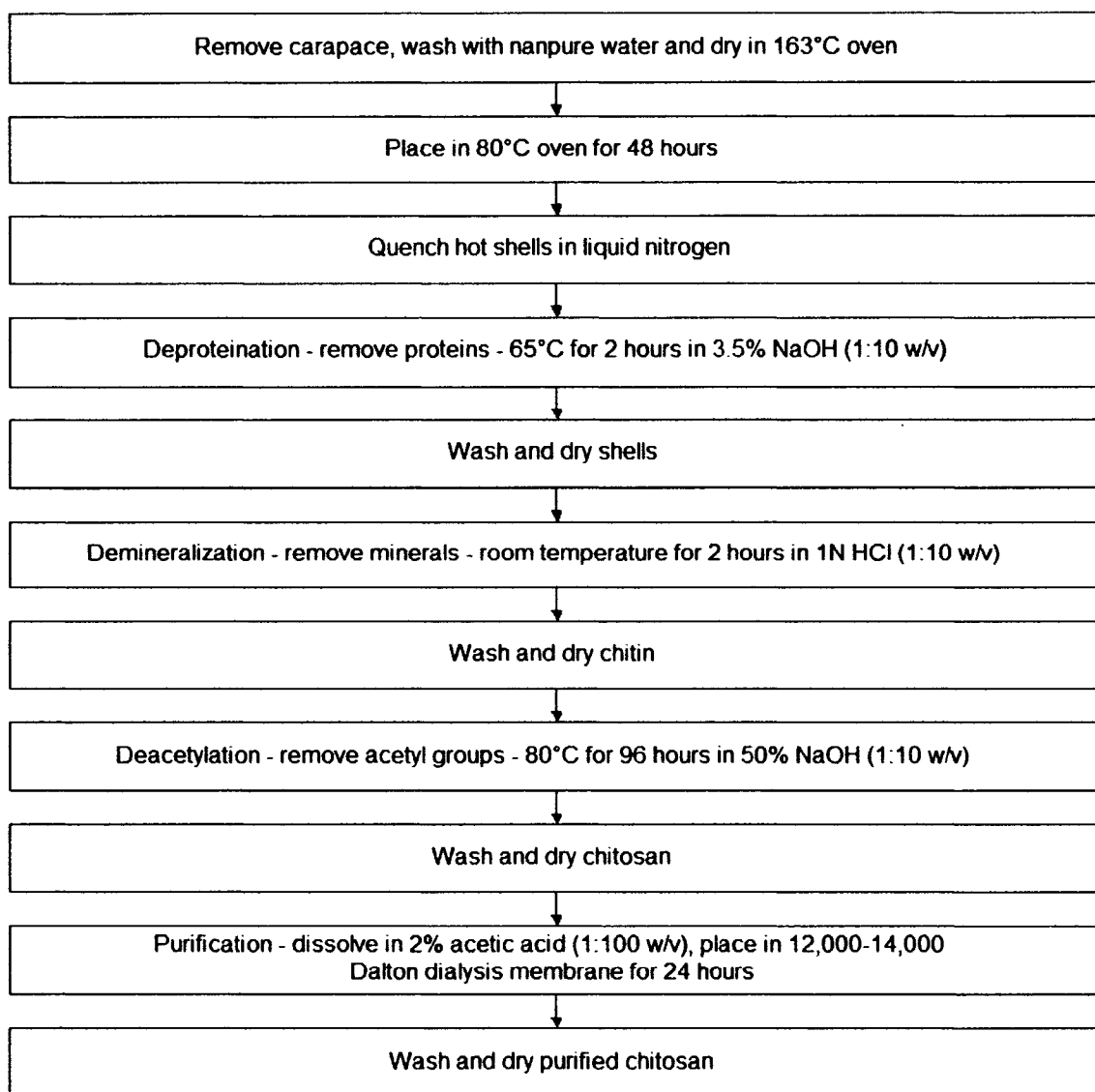
Osteoblast Cell Culture

Osteoblast cells were cultured from rat femoral bone marrow aspirate to an average concentration of 4.06×10^5 /ml, using published protocol [105]. The osteoblast cell culture protocol is in Appendix B.

Crawfish Chitosan Extraction

Crawfish chitosan was extracted per patented procedure [104] which followed the guideline in Table 1.

Table 1. Chitosan extraction from crawfish.



Crawfish Chitosan Bone Graft Preparation

Crawfish chitosan bone graft was prepared by combination of cultured osteoblasts, calcium sulfate (plaster of Paris), and crawfish chitosan. The ratio of chitosan to calcium sulfate was 1:4, ideally 0.1250g of crawfish chitosan to 0.5000g calcium sulfate. The actual average paste contents were 0.5104g of calcium sulfate and 0.1245g of crawfish chitosan with an average osteoblast

concentration of 2.30×10^5 /ml. The exact measurements of each component are listed in Appendix C.

Critical Size Defect Model

A critical defect is a defect which will not heal spontaneously during the lifetime of the animal [4,141]. In rats, critical defect size is three to four millimeters, in any bone excluding flat bones. Bone grafts are required for the repair of critical defects.

Surgical Procedure

To determine *in vivo* efficacy of this new chitosan synthetic bone graft a critical defect was created on the dorsal surface of the femur of male Lewis Rats, approximately two months of age and 200 to 250 grams in weight, per Institutional Animal Care and Use Committee (IACUC) protocol #P-04-001 (detailed in Appendix F). In order to reduce systematic error, the location of the defect was randomized from animal to animal. To sedate the animal prior to safely moving it to the surgical Table, light anesthesia was administered by lowering the animal into a plastic container containing paper towels coated lightly in 100% Isoflurane. Once anesthetized the animal was connected to a surgical gas administering device capable of administering 5% Isoflurane and oxygen.

All of the animals were oriented dorsal side up. Their limbs were taped down and the femoral location was determined by palpitation, Figure 7. The animal was shaved and the area was wiped down using 70% alcohol on sterile gauze followed by Betadine. An incision was made along the femur beginning at the femoral head and continuing the length of the femur.



Figure 7. Rat in surgical frame.

The incision was held open using a retractor and the muscle was cut in the same fashion. All soft tissue was removed from the femur and the four-hole plate was attached, screw holes were drilled with a Dremel tool. Once the plate was securely fashioned, a critical defect was created using a 2.5mm burring bit. The defect was approximately three millimeters wide and spanned the entire width of the femur. In the operated control group, once the defect was created, the muscle was sutured, with 3.0 Vicryl coated suture (Ethicon, Inc.). In the experimental group, the defect was filled with chitosan bone graft and the muscle was sutured. The skin incision was closed using staples. Staples were chosen because in previous experiments the animals chewed through sutures. A generous application of Polysporin, an antibiotic cream, was applied to the exterior of the wound. The animal was then returned to its cage, and allowed to regain consciousness. This typically occurred in ten to fifteen minutes. The animals were monitored very closely during the first two weeks. This initial monitoring was necessary to ensure the complete success of the surgeries as any noticeable problems would have been evident in the first two weeks.

Potential problems include: loss of foot use, loss of leg use, infection, lethargy, and pain. Approximately 10 days post surgery, the staples were removed.

Sacrifice

The animals were sacrificed using carbon dioxide asphyxiation, according to the following schedule listed in Table 2. The dated sacrifice table can be found in Appendix D.

Table 2. Sacrifice schedule (number of animals).

	Three month	Six month	Nine month
Operated control group	3	3	3
Experimental group	3	3	3
Unoperated control group	3	3	3

Harvest

Immediately after the animals were euthanized by carbon dioxide asphyxiation, soft tissue surrounding the femur was dissected. The femur was removed, placed into a 0.9% NaCl solution and frozen. The femurs remained frozen until testing.

Histological Sectioning

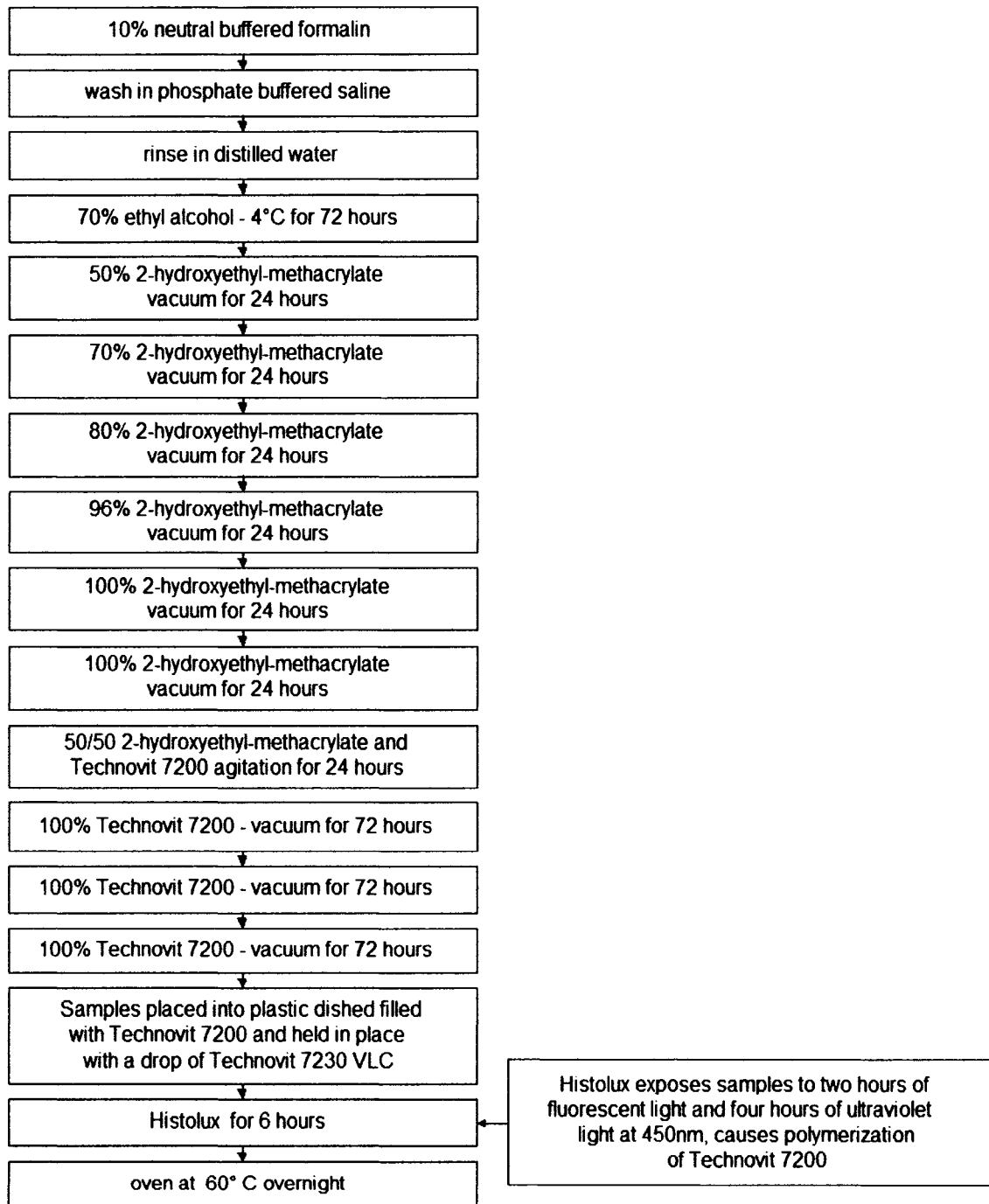
Undecalcified Sectioning

Undecalcified Materials. Technovit 7230 VLC (Exakt Corporation), Technovit 7210 VLC (Exakt Corporation), Technovit 7200 VLC resin (Exakt Corporation), Technovit 4000 (Exakt Corporation), small plastic slide 2"x3" (Exakt Corporation), large plastic slide 3"x4" (Exakt Corporation), 2-Hydroxyethyl-methacrylate 97% (Aldrich Corporation), Exakt standard cutting and grinding

system, 10% Carson Millonig formalin solution (Statlab medical products), phosphate buffered saline 1X (HyClone), 70% ethyl alcohol (Aaper Alcohol and Chemical Company), Histolux HX (Exakt Corporation).

Undecalcified Embedding. Femurs were stored in 10% solution of neutral buffered formalin, for tissue preservation. The time each femur was allowed to remain in Formalin varied according to the euthanizing schedule of subsequent groups. Minimum time required was 48 hours but no sample remained for less than two weeks. After removal from formalin, the bones were washed in phosphate buffered saline, rinsed in distilled water and transferred to 70% ethanol refrigerated. The bones underwent an increasing gradient of 2-hydroxyethyl-methacrylate/nanopure water followed by several changes of Technovit 7200VLC resin. The resin embedding procedure is shown in Table 3.

Table 3. Undecalcified histological embedding procedure.



Following embedding, samples were sandwiched between a large and small slide then sectioned using the specially designed diamond-tipped band saw, Figure 8, in the Exakt system. The sample was fixed to the large slide using Technovit 4000, which is a three part epoxy. After fixing the sample to the large slide, the resin block was ground down, using the grinder in Figure 9, until sample was in the surface plane of the block. A small slide was attached to the ground side of the block using Technovit 7210 VLC. After adherence of the sample to the small slide, the complex was attached to the Exakt saw. The blade was set to approximately 100 μ m and allowed to cut on a speed setting of two. This low setting caused slower cutting but less waste. After cutting, the slices were placed on the Exakt grinder, using increasing grits of sandpaper from 800 to 4000, and they were constantly measured until the specimen thickness was between 10 and 20 micrometers.

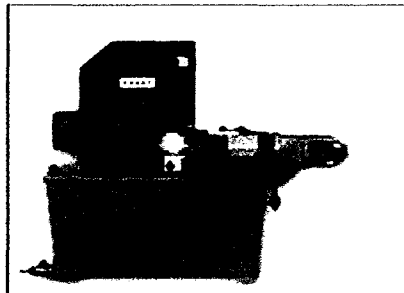


Figure 8. Exakt cutter.

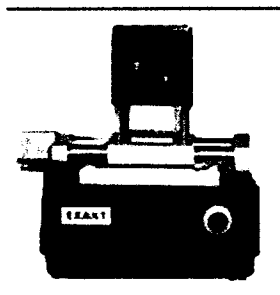
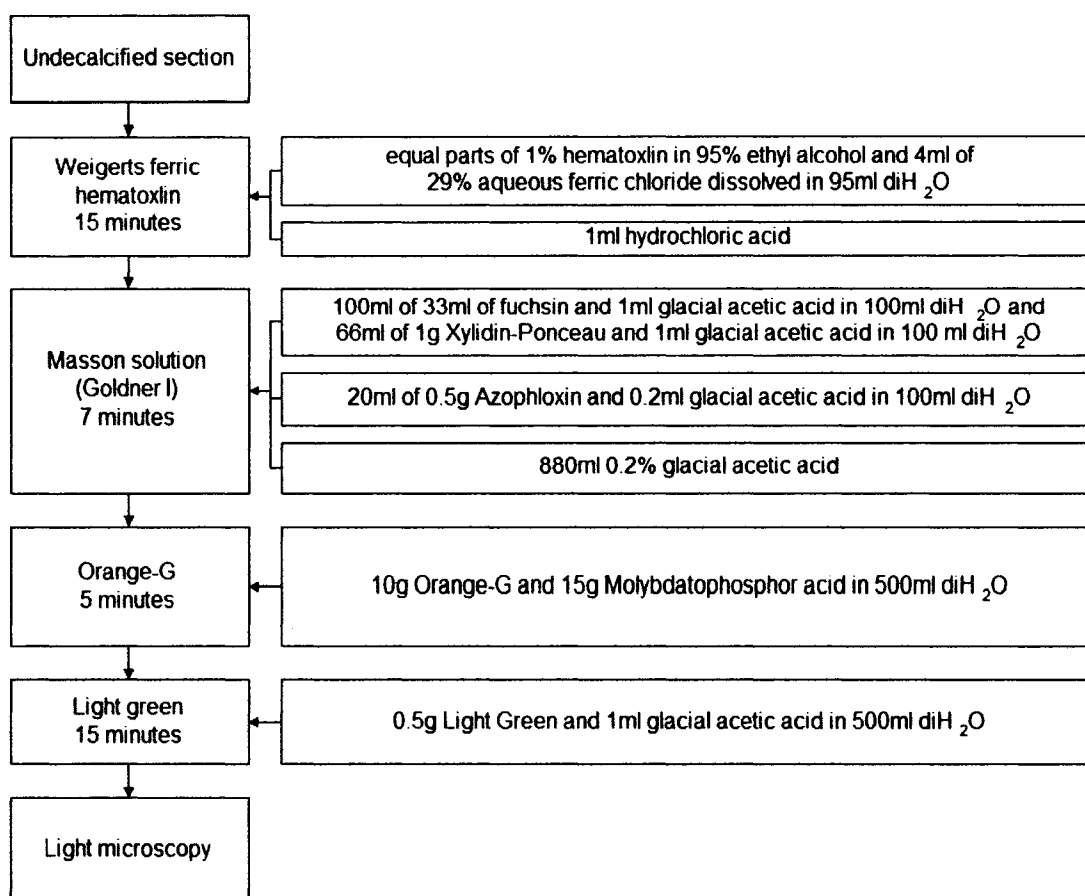


Figure 9. Exakt grinder.

Undecalcified Histological Staining Materials. Hematoxylin crystals (Acros Organics), 95% ethyl alcohol (Aaper Alcohol and Chemical Company), ferric chloride 29% aqueous (Sigma Chemical Company), hydrochloric acid (Fisher Scientific Company), acid fuchin (Sigma Chemical Company), glacial acetic acid (Fisher Scientific Company), Xylidin-Ponceau (Chroma), Azophloxin (Chroma), Orange-G (Sigma Chemical Company), Molybdato-phosphor acid (Sigma Chemical Company), Light Green (Sigma Chemical Company). Table 4 lists the undecalcified staining procedure.

Table 4. Undecalcified histological staining procedure.



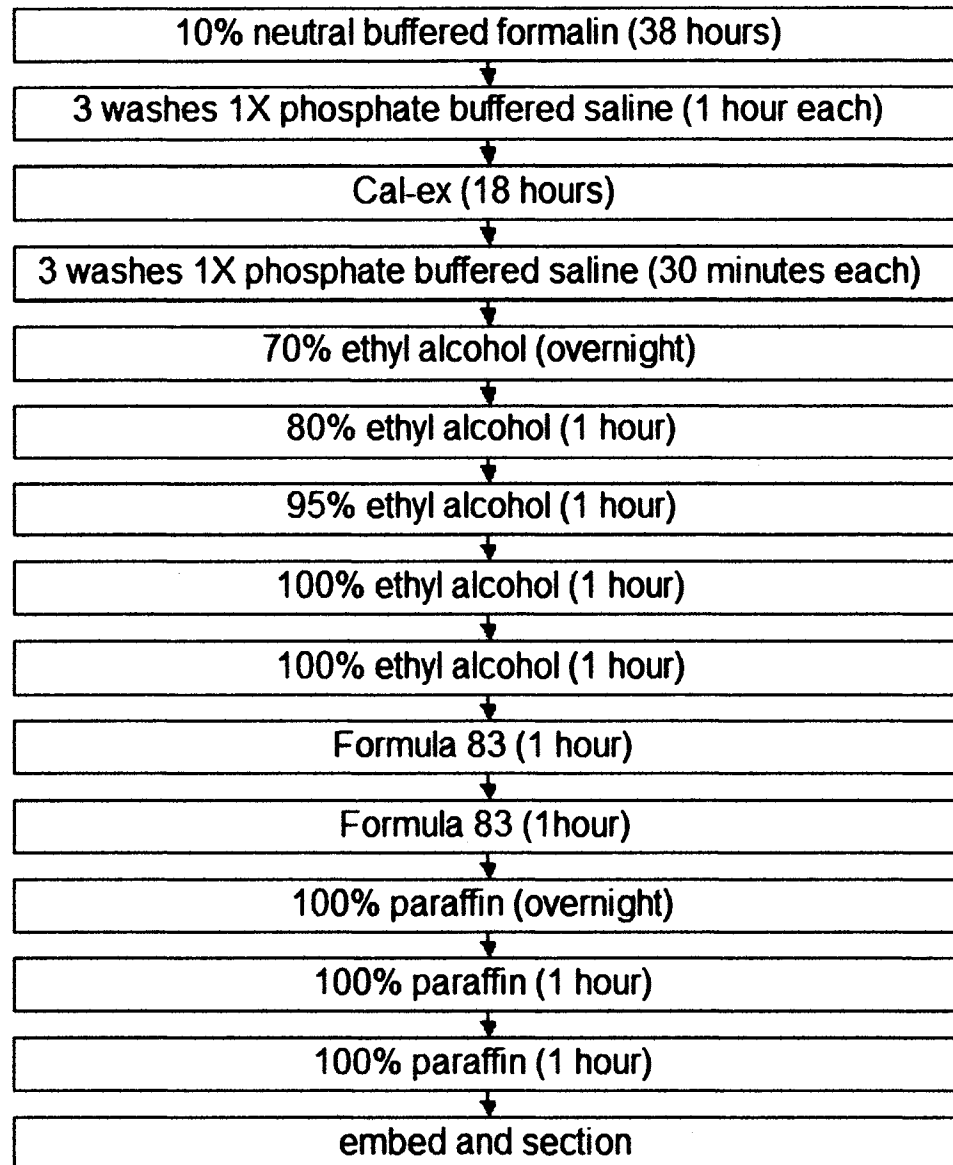
Decalcified Histology Materials

10% Carson Millonig formalin solution (Statlab medical products), Cal-Ex (Fisher Diagnostics), 100% ethyl alcohol (Aaper Alcohol and Chemical Company), Formula 83 (CBG Biotech), TissuePrep 2 paraffin wax (Fisher Scientific), sodium chloride (Fisher Scientific), potassium chloride (Aldrich Chemical Company, Inc.), potassium phosphate (Sigma Chemical Company), sodium phosphate (Sigma Chemical Company), nanopure water.

1X Phosphate Buffered Saline. 0.8g sodium chloride, 0.02g potassium chloride, 0.02g potassium phosphate, 0.11g sodium phosphate, 1L nanopure water, pH 7.2-7.4.

Decalcified Histological Procedure. The decalcified histological embedding procedure is shown in Table 5:

Table 5. Decalcified histological embedding procedure.



The samples were placed into a glass jar on top of gauze. The gauze allowed the dissolved calcium to fall away from the bone, preventing interference with further decalcification.

Following the final paraffin step, the samples were embedded into a paraffin block using Miles Tissue Tek II, Tissue Embedding Center 4603 (GMI, Inc.), Figure 10.

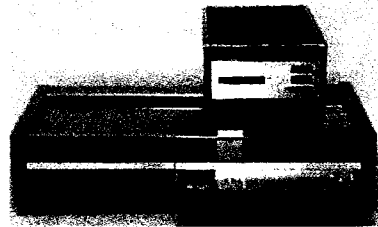


Figure 10. Miles Tissue Tek II.

The samples were cut into seven micrometer slices on an 820 Spencer microtome (American Optical Corporation).

Histological Analysis

Stained histological sections, undecalcified and undecalcified, were photographed using an Olympus digital camera connected to an Olympus CX41 light microscope at 4x magnification. Areas of bone were marked using Adobe Photoshop 7.0 edge finding option (areas not automatically selected were manually selected). Using the software, the number of pixels were found and compared to the overall number of pixels as well as to the number of pixels in other testing groups.

Post Harvest Analysis

Microcomputed Tomography

Microcomputed Tomography was performed (courtesy of Animal Resources, Louisiana State University Health Sciences Center, Shreveport,

Louisiana) on a MicroCAT II; model MCII-UAAI following standard operating procedure. Each femur, along with the contra-lateral side, was run for 512 scans along the defect site. This data was compiled into 2-D and 3-D images.

Mechanical Testing

Four point bend test was performed on an Instron 4202 (Instron Corporation, Norwood, MA) in a customized apparatus (see Figure 11). The fulcrum points were 8mm apart and the head speed was 10mm/min. Load was applied using either a 100N load cell or 10kN load cell.

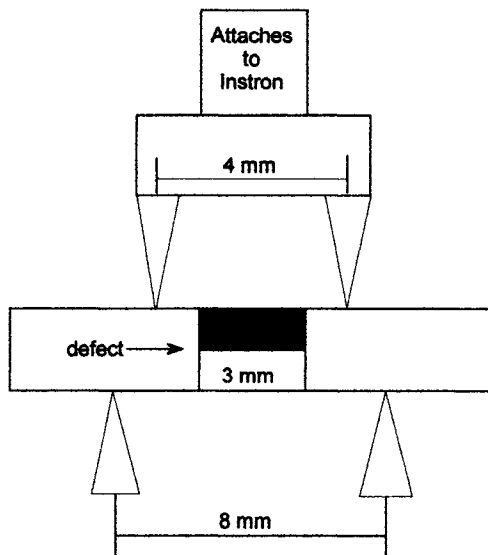


Figure 11. Mechanical testing apparatus.

CHAPTER 3

RESULTS

Chitosan Characterization

Fourier Transform Infrared Spectroscopy

Fourier transform infrared spectroscopy (FTIR) passes a known wavelength of infrared light through a sample and records amount of energy absorbed by the molecule. Spectra for crawfish chitosan, chitosan glutamate and crawfish chitosan, chitosan monomer is shown in Figures 12 and 13.

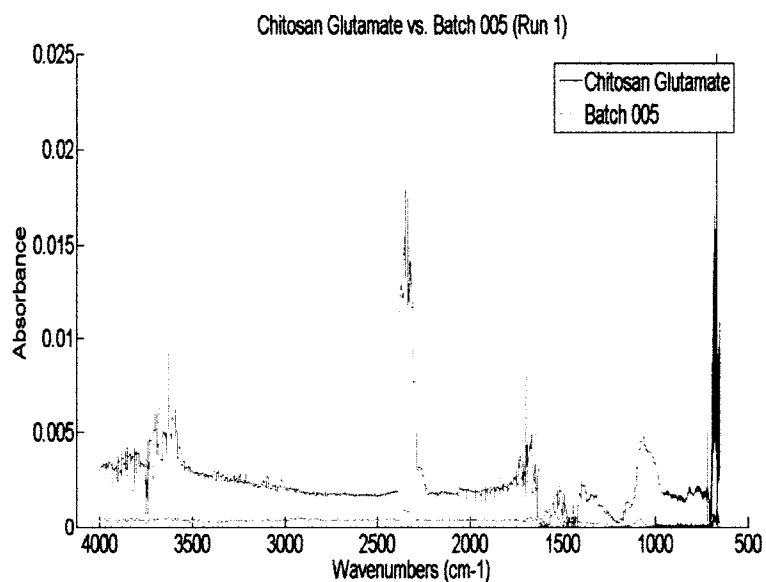


Figure 12. Crawfish chitosan and chitosan glutamate – FTIR.

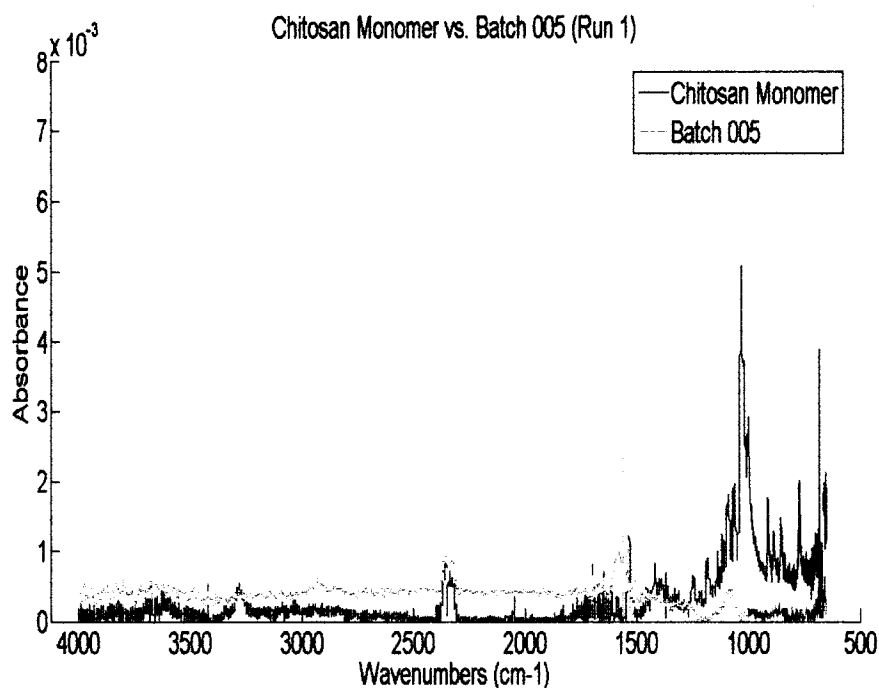


Figure 13. Crawfish chitosan and chitosan monomer – FTIR.

Chitosan glutamate, chitosan monomer and crawfish chitosan peak locations are located in Table 6. Peaks at 3628 cm^{-1} , 2344 cm^{-1} , 1654 cm^{-1} and 1089 cm^{-1} were all shared between chitosan glutamate, chitosan monomer and crawfish chitosan. The peak located at 3628 cm^{-1} is associated with hydroxyl groups. The peak located at 2344 cm^{-1} is associated with solid phase amine groups. The peak at 1654 cm^{-1} is associated with deformation vibration of primary amine groups and the peak at 1089 cm^{-1} is associated with CH-OH bonding.

Table 6. Common FTIR peak locations.

Common FTIR peak locations		
Chitosan Monomer	Chitosan Glutamate	Crawfish Chitosan
3628.893	3627.928	3628.893
2344.052	2353.212	2344.052
1654.426	1654.426	1654.426
1089.834	1089.798	1089.672

¹H Nuclear Magnetic Resonance Spectroscopy

¹H nuclear magnetic resonance spectroscopy (NMR) aligns protons with intrinsic magnetic moments with a powerful external magnetic field and perturbs the alignment using an electromagnetic field. Perturbations are measured and recorded. All nuclei with odd numbers of protons and some with even number of protons have intrinsic magnetic moments; ¹H and ¹³C are most widely used.

Similar peaks were located in all three ¹H NMR spectra: crawfish chitosan, chitosan monomer, and chitosan glutamate. ¹H NMR spectral analysis is in Figure 14. Peak locations were noted by distance from peak center to nearest quantitative part per million. Common peaks were: 0.235 inches to the right of one part per million, 0.149 inches to the right of two parts per million, 0.070 inches to the right of three parts per million, and 0.050 inches to the left of four parts per million. The peaks located 0.235 inches to the right of one part per million and 0.070 inches to the right of three parts per million are associated with amine groups. The peak located at 0.149 inches to the right of two parts per million is associated with hydroxyl groups.

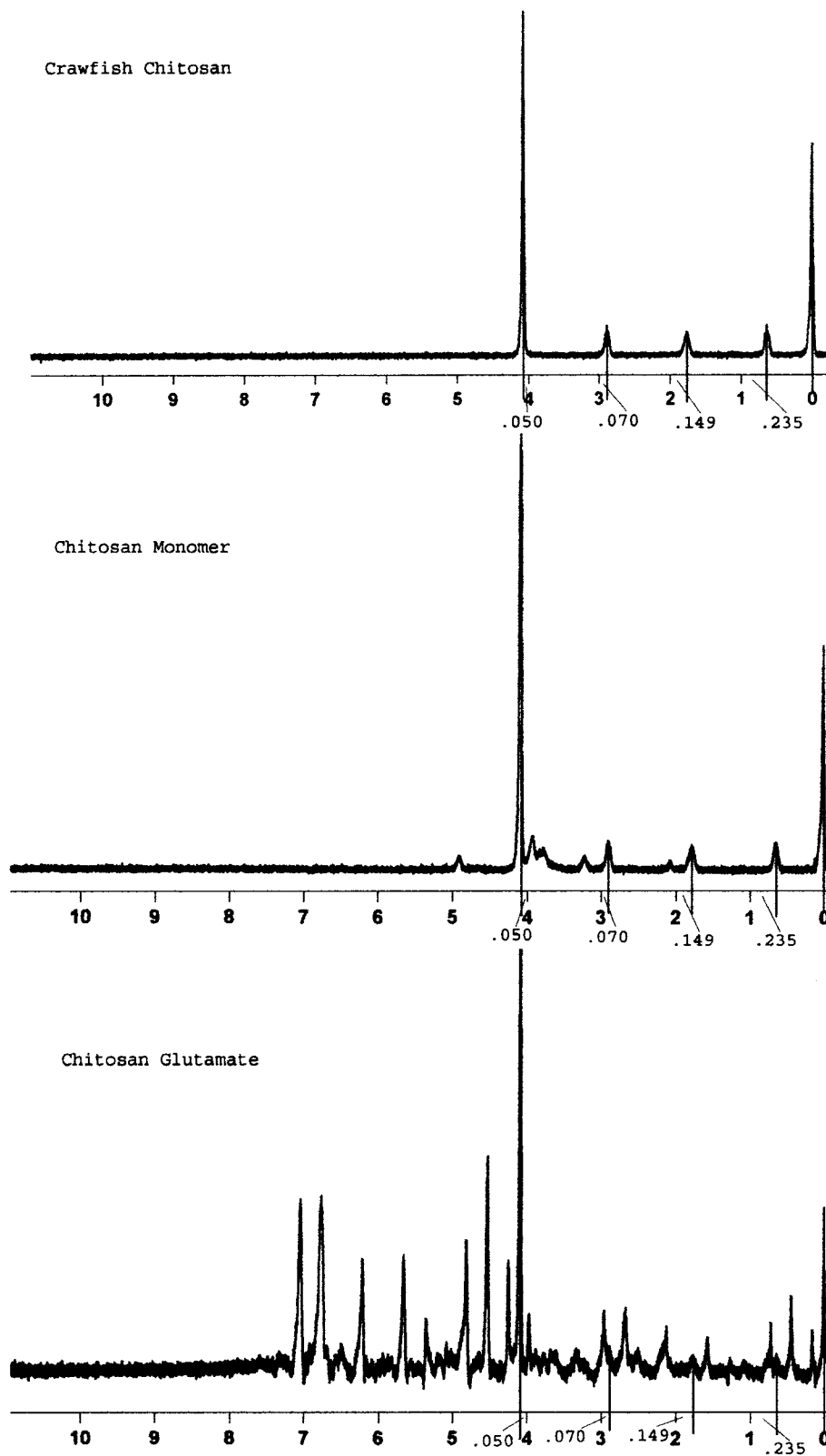


Figure 14. Comparison of NMR spectra.

Differential Scanning Calorimetry

In differential scanning calorimetry (DSC), differences in amount of heat required to increase the temperature of a sample and a reference are measured as a function of temperature. During melting, more heat is flowing to the sample, this is an endothermic reaction. During crystallization, less heat is required to raise the temperature (less heat is flowing to the sample), this is an exothermic reaction. DSC measures amount of energy absorbed or released compared to a control. In Figure 15, crawfish chitosan DSC results are shown for control (empty pan, left) and crawfish chitosan (right). In Figure 16, industrial chitosan DSC results are shown with control (empty pan, left) and industrial chitosan (right). Crawfish chitosan appears more amorphous than industrial chitosan due lack of peak and troughs in the DSC spectra of crawfish chitosan, compared to various endothermic and exothermic cycles from the industrial chitosan DSC spectra.

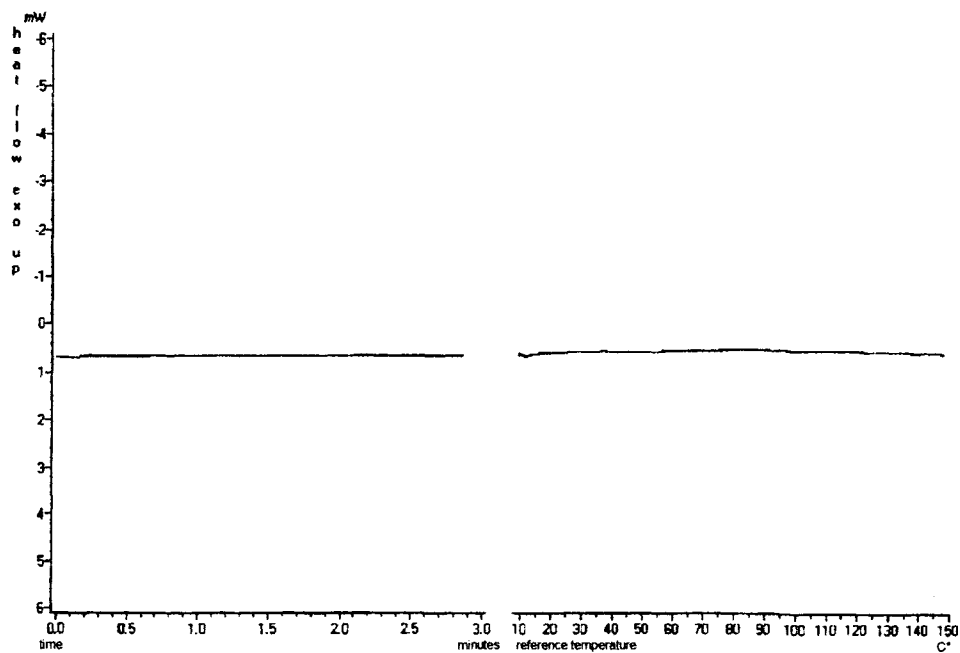


Figure 15. Crawfish chitosan – DSC.

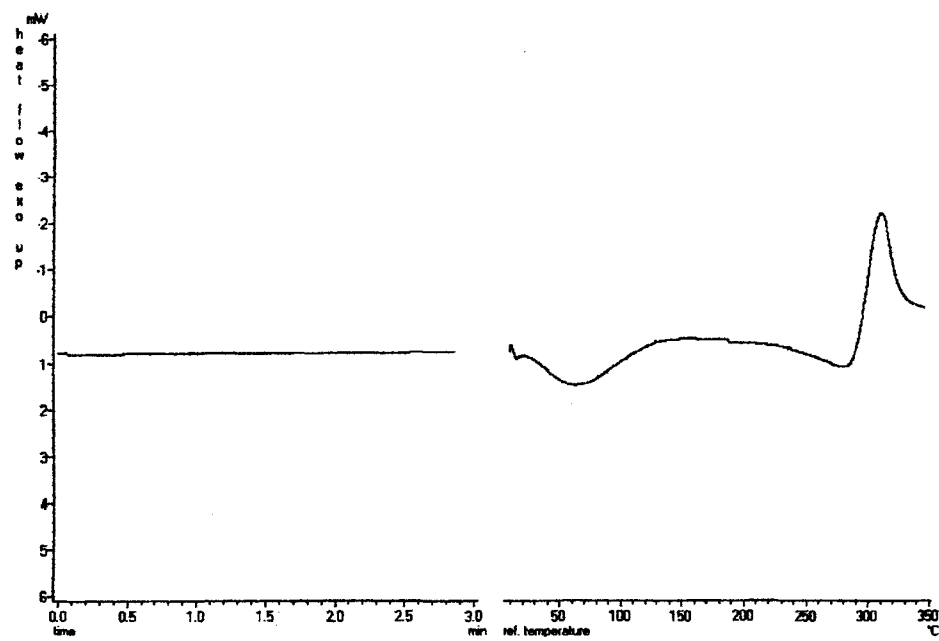


Figure 16. Industrial chitosan – DSC.

Gross Anatomy

Six Month

From gross anatomical analysis, operated control samples grew deformed with the defect completely filled with fibrous tissue (Figure 17). Bone growth along the dorsal side of the plate was significantly increased compared to the three month operated control. In experimental samples, the defect was either partially healed with a slight defect present (Figure 18) or completely healed with slight visual evidence of small amounts of fibrous tissue (Figure 19).

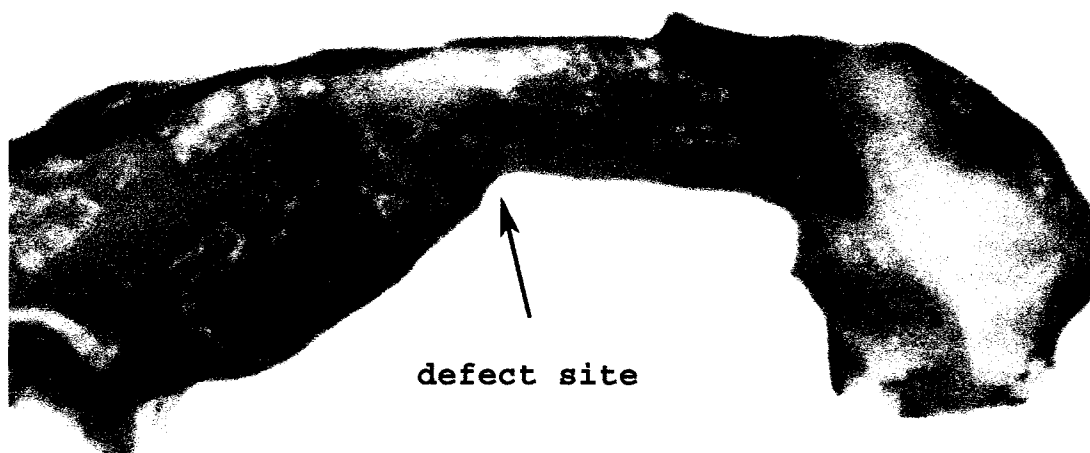


Figure 17. Six mo. Rat 6 left operated control – gross.

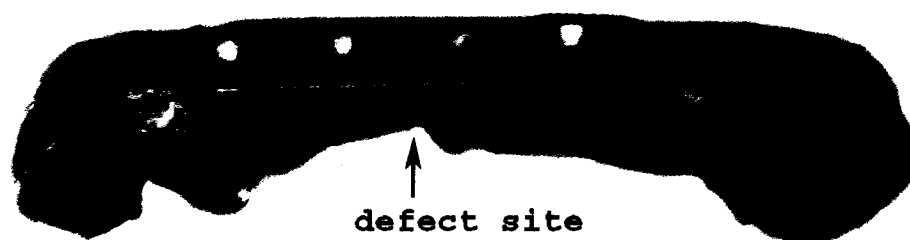


Figure 18. Six mo. Rat 13 left experimental – gross.



Figure 19. Six mo. Rat 14 left experimental – gross.

Nine Month

From the gross anatomical analysis, operated control samples showed complete fibrous ingrowth (Figure 20). Upon removal of the plate, the defect was present and the bone had no structural support. Bone growth was observed along the dorsal side of the plate, increased from the six month operated control group. In the experimental group, the defect was completely healed with no evidence of fibrous tissue (Figure 21). No bone growth was visualized along the dorsal plane of the plate.



Figure 20. Nine mo. Rat 19 left operated control – gross.



Figure 21. Nine mo. Rat 18 left experimental – gross.

Undecalcified Histological Sectioning

In order to determine the presence of bone, a sample from each time frame and tested group underwent undecalcified sectioning and staining with Goldner's' Trichrome Method (muscle – red, collagen (bone) – green, cytoplasm (fibrous tissue) – bright red, nucleus – brownish black). All photographs were taken at 4x magnification with a light microscope, unless otherwise noted.

Six Month

At six month time interval, in the operated control group, fibrous tissue was present in the defect site (Figure 22). Bone was present juxtaposed to fibrous tissue. In the experimental group, the defect was filled with bone with

voids, indicated by white areas (Figure 23). Undisturbed bone from the six month group is in Figure 24.

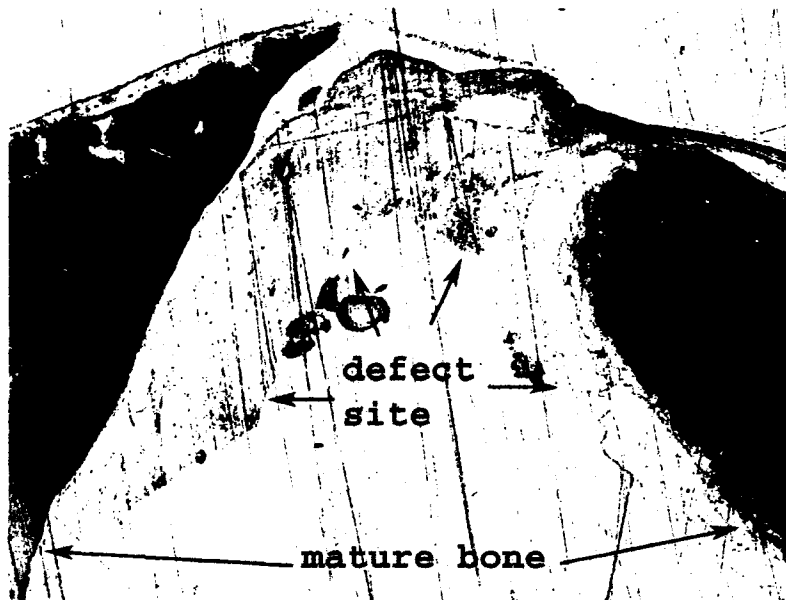


Figure 22. Six mo. operated control (Goldner's, undecal., 5L-VV).



Figure 23. Six mo. experimental (Goldner's, undecal., 13L-SS).



Figure 24. Six mo. unoperated control (Goldner's, undecal., 25L-MM).

Nine Month

At nine month time interval, in the operated control group, fibrous tissue was present in the defect site (Figures 25, 26, 27 & 28). The amount of fibrous tissue increased from the six month group. Delineation between fibrous tissue and bone improved and the fibrous tissue appears denser. In the experimental group, the defect was almost entirely repaired. Repair occurred in the medial to lateral direction as observed in Figure 29 and 30 (Figure 29 was sectioned prior to Figure 30). Bone was organized and the intermedullary canal was well defined (Figure 30). Undisturbed bone from the unoperated control group is in Figure 31.



Figure 25. Nine mo. operated control (Goldner's, undecal., 7R-69).



Figure 26. Nine mo. operated control (Goldner's, undecal., 7R-69).



Figure 27. Nine mo. operated control (Goldner's, undecal., 7R-76).

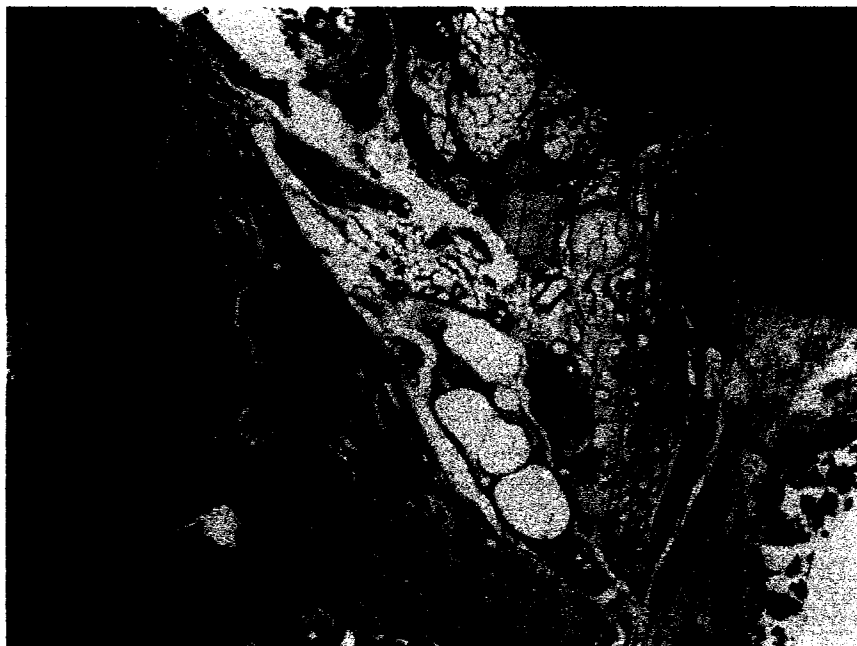


Figure 28. Nine mo. operated control (Goldner's, undecal., 7R-81).



Figure 29. Nine mo. experimental (Goldner's, undecal., 17L-62).



Figure 30. Nine mo. experimental (Goldner's, undecal., 17L-64).

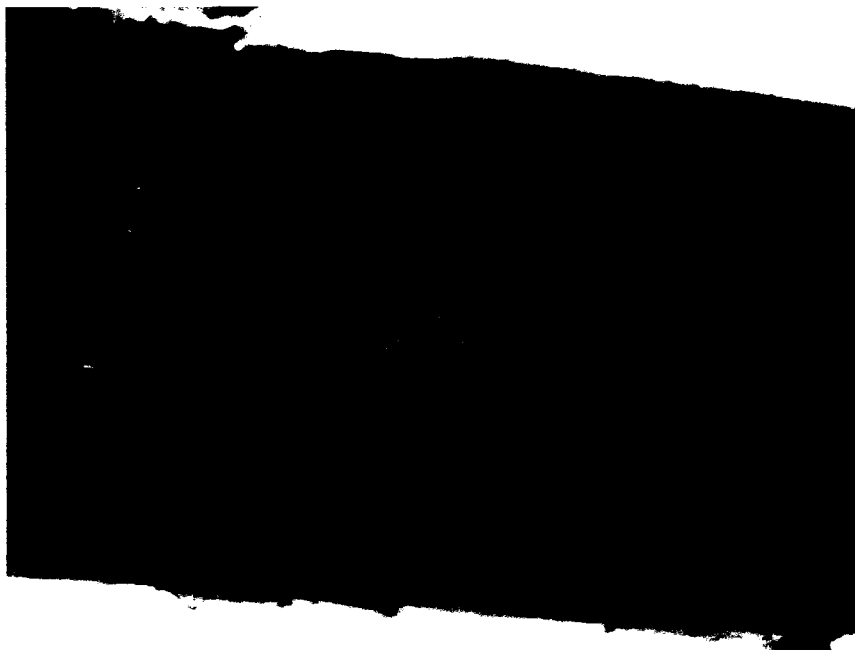


Figure 31. Nine mo. unoperated control (Goldner's, undecal., 27R-59).

Histological Quantitative Data

From bone pixilation, the percentage of bone in each group can be compared (Figure 32). In each time interval, more bone was present in the experimental group compared to the operated control group. At the six month time interval, 35.58% bone growth was calculated in the experimental group and 30.09% bone growth was recorded in the operated control group. As expected, nine month time interval demonstrated the highest percentage of bone growth in both groups. The experimental group experienced 42.82% bone growth while the operated control group experienced 40.16%.

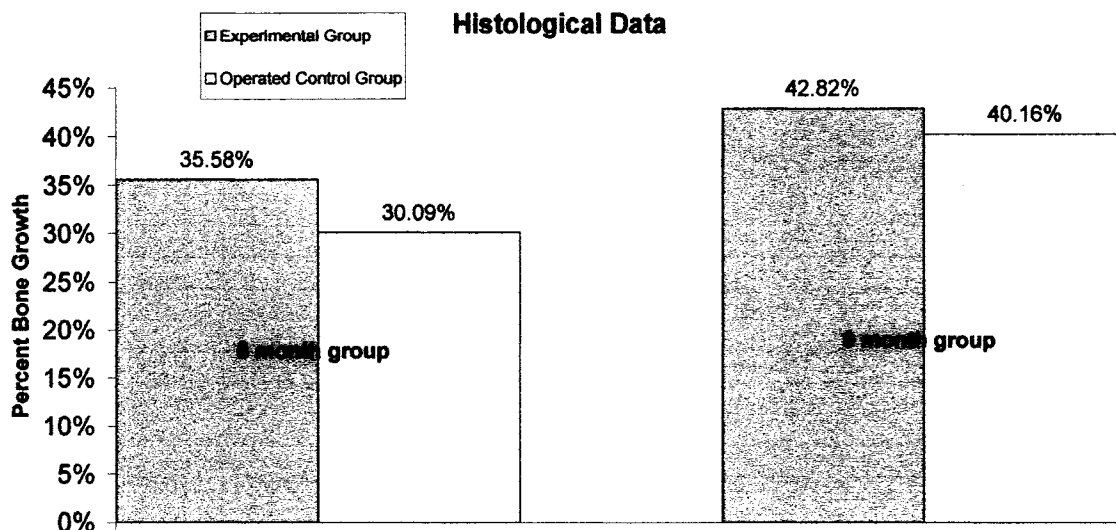


Figure 32. Histological data - percent bone growth.

Decalcified Histological Sectioning

Multiple slices were cut from each sample and stained with either Hematoxylin and Eosin or Safranin O. Hematoxylin is a basophilic dye, it binds to basic tissue components whereas Eosin is an acidophilic dye, and it binds to acidic tissue components. With H&E staining, nuclei stain blue to blue/black, collagen and skeletal muscle stain bright red, smooth muscle stain pink/red and red blood cells and fibrin stain bright red/orange. All photographs were taken with a light microscope at 4x magnification. The purpose of H&E staining was to provide a simple secondary method for determining the presence of bone. The purpose of Safranin O staining was to determine if residual cartilage remained in presence of the crawfish chitosan bone graft. Across all three groups (operated control, experimental and unoperated control) and time intervals, H&E staining was consistent with bone. None of the groups (operated control, experimental and unoperated control) at any time interval stained positive with Safranin O for

cartilage. Hematoxylin and Eosin stained three month slides are in Figures 33, 34 and 35, Safranin O stained specimens are in Figures 36, 37 and 38. Hematoxylin and Eosin stained six month slides are in Figures 39 and 40, Safranin O stained specimens are in Figures 41 and 42. Hematoxylin and Eosin stained nine month slides are in Figures 43, 44 and 45, Safranin O stained specimens are in Figures 46, 47 and 48.



Figure 33. Three mo. operated control (H&E, decal., 8L-1).

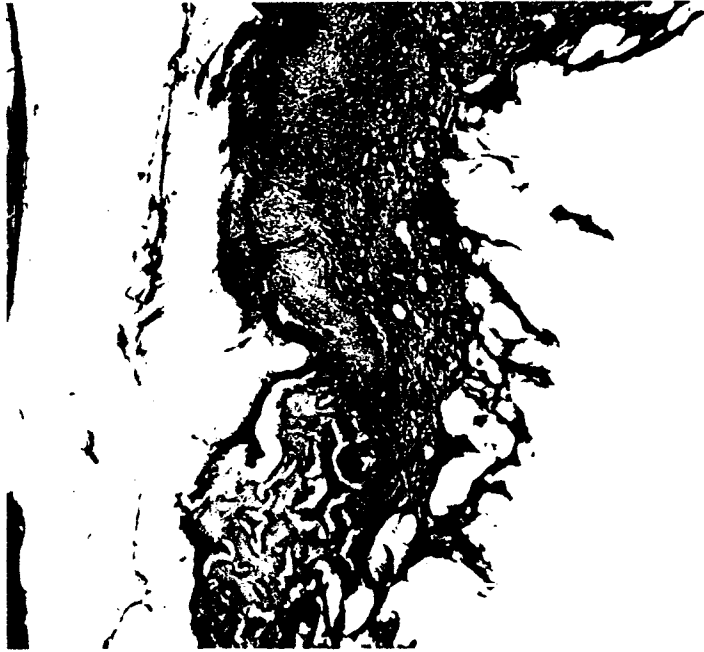


Figure 34. Three mo. experimental (H&E, decal., 11L-1).

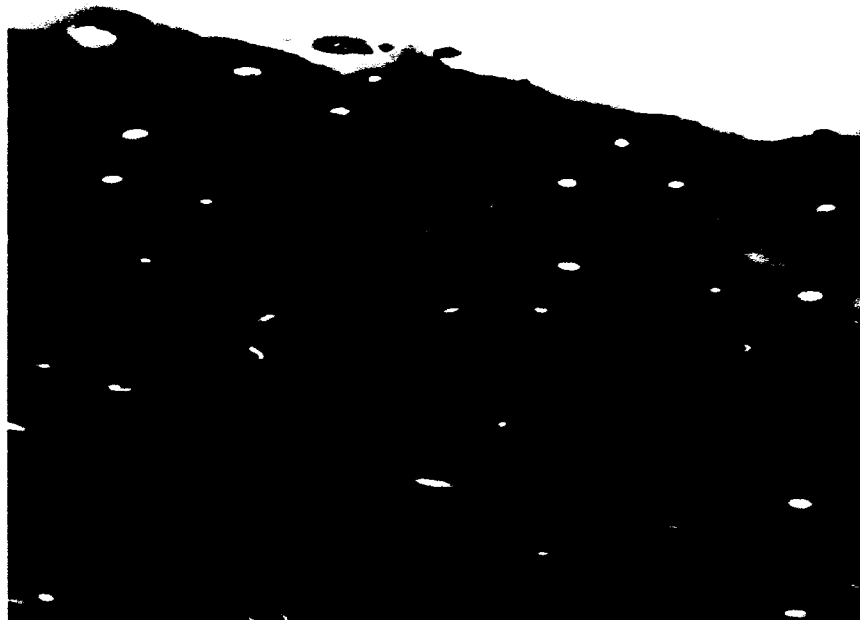


Figure 35. Three mo. unoperated control (H&E, decal., 3L-1).



Figure 36. Three mo. operated control (Safranin O, decal., 1L-2).

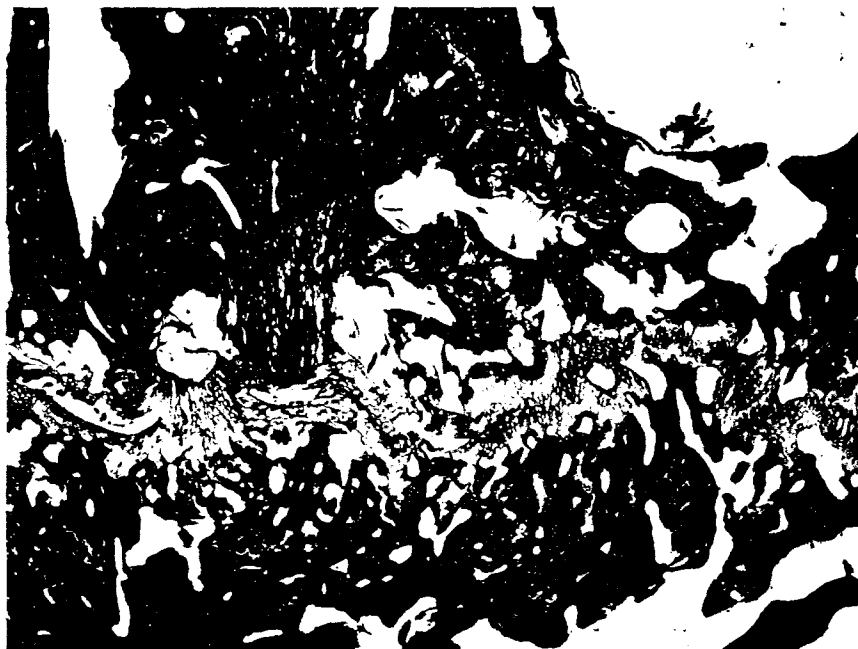


Figure 37. Three mo. experimental (Safranin O, decal., 10R-3).



Figure 38. Three mo. unoperated control (Safranin O, decal., 3L-2).



Figure 39. Six mo. operated control (H&E, decal., 6L-1).

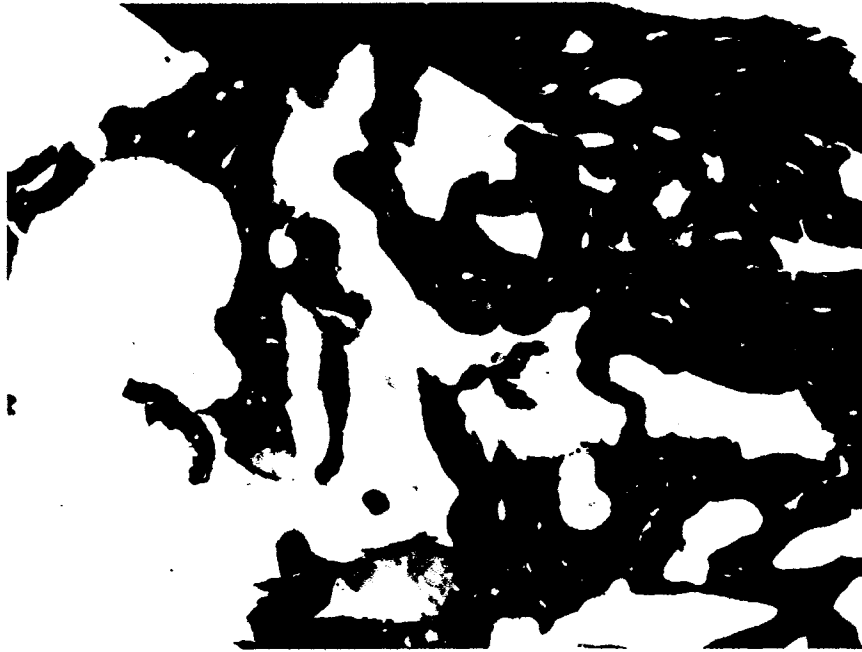


Figure 40. Six mo. experimental (H&E, decal., 14L-2).

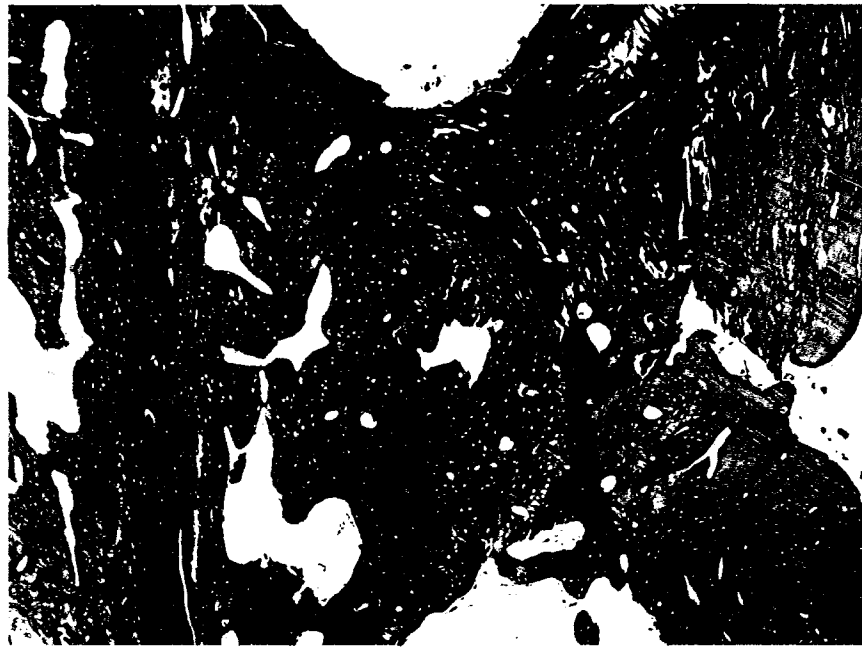


Figure 41. Six mo. operated control (Safranin O, decal., 4R-2).

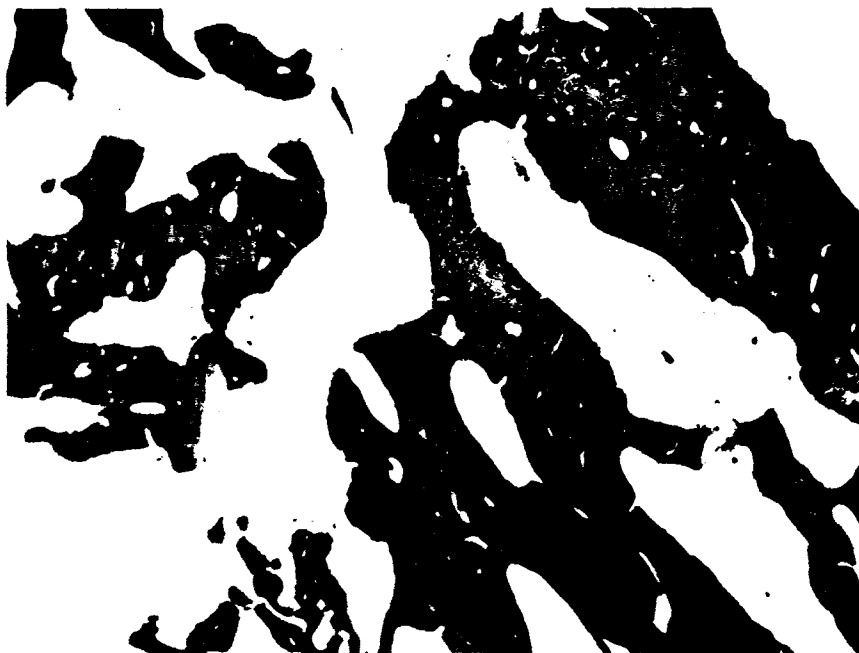


Figure 42. Six mo. experimental (Safranin O, decal., 14L-1).



Figure 43. Nine mo. operated control (H&E, decal., 20L-1).



Figure 44. Nine mo. experimental (H&E, decal., 18L-2).



Figure 45. Nine mo. unoperated control (H&E, decal., 20R-2).

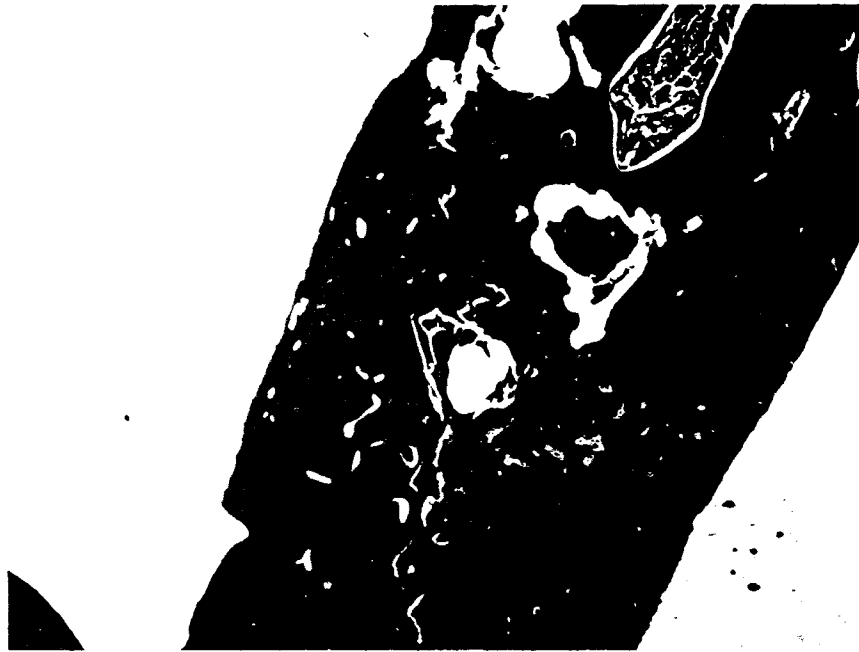


Figure 46. Nine mo. operated control (Safranin O, decal., 20L-3).

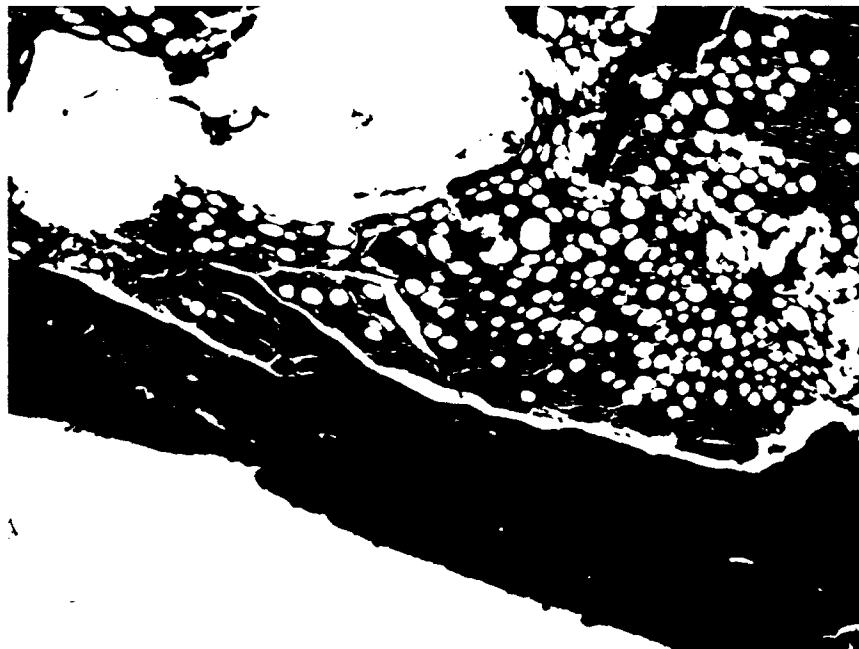


Figure 47. Nine mo. experimental (Safranin O, decal., 18L-3).

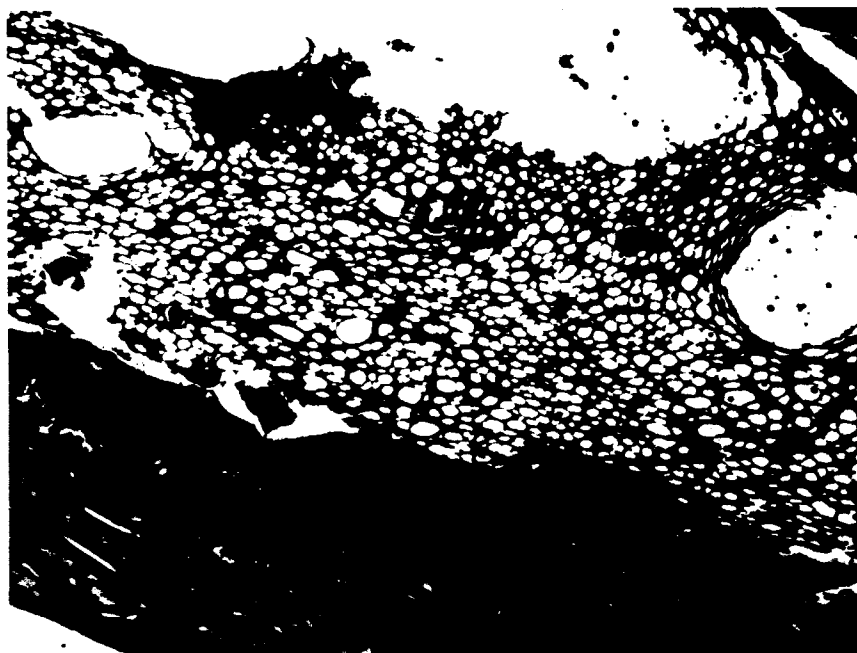


Figure 48. Nine mo. unoperated control (Safranin O, decal., 29L-2).

Post Harvest Analysis

Microcomputed Tomography

Microcomputed tomography was performed on a MicroCAT II; model MCII-UAAI following standard operating procedure. Each femur, along with the contra-lateral side, was run for 512 scans along defect site. This data was compiled into 2-D and 3-D images.

Six Month. In the six month operated control group, defect was still visible (Figure 49 & 50) and bone underwent deformed repair (Figure 49). In Figure 50, denser cortical bone is lining the defect, thereby preventing formation of the intermedullary canal and halting further repair processes. In the experimental six month group, repair is significantly improved compared to the operated control group during the same time interval. The intermedullary canal is continuous throughout the femur. Defect site has a slight defect in cortical bone on ventral

surface. Figures 51 and 52 show defects which slightly impede the intermedullary canal. In the three dimensional rendering (Figure 53), the dorsal plane of the defect is completely healed and undistinguishable from surrounding bone. Figure 54 demonstrates an undefected femur at this time interval.

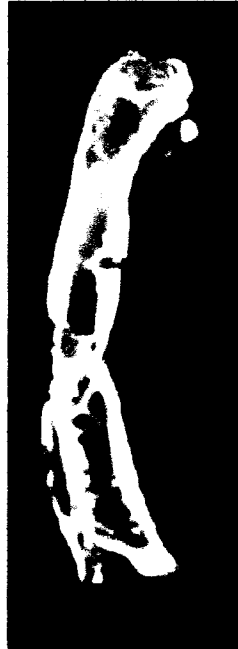


Figure 49. Six mo. Rat 6 operated control (single slice) - μ CT.

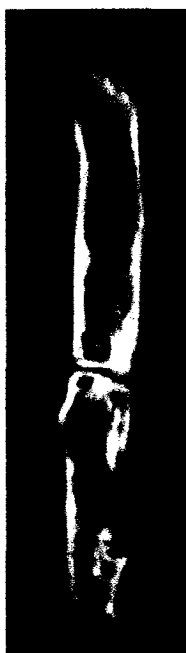


Figure 50. Six mo. Rat 6 operated control (single slice) - μ CT.



Figure 51. Six mo. Rat 14 experimental (single slice) - μ CT.



Figure 52. Six mo. Rat 14 experimental (single slice) - μ CT.

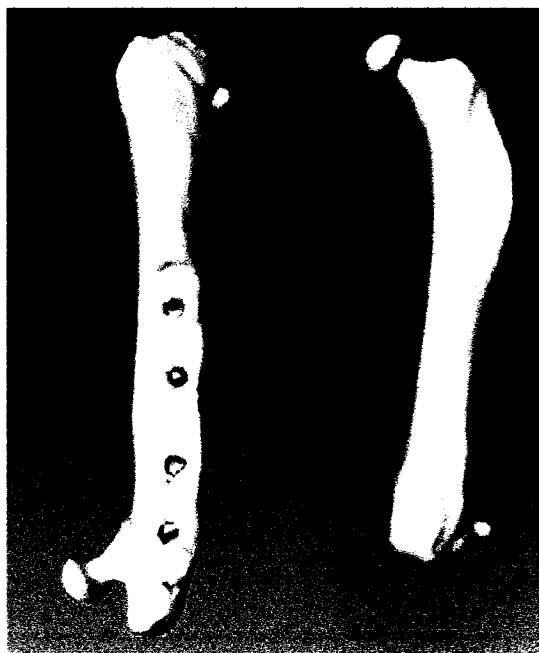


Figure 53. Six mo. Rat 14 experimental (3-D) - μ CT.

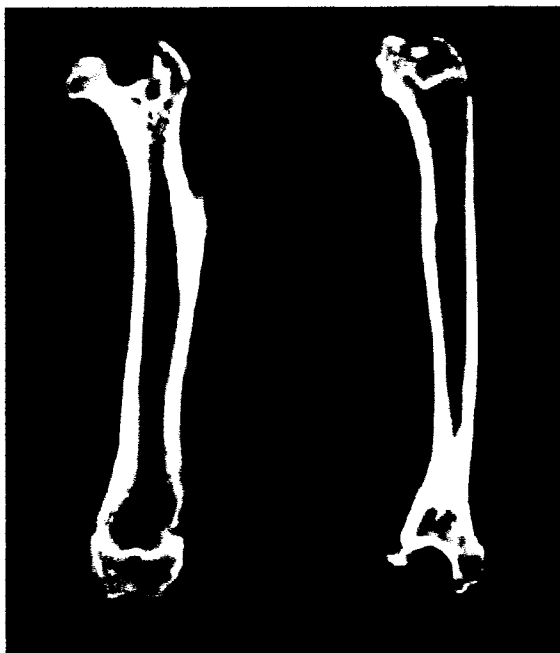


Figure 54. Six mo. Rat 24 unoperated control (single slice) - μ CT.

Nine Month. In the nine month operated control group, cortical bone defined edges of the defect (Figure 55) and prevented complete repair of the intermedullary canal. In Figures 55, 56 and 57, lack of repair is visually definable. In the nine month experimental group, repair is essentially complete with only small amounts of defects present. The intermedullary canal is virtually complete (Figure 58) and three dimensional rendering shows lack of a visually apparent defect (Figure 59) and presence of a complete intermedullary canal (Figure 60). Figures 61 and 62 show unaltered nine month femurs.

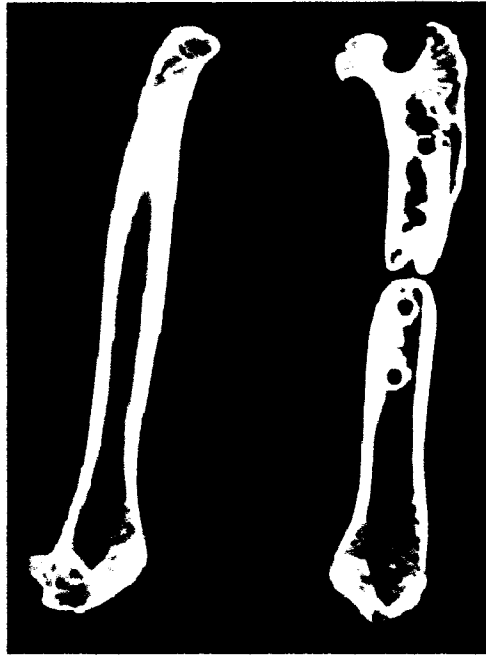


Figure 55. Nine mo. Rat 19 operated control (single slice) - μ CT.



Figure 56. Nine mo. Rat 19 operated control (3-D) - μ CT.

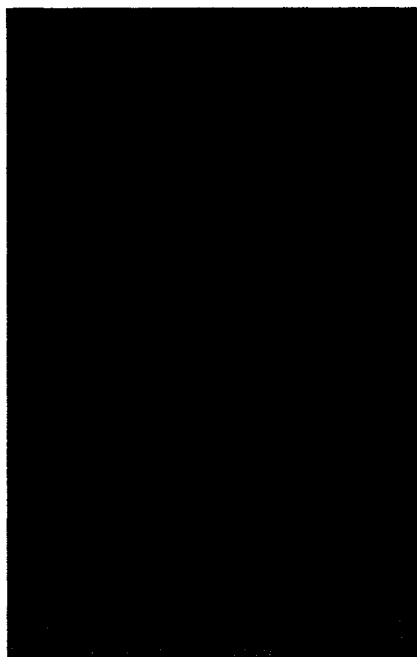


Figure 57. Nine mo. Rat 19 operated control (3-D) - μ CT.



Figure 58. Nine mo. Rat 18 experimental (single slice) - μ CT.



Figure 59. Nine mo. Rat 18 experimental (3-D) - μ CT.



Figure 60. Nine mo. Rat 18 experimental (3-D) - μ CT.



Figure 61. Nine mo. Rat 28 unoperated control (3-D) - μ CT.

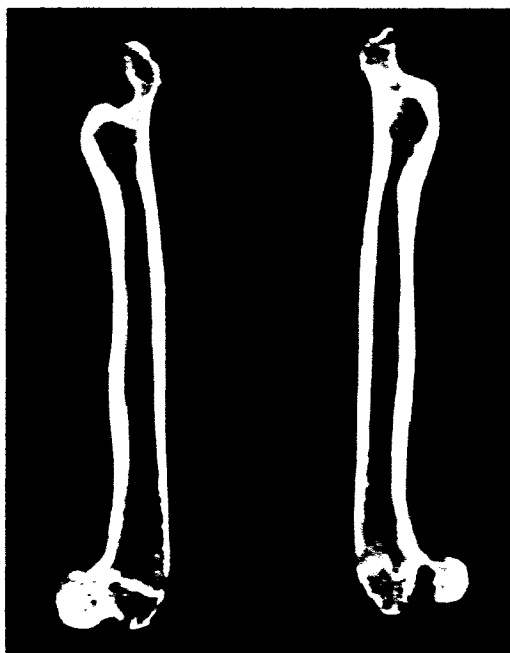


Figure 62. Nine mo. Rat 28 unoperated control (single slice) - μ CT.

Mechanical Testing

Mechanical testing was performed to compare stiffnesses and fracture loads between the groups and time intervals. Due to the small nature of the samples, a custom four point bending apparatus was designed to distribute load over the sample length (Figure 11). The results are compiled in Figure 67 and Table 7.

Six Month. Figures 63, 64 and 65 illustrate bending moment versus displacement for the six month group. All four point bending tests were carried out to failure. Sample size and load data was used to calculate bending moment.

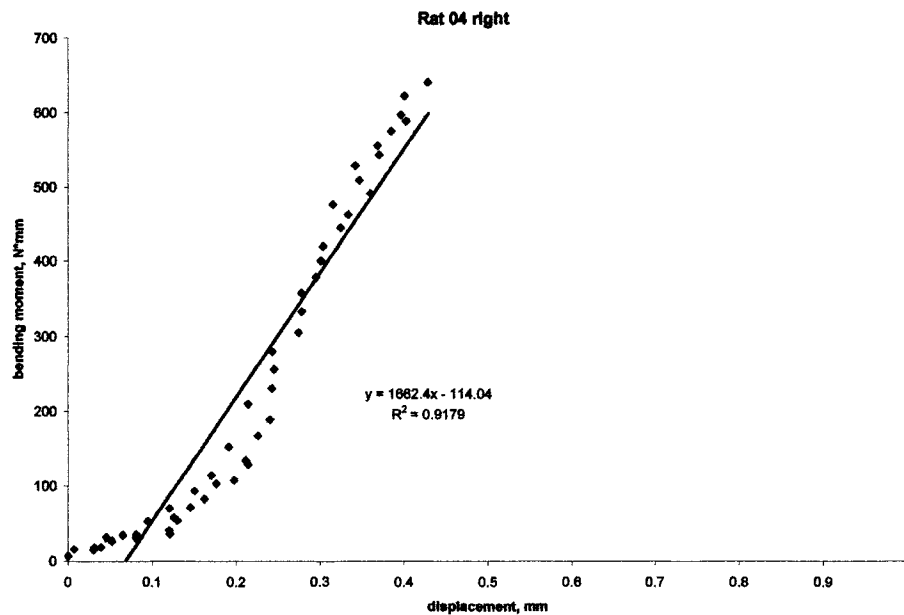


Figure 63. Six mo. Rat 04 right operated control - 4-point bending.

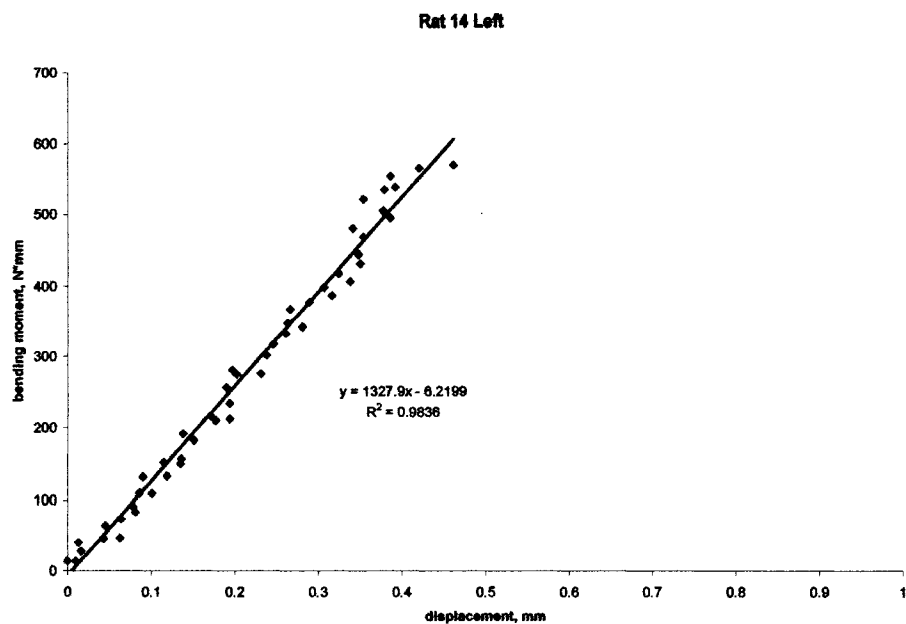


Figure 64. Six mo. Rat 14 left experimental - 4-point bending.

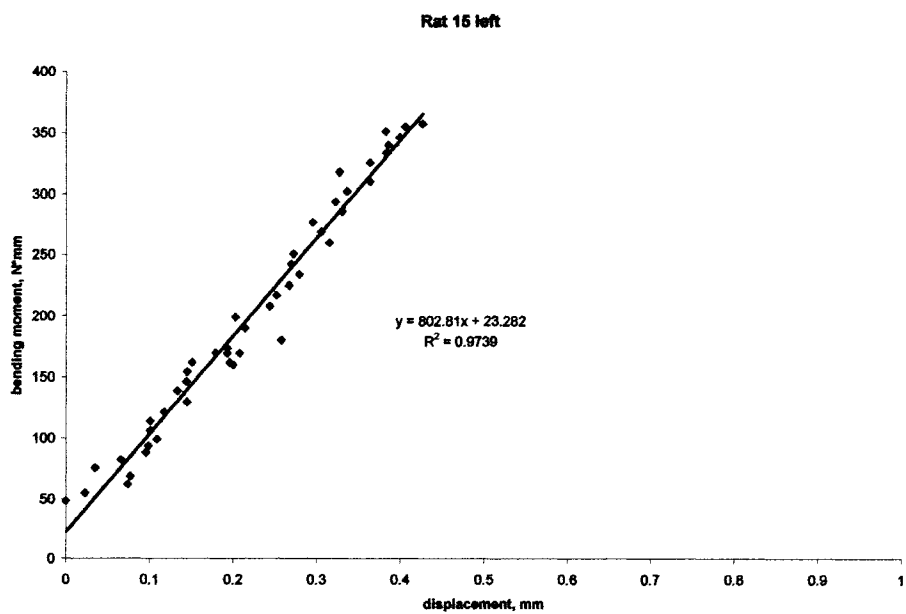


Figure 65. Six mo. Rat 15 left experimental - 4-point bending.

Nine Month. Figure 66 illustrates bending moment versus displacement for the nine month group. All four point bending tests were carried out to failure. Sample size and load data was used to calculate bending moment.

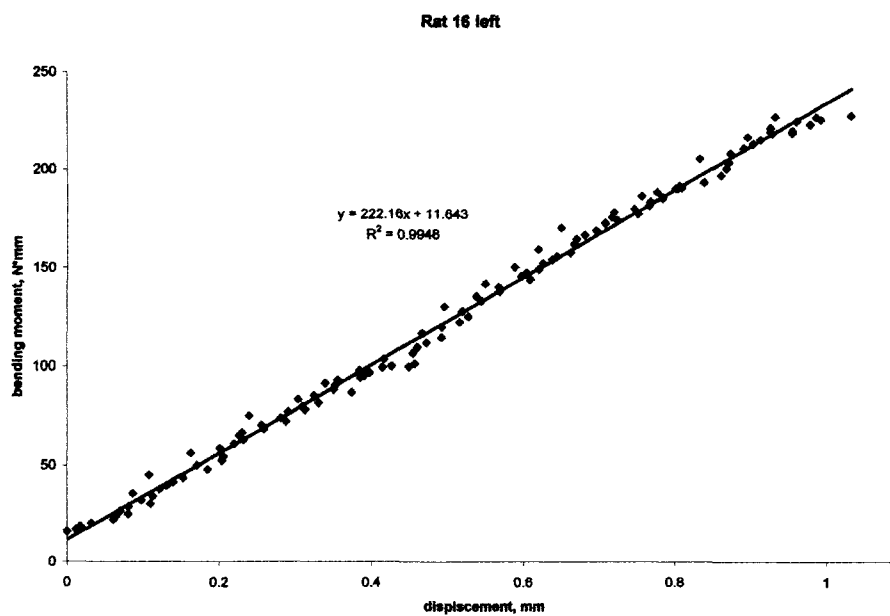


Figure 66. Nine mo. Rat 16 left experimental - 4-point bending.

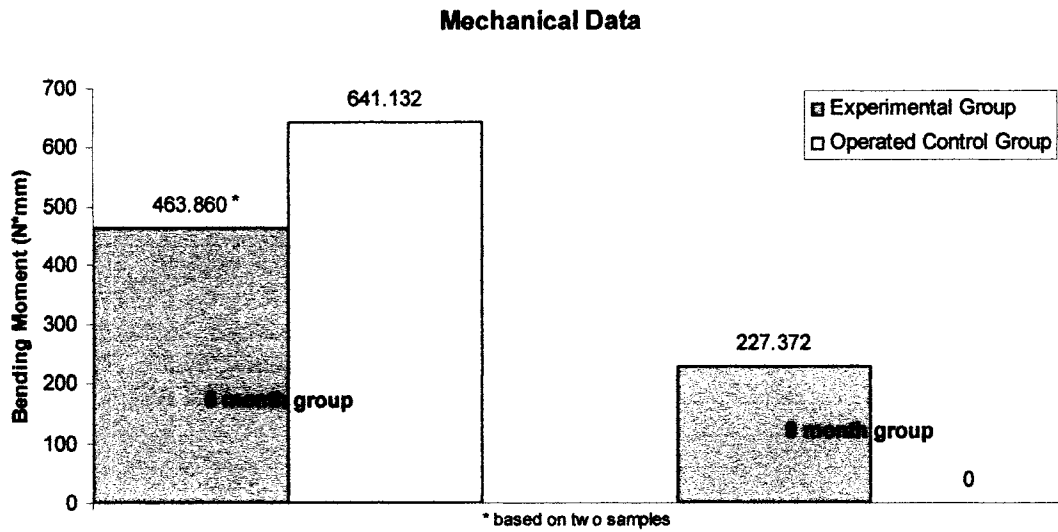


Figure 67. Mechanical data - bending moments at failure.

Table 7. Stiffness, bending moment and displacement.

Sample ID	Month	Description	Stiffness ((N*mm)/mm)	Bending moment (N*mm)	Displacement (mm)
Rat 4	Six	Operated control group	1662.400	641.132	0.429
Rat 14	Six	Experimental group	1327.900	570.332	0.461
Rat 15	Six	Experimental group	802.810	357.388	0.426
Rat 16	Nine	Experimental group	222.160	227.372	1.032
Rat 19	Nine	Operated control	defect filled with fibrous growth		

CHAPTER 4

DISCUSSION

Characterization

The purpose of crawfish chitosan characterization is to create a “fingerprint”, a series of test results that describe the chemical and physical composition of the compound. The importance of chemical fingerprinting is to identify crawfish chitosan from patented procedure [104] from other types of chitosan. In order to distinguish crawfish chitosan from non-chitosan product, “fingerprinting” tests are run on known chitosan samples in parallel with crawfish chitosan and similarities are noted. Determining exact functional groups associated with peak location is beyond the scope of this project. Noting similarities between crawfish chitosan (extracted using patented procedure [104]) and a control not only defines crawfish chitosan’s individuality, it also determines whether or not chitosan is present.

Fourier Transform Infrared Spectroscopy

Fourier transform infrared spectroscopy (FTIR) passes a known wavelength of infrared light through a sample and records the amount of energy absorbed by the molecule. In this experiment, crawfish chitosan, chitosan monomer and industrial chitosan were run on Fourier transform infrared

spectroscopy to determine the presence of similar chemical groups. Similar peaks were found at 3628 cm^{-1} , 2344 cm^{-1} , 1654 cm^{-1} and 1089 cm^{-1} . From this data, the presence of similar chemical groups can be ascertained. The peak located at 3628 cm^{-1} is associated with hydroxyl groups. The peak located at 2344 cm^{-1} is associated with solid phase amine groups. The peak at 1654 cm^{-1} is associated with the deformation vibration of primary amine groups and the peak at 1089 cm^{-1} is associated with CH-OH bonding.

Nuclear Magnetic Resonance Spectroscopy

Nuclear magnetic resonance spectroscopy (NMR) aligns protons with intrinsic magnetic moments with a powerful external magnetic field and perturbs the alignment using an electromagnetic field. The perturbations are measured and recorded. Each chemical group perturbs differently depending on composition (i.e. chemicals involved and bond types). From similar perturbations (peak locations) we can ascertain the presence of similar chemical groups.

To determine exact location of a peak, the corresponding peak centerpoint location was found on the x-axis. This distance was measured to the nearest whole number. Comparison of chitosan glutamate, crawfish chitosan and chitosan monomer, through NMR analysis, displayed the presence of three similar peaks (i.e. three similar chemical groups). The peak at zero is a control used to determine the location of zero parts per million, and the peak around four is deuterated (heavy) water (water containing deuterium atoms instead of hydrogen, deuterium is twice as heavy as hydrogen because it contains an additional neutron). Similar peaks were found 0.235 inches to the right of one

part per million, 0.149 inches to the right of two parts per million, 0.070 inches to the right of three parts per million, and 0.050 inches to the left of four parts per million (Figure 13). The common peak locations define the presence of chemical groups similar among the three different types of chitosan tested (crawfish chitosan, chitosan glutamate and chitosan monomer). The peaks located 0.235 inches to the right of one part per million and 0.070 inches to the right of three parts per million are associated with amine groups. The peak located at 0.149 inches to the right of two parts per million is associated with hydroxyl groups.

Differential Scanning Calorimetry

In differential scanning calorimetry (DSC), differences in amount of heat required to increase the temperature of a sample and a reference are measured as a function of temperature. During melting, more heat is flowing to the sample, this is an endothermic reaction. During crystallization, less heat is required to raise the temperature (less heat is flowing to the sample), this is an exothermic reaction. DSC measures the amount of energy absorbed or released. Lack of well defined peaks (crystallization) or troughs (melting) defines an amorphous polymer. Amorphous biopolymers degrade quicker than crystalline polymers and more completely, in addition the structure is more uniform and properties are more predictable.

Differential scanning calorimetry was performed on crawfish chitosan and a control (empty pan) to determine lack of crystalline form (for comparison, industrial chitosan was also run). Results demonstrated that crawfish chitosan appears amorphous due to the lack of peaks and troughs in the crawfish chitosan

DSC spectra, compared to industrial chitosan which undergoes several cycles of melting and crystallization.

Experimental Design

Experimental design consisted of an experimental group, an operated control group and an unoperated control group. The experimental group consisted of animals with a plated femur, critical sized defect and crawfish chitosan bone graft paste. The operated control group consisted of animals with a plated femur and a critical sized defect (no crawfish chitosan bone graft paste). The unoperated control group contained animals that did not undergo any surgical procedure. An unoperated control group was necessary, as opposed to obtaining undefected bone data from contra-lateral femurs, because surgical conditions dispose the animal to preferential leg treatment thereby tainting the unoperated control results. In addition to the groups listed above, a sham group should have been included. A sham group (plated bone with no critical defect) would have provided data regarding the effect of the plate on the femur and animal bias, due to surgery the animal will preferentially use their contra-lateral leg.

Each group consisted of three animals across three time periods. The number of animals in each group is described in the table two. Following the current study, surgeries were performed on an additional ten animals as part of an ongoing study (Appendix E) in an attempt to increase sample size and obtain more sophisticated test results. These additional femurs were harvested following a three month repair period and sent to the Materials Science

Department at Massachusetts Institute of Technology (MIT) for nano-indentation testing and backscatter electron microscopy.

Discrepancies in mechanical data are probably due to small sample size. Most of the mechanical data was based off of one sample thereby negating the ability to perform statistical analysis. The number of animals used was dictated by lack of funding for this project. With adequate funding, sample size can be increased and statistical analysis could be preformed thereby possibly providing more accurate results. This was a preliminary study to determine the efficacy of crawfish chitosan as a cell delivery vehicle. The small sample size could have possibly provided inaccurate results regarding bone growth. As a preliminary study, the results provided are sufficient to instigate additional studies to find out the exact role of crawfish chitosan in bone defect repair.

Gross Anatomy

In the six month group, profound visualizations can be made due to deformities present in the operated control femur. Operated control femurs appeared to have a high amount of fibrous tissue along with a deformed anatomy (Figure 68). Fibrous tissue caused bone discoloration.

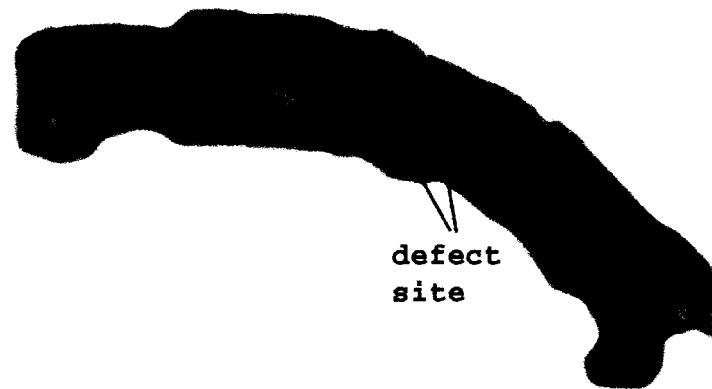


Figure 68. Deformed femur, six month operated control group (5L).

Experimental femurs, six month group, displayed appropriate morphology with presence of a slight defect along the ventral femoral surface. Upon plate removal, experimental femurs displayed rigidity and structural soundness compared to operated control femurs which displayed flexibility at the defect site. In the nine month group, experimental femurs visually demonstrated complete repair with no signs of defects present. Operated control femurs exhibited fibrous growth throughout the defect site. Upon plate removal, experimental femurs showed complete repair and inflexibility whereas operated control femurs demonstrated severe flexibility and lack of structural soundness. All plated femurs demonstrated flattened morphology, at plate location, due to plate presence. On some femurs bone began to slightly encompass the plate on the proximal portion. Since mechanostimulation promotes bone growth, change in load distribution due to the plate, along with angle at which a rat's leg naturally splays is a probable cause (Figure 69).



Figure 69. Lewis rat skeleton.

After surgery, rats gain weight due to lack of significant movement and therefore have less space for movement. This lack of significant movement reduces mechanostimulation on all loaded skeletal structures. Since repair processes strive under loaded conditions and these lethargic animals presented reduced loaded conditions, bone growth decreased from the three month group to the nine month group. Mechanostimulation is an important part of bone growth and repair. During all time intervals, animals were confined to cages 10.5" W x 19" L x 8" H (Allentown Caging Equipment, Inc., Allentown, N.J.) (Figure 70), physical activity was negligible and feed intake was constant (free choice). Reduced physical activity led to decreased mechanostimulation which led to weakened repaired bone [166,167].

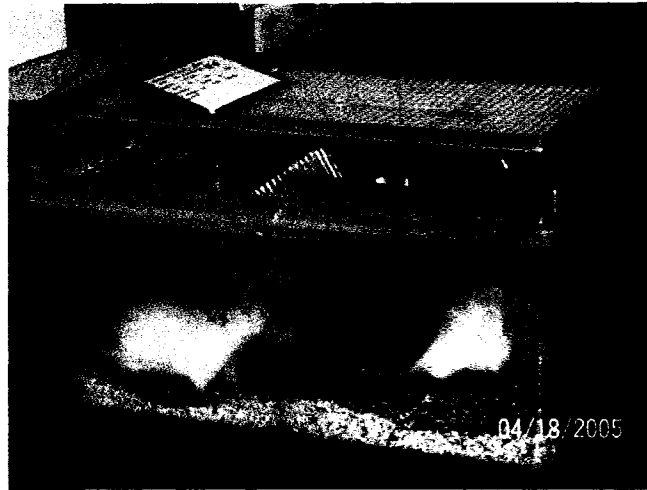


Figure 70. Rat housing.

Undecalcified Histological Sectioning

During each time interval (three, six and nine months) repair occurred faster in experimental groups compared to operated control groups. Repair, in the experimental group, lacked fibrous tissue and, histologically, appeared to consist primarily of cortical bone. In comparison, operated control samples demonstrated repair with a relative high concentration of voids and fibrous tissue. Defects were present, in operated control femurs, after nine months of repair time.

Slide color variation is due to specimen thickness, whereby more tissue is stained. General colors are the same with slight shade variation. Exact duplication in slide thickness was attempted but not always achieved. The process of grinding resin embedded specimens to exact thickness consisted of periodically removing the slide from the grinder and measuring thickness with a micrometer and either replacing the slide onto the grinder or removing it for staining.

Histological analysis demonstrated presence of bone. Mechanical analysis demonstrated decreased strength probably due to decreased mechanostimulation. Jarvinen et al. [166] and Umeruma et al. [167] described minimodeling caused by mechanostimulation. Minimodeling is growth/repair initiated by mechanostimulation which influences alignment and thickness of trabeculae. Minimodeling does not affect external bone dimensions.

Six Month

Six month undecalcified histological operated control sections displayed significant fibrous growth at defect site. Tissue juxtaposed to defect site was highly infiltrated with fibrous tissue (Figure 22). Analysis of later sections revealed fibrous tissue decreased to area in defect site. Six month experimental histological sections displayed superior growth compared to the operated control samples. Repaired bone tissue displayed continuous growth although large voids, white spaces, were noticed (Figure 23).

Six month experimental histological sections showed improved repair compared to operated control samples. While voids were present in experimental samples, operated control samples had complete defects present.

Nine Month

Nine month undecalcified operated control sections displayed a high relative percentage of fibrous tissue in the defect site. Unlike the six month group, fibrous tissue was juxtaposed to cortical bone. In nine month undecalcified experimental sections, defects were only slightly present with no

signs of fibrous tissue or voids. All defects, in experimental femurs, were repaired with, histologically, cortical bone.

Nine month experimental group demonstrated a relative higher percentage of bone compared to operated control femurs from the same time period.

Decalcified Histological Sectioning

Bone repair occurs by endochondral ossification, whereby mesenchymal cells differentiate into chondrocytes which form scaffolding for osteoblasts and mineral deposition. Chitosan is described in several published papers [1, 61, 62, 70, 83] as a successful biomaterial in cartilage tissue engineering. Specimens were stained with Safranin O staining to determine presence of residual cartilage remaining from the crawfish chitosan bone graft repair process. Both groups (operated control and experimental) tested negative for the presence of residual cartilage which implies that the crawfish chitosan bone graft does not cause residual cartilage formation, although results may have been different if samples were observed at shorter time intervals.

Hematoxylin and Eosin (H&E) is a general stain. For this experiment, H&E was used as a secondary detector of bone; undecalcified Goldner's Trichrome sections were primary. After comparing stained slides, H&E and Goldner's Trichrome, from the operated control and experimental groups to slides from the unoperated control groups, presence of bone was verified. All experimental samples displayed bone at defect sites, in varying degrees, while

operated control samples displayed fibrous tissue, histologically, during all time intervals.

Post Harvest Analysis

Four-Point Bending

In Table 7, values of bending moments at failure are listed. Values are higher at six months and lower at nine months. This trend is opposite what we would expect. According to Umemura et al. [167] and Järvinen et al. [166] loading results increase bone strength but not bone size. According to Järvinen et al. [166] loading (exercise) for 20 minutes a day / five days a week for nine weeks causes mini-modeling in bone, which is a change in the alignment of trabeculae without changing bone dimensions or adding bone minerals. Loading created more dense trabeculae, thereby creating stronger bones. The decreased bending moment for failure at nine months is probably a consequence of lack of loading caused by a confining environment and a constant food supply which led to a lethargic lifestyle. Another possible explanation for the decrease is natural aging. The average lifespan of a male Lewis rat is approximately two years. The animals were two months old pre-surgery and, in the case of the longest group, kept until they were approximately 11 months old. Bones heal more rapidly in juveniles compared to adults. At the inception of this project, the animals were juveniles and at the conclusion of the study they were mature adults.

Microcomputed Tomography

Microcomputed tomography (μ CT) is a series of x-ray images compiled together into a three dimensional image. Individual slices are available for viewing as well as three dimensional images. Microcomputed tomography images of the bone graft site displayed progressive repair in experimental samples compared to operated control femurs, which displayed a complete defect throughout all time periods. Operated control femurs, across all time intervals, displayed similar characteristics. All operated control samples had incomplete intermedullary canals, defect presence (appropriate for a critical sized defect) and dense tissue growth over bone ends at defect site. Likewise, experimental samples displayed similar characteristics across all time intervals. All experimental samples had a slight surface defect present (although size decreased as time progressed) and intermedullary canal was continuous throughout entire femoral length. Microcomputed tomography provided a non-destructive technique to view internal composition without compromising sample integrity. Non-destructive microcomputed tomography testing allowed femurs to undergo additional testing, thus maximizing the quantity of data per sample.

Conclusion

The objective of this study was to extract, characterize and evaluate chitosan made from crawfish shells [104] in a critical size defect model [4,141] in rats as a synthetic bone graft material. The composite of this purified chitosan and calcium sulfate, in a paste form, was successfully used as a delivery system

for osteoblasts and the results confirmed our hypothesis that such a system promotes bone growth.

The specific conclusions were:

1. The physical characterization by Fourier transform infrared spectroscopy (FTIR) of purified crawfish chitosan showed similar characteristics to that of a commercially pure and medical grade chitosan glutamate.
2. Differential scanning calorimetry (DSC) confirmed the amorphous nature of chitosan made from crawfish shells using Dr. Debi Mukherjee's patented procedure.
3. Chemical characterization by nuclear magnetic resonance spectroscopy (NMR), when benchmarked against chitosan glutamate and chitosan monomer, showed remarkable similarity.
4. The animal evaluations of the composite paste for three, six & nine months examined by histology (undecalcified and decalcified), and microCT (μ CT) demonstrated a high degree of bone ingrowth for the experimental group as compared to samples in the operated control group (defected and repaired without paste).
5. The use of μ CT as a non-destructive tool to follow bone ingrowth was found to be very valuable. Although we used this technique mainly for qualitative purpose the data can be digitized to make more quantitative predictions.
6. Four point bending data at six months was somewhat anomalous, which may be due to small sample size and loss of strength due to lack of

activity as the rats gained weight. In the nine month group, experimental bending stiffness and failure load was higher compared to operated control samples, defects in the operated control femurs were filled with fibrous tissue and therefore could not be tested.

In this study, chitosan was extracted from crawfish shells, combined with plaster of Paris and cultured osteoblasts and used as a synthetic bone graft in a critical sized defect model. In addition to the novel method used for chitosan extraction from crawfish shells, this research demonstrates chitosan's successful use as a cell delivery system.

Future Work

This preliminary study has great potential provided proper follow-up experiments are preformed. One possible experiment is comparing crawfish chitosan bone graft against a bone graft containing all components, except crawfish chitosan (i.e. the graft would contain plaster of Paris and osteoblasts). This would give a better description of the exact role of crawfish chitosan. In addition, more animals should be included to decrease biological variability and provide a basis for statistical analysis. A sham group (plate is attached to the femur but no defect is made) should be included. A sham group removes biological variability due to the plate by recording effects of the plate on the femur as well as effects of animal bias on the femur, as the animal will preferentially use the contra-lateral leg over the operated one. This data can be compared to the experimental groups to better define the role of crawfish chitosan. In Table 8 is an experimental design for a future study, based on identical analysis to the

current study being performed. In defected bone, repair should be complete within six months (unless a non-union has occurred); based on this the proposed study should only be carried out for six months. Since the purpose of this study is development of a bone graft that is osteoconductive, osteoinductive and osteogenic in a critical defect, the final graft repair is most important. Each group, excluding the unoperated control group, consists of 30 male Lewis rats. This provides 10 animals for each of the three destructive testing methods currently being used, decalcified histology sections, undecalcified histology sections and mechanical testing (all samples should undergo microcomputed tomography). The unoperated control group consists of 18 animals, six of each of the testing methods. The unoperated control animals will provide baseline data, therefore fewer animals are needed. Six animals in each testing group are enough to perform statistical analysis.

Prior to graft implantation, but post graft creation, osteoblast viability should be determined. This can be accomplished by a live-dead count on a hemocytometer. A count would provide the actual number of viable cells being used in the graft as well as reconfirm the non-toxicity of graft components. Osteoblasts are the components that are hypothesized to play an integral role in providing the crawfish chitosan bone graft with osteogenic properties. In order for the results to be as accurate as possible, osteoblast viability should be noted so any differences can be taken into account. This data would be useful as a possible source of discrepancies among post harvest results.

The characterization of crawfish chitosan is important because it defines a “fingerprint” that signifies the presence of crawfish chitosan. Further analysis should be performed to clearly define the location of specific molecular groups associated with specific peaks. To aid in fingerprinting, crawfish chitin should be tested along with crawfish chitosan. This will aid characterization by demonstrating the removal of acetyl groups as well as reconfirming the relationship between crawfish chitin and crawfish chitosan (i.e. does deacetylation do more than remove an acetyl group?).

In the current study, it is recommended to generate better mechanical data by using a more sophisticated technique and increase the number of animals. With this in mind an additional six rats with necessary controls were studied for three months. The animals were sacrificed and femurs were sent to the Biomaterials Laboratory at Massachusetts Institute of Technology (MIT) for nanoindentation testing and backscatter electron microscopy. The details are shown in the Appendix E. Table eight describes a possible future study.

Table 8. Experimental design for a future study.

	Number of animals				
	Unoperated control group	Operated control group	Sham group	Experimental group 1	Experimental group 2
Group specifics	No surgery	Critical defect and crawfish chitosan bone graft paste	Plated femur	Critical defect with plaster of Paris and osteoblasts	Critical defect and crawfish chitosan bone graft paste
6 month	18	30	30	30	30

APPENDIX A

NUCLEAR MAGNETIC RESONANCE SPECTROSCOPY PROTOCOL

APPENDIX A

NUCLEAR MAGNETIC RESONANCE SPECTROSCOPY PROTOCOL

The nuclear magnetic resonance spectroscopy (NMRS) protocol includes a four hour incubation. To maximize time and ensure test completion in a timely fashion, deuterium chloride (DCI) and sodium deuterioxide (NaOD) were prepared 24 hours before test run. ^1H NMRS aligns ^1H molecules with an electromagnet and measures the amount of energy released when the molecule returns to its natural state. In order to prevent false readings, any reagents used in ^1H NMRS preparation that contain hydrogen are replaced with a deuterated version. The deuterated version is molecularly heavier as it contains an additional neutron and is recorded on the spectra in a different location.

The nuclear magnetic resonance spectroscopy protocol is listed below:

The day prior to testing a 20% DCI solution is prepared in a 0.1M solution and a 1M solution along with a 0.1M and 1M solution of NaOD, the diluent is deuterated water.

On the day of testing 33mg of crawfish chitosan was added to 3.3ml of D₂O. After two to three minutes, 250 μ l of 1M DCI is added to the crawfish chitosan mixture. After two to three minutes, 100 μ l of freshly made NaNO₂ is added. This mixture is allowed to sit in the dark for four hours at room temperature. During this incubation, 0.15M of the control, sodium 3-trimethylsilylpropionate-2,2',3,3'-d₄ (TMSP) is prepared. Following the incubation

period, the pH of the sample is checked and adjusted to between 3.8 and 4.2 using DCl and NaOD. Once the pH was adjusted, the solution was centrifuged to remove any large particulate matter. Following centrifugation, 700 μ l of the supernatant was placed into an NMR sample tube and 5 μ l TMS was added. The tubes were inverted to mix and run on the NMR using the following specifications:

Temperature: 90°C

Sample spinning: 20Hz

Number of scans: 64

Proton spectral width: 10ppm

Relaxation delay: 5s

Pulse angle: 90°

APPENDIX B

CELL CULTURE PROTOCOL

APPENDIX B

CELL CULTURE PROTOCOL

1. **Stromal osteoblastic cells were obtained from the bone marrow of male Lewis rats, approximately six months old and 200-250 grams.**
2. **Following euthanasia by carbon dioxide asphyxiation, femora were aseptically excised, cleaned of soft tissue, washed in Dulbecco's Modified Eagle's Medium (DMEM), Penicillin G Streptomycin (antibiotic) and Amphotericin B (antimycotic). Concentration of the antibiotic-antimycotic solution is ten times the normal amount that is used in the media for growing cells.**
3. **The metaphyseal ends were cut off and the bone marrow was flushed from the midshaft with five milliliters of media (DMEM + 10% fetal bovine serum (FBS) + antibiotic-antimycotic solution) using a sterile syringe and collected in a sterile test tube.**
4. **Cell clumps were broken by repeatedly pipetting the cell suspension.**
5. **The cell suspension was centrifuged at 1200 rpm for 10 minutes.**
6. **The cell pellet was resuspended in media (DMEM + 10% FBS + antibiotic-antimycotic solution + 10% Interleukin three) and seeded in a flask.**
7. **The following day, the media was removed and the cells were washed with a 10x concentration of antibiotic-antimycotic solution in phosphate buffered saline (PBS). New media (DMEM + 10% FBS + antibiotic-**

antimycotic solution + 10% Interleukin three) was put back into the flask.

8. The media was exchanged every two to three days until confluent then trypsinized.

APPENDIX C

GRAFT COMPONENTS

APPENDIX C

GRAFT COMPONENTS

Animal	Month	Calcium Sulfate (g)	Crawfish Chitosan (g)	Osteoblast Concentration (cells per ml)
10	3	0.5059	0.1250	2.60×10^5
11	3	0.5048	0.1249	1.98×10^5
12	3	0.5048	0.1249	2.28×10^5
13	6	0.5022	0.1244	2.78×10^5
14	6	0.5050	0.1234	2.65×10^5
15	6	0.5656	0.1243	2.05×10^5
16	9	0.5004	0.1246	1.98×10^5
17	9	0.5017	0.1240	2.40×10^5
18	9	0.5030	0.1247	1.90×10^5

APPENDIX D

SACRIFICE TIME TABLE

APPENDIX D

SACRIFICE TIME TABLE

		Surgery Date	6 months	9 months
Operated Control Group	Rat 4	4/20/2005	10/20/2005	
	Rat 5	4/21/2005	10/20/2005	
	Rat 6	4/21/2005	10/20/2005	
	Rat 7	4/22/2005		1/27/2006
	Rat 9	4/27/2005		2/8/2006
	Rat 19	5/5/2005		2/8/2006
	Rat 20	5/5/2005		2/8/2006
Experimental Group	Rat 13	4/28/2005	10/27/2005	
	Rat 14	4/28/2005	10/27/2005	
	Rat 15	4/28/2005	10/27/2005	
	Rat 16	4/29/2005		2/1/2006
	Rat 17	4/29/2005		2/1/2006
	Rat 18	4/29/2005		2/1/2006
	Unoperated Control Group	Rat 24		10/30/2005
Rat 25			10/30/2005	
Rat 26			10/30/2005	
Rat 27				2/7/2006
Rat 28				2/7/2006
Rat 29				2/7/2006

APPENDIX E

ADDITIONAL ANIMAL SAMPLES

APPENDIX E

ADDITIONAL ANIMAL SAMPLES

Following completion of the primary study, ten additional animals underwent surgery. Five of the additional animals were in an experimental group and the remaining were in an operated control group. Surgical methods were the same with animals in the experimental group receiving the crawfish chitosan paste and the operated control animals received no paste.

The purpose of the additional animals is to better characterize the graft with additional samples. The additional samples underwent microcomputer tomography (courtesy of Louisiana State University Health Sciences Center, Animal Resources, Shreveport, Louisiana) and were sent to the Biomaterials Laboratory at Massachusetts Institute of Technology for Backscatter Electron Microscopy and Nanoindentation. Results are pending.

APPENDIX F

**ANIMAL CARE AND USE INSTITUTIONAL REVIEW
BOARD FORM FROM LOUISIANA
STATE UNIVERSITY –
SHREVEPORT**



SCHOOL OF MEDICINE IN SHREVEPORT
Animal Care and Use Committee

Notice of Committee Action for ADDENDUM

Proposal Number: P-04-001

Title: Evaluation of a Chitosan and Plaster of Paris in a Segmental Bone Defect Model

Investigator: Dr. Debi Mukherjee/Orthopedics

This is to certify that the Animal Care and Use Committee has reviewed the above proposal on
November 16, 2004, at which time a quorum of the members was present.

Recommendations of this committee:

APPROVED

Jill Williams
Chairman, ACUC

11-17-04
Date

[Signature]
Director, Animal Resources

11-17-04
Date

Copies to: ACUC Coordinator's Office
Investigator
Grants Office

Section II. OVERVIEW AND RATIONALE OF STUDY:

- The following information is required to assist the committee with evaluating the appropriateness of the animal model and procedures to be used. All questions must be answered. Use additional pages if necessary. Abstracts from grant application forms are not acceptable. Be concise and respond in lay terms.

A. State the objective(s) of this protocol, significance, scientific merit, and what population this research will affect.

The objectives are:

1. To follow the time course 3, 6 & 9 months of healing of the rat femoral segmental bone defect filled with chitosan and Plaster of Paris composite paste and osteoblasts. The protocol of this fracture model was developed based on a 3-month pilot study (Protocol No. S-02-00) that was completed early this year. This paste is intended to be used as a synthetic bone graft substitute to repair bone defects in osteoarthritic patients.

2. To apply the new technique of microcomputer tomography (μ CT) to identify the development of bone in the segmental defect in the rat femur. This is a promising technique to quantify the changes in bone density and porosity. The Research Core Facility of LSUHSC is in the process of acquiring this instrument and it will be available to us on a fee basis in the near future.

3. To generate the safety and efficacy data of our chitosan paste for future Investigational Device Exemption (IDE) filing to Food and Drug Administration (FDA) which is needed before starting human clinical trials. This data will also increase the potential chances of licensing our chitosan patent (US 6,310, 188B1) to interested companies.

This research study is aimed towards the delivery of osteoblasts to treat osteoarthritis. Currently the annual US sales of bone graft substitute are \$50 million and growing substantially (JBJS, 2001 Supplement 2, 98-103). This study is pivotal to complete the FDA regulatory needs and product licensing for commercialization.

B. Give the rationale for using animals in this project, the justification of the animal model chosen, and a justification for the number of animals requested. (Be Specific)

The animal model was chosen based on the following papers:

1. Einhorn TA, Lane JM, Burstein AH, Kopman CB, and Vigorita VJ. "The healing of segmental defects induced by demineralized bone matrix". J. of Bone and Joint Surgery, 1984, 66-A, 274-279.
2. Wolff DW, Goldberg VM, and Stevenson S. "Histomorphometric analysis of the repair of a segmental diaphyseal defect with ceramic and titanium fiber metal implants: effects of bone marrow". J. Of Orthopaedic Research, 1994, 12 (3) 439-446.

There is no computer model to simulate the bone growth hence it needs animal experiments.

We will create a unilateral segmental defect of about 3 mm in a rat femur and fix the defect with a 4-hole titanium plate and four 2-mm screws following the protocol that we developed in our pilot study (S-02-00). In the first group the defects, in the rat femur will be fixed with a plate and screws and filled with chitosan paste. In the second group, the defect will be fixed with a plate and screws only without the paste. The third group would be the sham-operated control. We must have a minimum of 6 rats per group for analysis of statistical significance. For our time periods of 3, 6 & 9 months we would need 54 rats (3x6x3 =54). Additionally, we would also need a minimum of 6 rats to collect the bone marrow needed to expand the osteoblasts. Hence we are requesting for a total of 60 rats.

REFERENCES

1. **AdiMartino, M.S., and M. Risbud, Chitosan: A versatile biopolymer for orthopaedic tissue-engineering. *Biomaterials*, 2005. 26: p. 5983-5990.**
2. **Agnihotri, S., Aminabhavi, T., Controlled release of clozapine through chitosan microparticles prepared by a novel method. *Journal of Controlled Release*, 2004. 96: p. 245-259.**
3. **Alderman, N.E., Sterile Plaster of Paris as an implant in the infrabony environment: a preliminary study. *Journal of Periodontology*, 1969. 40(1): p. 11-13.**
4. **Anderson, M., Dhert, W., Bruijn, J., Dalmeijer, R., Leenders, H., van Blitterswijk, C., Verbout, A., Critical size defect in the goat O's ilium. *Clinical Orthopaedics and Related Research*, 1999. 364: p. 231-239.**
5. **Aubin, J.E., Triffitt, J.T., Mesenchymal Stem Cells and Osteoblast Differentiation, in Principles of Bone Biology, J.P. Bilezikian, Raisz, L.G., Rodan, G.A., Editor. 2002. p. 59-81.**
6. **Auerbach, B.L., The Structure of Chitin and Chitosan. *IEEE Ocean*, 1975: p. 454-456.**
7. **Azevedo, H.S., Gama, F.M., Reis, R.L., *In Vitro* Assessment of the Enzymatic Degradation of Several Starch Based Biomaterials. *Biomacromolecules*, 2003. 4: p. 1703-1712.**
8. **Barrack, R., Bone graft extenders, substitutes, and osteogenic proteins. *The Journal of Arthroplasty*, 2005. 20(4 Suppl. 2): p. 94-97.**
9. **Bauer, T.W., Muschler, G.F., Bone Graft Materials. *Clinical Orthopaedics and Related Research*, 2000. 371: p. 10-27.**
10. **Beppu, M.M., Santana, C.C., *In Vitro* Biomineralization of Chitosan. *Key Engineering Materials*, 2001. 192-195: p. 31-34.**
11. **Biagini, G., Muzzarelli, R.A.A., Giardino, R., Castaldini, C., Biological Materials for wound healing, in Advances in Chitin and Chitosan, P.A. Charles J. Brine, Sandford, John P. Zikakis, Editor. 1992, Elsevier. p. 16-24.**

12. Borah, G., Scott, G., Wortham, K., Bone Induction by Chitosan in Endochondral Bones of the Extremities, in *Advances in Chitin and Chitosan*, P.A. Charles J. Brine, Sandford, John P. Zikakis, Editor. 1992. p. 47-53.
13. Bucholz, R.W., Nonallograft Osteoconductive Bone Graft Substitutes. *Clinical Orthopaedics and Related Research*, 2002. 395: p. 44-52.
14. Bumgardner, J.D., Wiser, R., Gerard, P.D., Bergin, P., Chestnutt, B., Marini, M., Ramsey, V., Elder, S.H., Gilbert, J.A., Chitosan: potential use as a bioactive coating for orthopaedic and craniofacial/dental implants. *Journal of Biomaterials Polymer Edition*, 2003. 14(5): p. 423-438.
15. Burchardt, H., The biology of bone graft repair. *Clinical Orthopaedics and Related Research*, 1983. 174: p. 28-42.
16. Burg, K., Porter, S., Kellam, J., Biological developments for bone tissue engineering. *Biomaterials*, 2000. 21: p. 2347-2359.
17. Cardenas, G., Miranda, S.P., FTIR and TGA Studies of Chitosan Composite Films. *Journal of the Chilean Chemical Society*, 2004. 49(4): p. 291-295.
18. Carraher, C., Natural Functional Condensation Polymer Feedstocks, in *Functional Condensation Polymers*, C. Carraher, Swift, G., Editor. 2002. p. 151-183.
19. Cervera, M.F., Hienamaki, J., Krogars, K., Jorgensen, A.C., Karjalainen, M., Colarte, A.I., Yliruusi, J., Solid-State and Mechanical Properties of Aqueous Chitosan-Amylose Starch Films Plasticized with Polyols. *AAPS PharmSciTech*, 2004. 5(1): p. 1-6.
20. Chandy, T., Sharma, C.P., Chitosan as a Biomaterial. *Biomaterials, Artificial Cells and Artificial Organs*, 1990. 18(1): p. 1-24.
21. Chaussard, G., Domard, A., New Aspects of the Extraction of Chitin from Squid Pens. *Biomacromolecules*, 2004. 5: p. 559-564.
22. Chen, Y., Chung, Y., Wang, L., Chen, K., Li, S., Antibacterial Properties of Chitosan in Waterborne Pathogens. *Journal of Environmental Science and Health*, 2002. A37(7): p. 1379-1390.
23. Chevrier, A., Hoemann, C.D., Sun, J., Buschmann, M.D., In Situ Solidifying Chitosan-GP/Blood Implants Promote Intramembranous Bone Formation in Microdrilled Chondral Defects of Adult Rabbits, in 51st Annual Meeting of the Orthopaedic Research Society. 2005.

24. Chirkov, S., The antiviral activity of chitosan (Review). *Applied Biochemistry and Microbiology*, 2002. 38(1): p. 1-8.
25. Cho, B.C., Park, J.W., Baik, B.S., Kwon, I.C., Kim, I.S., The Role of Hyaluronic Acid, Chitosan, and Calcium Sulfate and Their Combined Effect on Early Bony Consolidation on Distraction Osteogenesis of a Canine Model. *The Journal of Craniofacial Surgery*, 2002. 13(6): p. 783-793.
26. Cho, B.C., Kim, T.G., Yang, J.D., Chung, H.Y., Park, J.W., Kwon, I.C., Roh, K.H., Chung, H.S., Lee, D.S., Park, N.U., Kim, I.S., Effect of Calcium Sulfate-Chitosan Composite Pellet on Bone Formation in Bone Defect. *The Journal of Craniofacial Surgery*, 2005. 16(2): p. 213-224.
27. Chou, T., Fu, E., Wu, C., Yeh, J., Chitosan enhances platelet adhesion and aggregation. *Biochemical and Biophysical Research Communications*, 2003. 302: p. 480-483.
28. Clokie, C.M.L., Moghadam, H., Jackson, M.T., Sandor, G.K.B., Closure of Critical Sized Defects with Allogenic and Alloplastic Bone Substitutes. *Journal of Craniofacial Surgery*, 2002. 13(1): p. 111-123.
29. Cremades, O., Ponce, E., Corpas, R., Gutierrez, J.F., Jover, M., Alvarez-Ossorio, M.C., Parrado, J., Bautista, J., Processing of Crawfish (*Procambarus clarkii*) for the Preparation of Carotenoproteins and Chitin. *Journal of Agricultural and Food Chemistry*, 2001. 49: p. 5468-5472.
30. Cullinane, D.M., Einhorn, T.E., Biomechanics of Bone, in Principles of Bone Biology, J.P. Bilezikian, Raisz, L.G., Rodan, G.A., Editor. 2002. p. 17-32.
31. Daly, W.H., Chitin: The Neglected Biomaterial, in Polymers from Biobased Materials, H.L. Chum, Editor. 1991, William Andrew Publishing. p. 81-89.
32. Damien, C.J., Parsons, J.R., Bone Graft and bone graft substitutes; a review of current technology and applications. *Journal of Applied Biomaterials*, 1991. 2(3): p. 187-208.
33. Devlieghere, F., Vermeulen, A., Debevere, J., Chitosan: antimicrobial activity, interactions with food components and applicability as a coating on fruit and vegetables. *Food Microbiology*, 2004. 21: p. 703-714.
34. Domard, A., Rinaudo, M., Preparation and Characterization of fully deacetylated chitosan. *International Journal of Biological Macromolecules*, 1983. 5: p. 49-52.

35. Don, T., Chuang, C., Chiu, W., Studies on the Degradation Behavior of Chitosan-g-Poly (acrylic acid) Copolymers. *Tamkang Journal of Science and Engineering*, 2002. 5(4): p. 235-240.
36. Dong, Y., Ruan, Y., Wang, H., Zhao, Y., Bi, D., Studies on Glass Transition Temperature of Chitosan with Four Techniques. *Journal of Applied Polymer Science*, 2004. 93: p. 1553-1558.
37. Draenert, Y., Draenert, K., Gap healing of compact bone. *Scanning Electron Microscopy*, 1980. 4: p. 103-111.
38. Duarte, M.L., Ferriera, M.C., Marvao, M.R., Rocha, J., An optimized method to determine the degree of acetylation of chitin and chitosan by FTIR spectroscopy. *International Journal of Biological Macromolecules*, 2002. 31: p. 1-8.
39. Dutta, P.K., Ravikumar, M.N.V., Dutta, J., Chitin and Chitosan for versatile applications. *Journal of Macromolecular Science*, 2002. C42; Part C(3): p. 307-354.
40. Dutta, P.K., Dutta, J., Chattopadhyaya, M.C., Tripathi, V.S., Chitin and Chitosan: Novel Biomaterials Waiting for Future Development. *Journal of Polymer Materials*, 2004. 21(3): p. 321-333.
41. Dutta, P.K., Dutta, J., Tripathi, V.S., Chitin and chitosan: Chemistry, properties and applications. *Journal of Scientific & Industrial Research*, 2004. 63(1): p. 20-31.
42. Elder, S.H., Nettles, D.L., Bumgardner, J.D., Synthesis and Characterization of Chitosan Scaffolds for Cartilage-Tissue Engineering, in *Biopolymer Methods in Tissue Engineering*, A.P. Hollander, Hatton, P.V., Editor. 2004, Humana Press. p. 41-48.
43. Fakhry, A., Schneider, G.B., Zaharias, R., Senel S., Chitosan supports the initial attachment and spreading of osteoblasts preferentially over fibroblasts. *Biomaterials*, 2004. 25: p. 2075-2079.
44. Fei, X., Guan, Y., Yang, D., Li, Z., Yao, K., Antibacterial action of chitosan and carboxymethylated chitosan. *Journal of Applied Polymer Science*, 2001. 79(7): p. 1324-1335.
45. Felse, P.A., Panda, T., Studies on applications of chitin and its derivatives. *Bioprocess and Biosystems Engineering*, 1999. 20(6): p. 505-512.
46. Fernandez-Kim, S., Physicochemical and Functional Properties of Crawfish Chitosan as affected by different processing protocols, in *Food Science*. 2004, Louisiana State University: Baton Rouge. p. 99.

47. Fernandez-Megia, E., Novoa-Carballal, R., Quinoa, E., Riguera, R., Optimal routine conditions for the determination of the degree of acetylation of chitosan by $^1\text{H-NMR}$. *Carbohydrate Polymers*, 2005. 61: p. 155-161.
48. Fradet, G., Brister, S., Mulder, D.S., Lough, J., Averbach, B.L., Evaluation of Chitosan as a New Haemostatic Agent: *In Vitro* and *In vivo* Experiments, in *Chitin in Nature and Technology*, C.J. R. Muzzarelli, G. Gooday, Editor. 1986, Plenum Press. p. 443-451.
49. Francis-Suh, J., Matthew, H., Application of chitosan-based polysaccharide biomaterials in cartilage tissue engineering. *Biomaterials*, 2000. 21: p. 2589-2598.
50. Freier, T., Montenegro, R., Koh, H., Shoichet, M., Chitin-based tubes for tissue engineering in the nervous system. *Biomaterials*, 2005. 26: p. 4624-4632.
51. Freier, T., Koh, H., Kazazian, K., Shoichet, M., Controlling cell adhesion and degradation of chitosan films by N-acetylation. *Biomaterials*, 2005. 26: p. 5872-5878.
52. Funakoshi, T., Majima, T., Iwasaki, N., Sawaguchi, N., Simode, K., Harada, K., Suenaga, N., Minami, A., Minami, M., Nishimura, S., Application of Tissue Engineering Technique to Rotator Cuff Repair using the Novel Scaffold Material, in 50th Annual Meeting of the Orthopaedic Research Society. 2004: San Francisco, CA.
53. Gazdag, A.R., Lane, J.M., Glaser, D.G., Forster, R.A., Alternatives to Autogenous Bone Graft: Efficacy and Indications. *Journal of the American Academy of Orthopaedic Surgeons*, 1995. 3(1): p. 1-8.
54. Gilbert, S.F., Osteogenesis: The development of Bones, in *Developmental Biology*. 2000.
55. Greenwald, A.S., Boden, S.D., Goldberg, V.M., Khan, Y., Laurencin, C.T., Rosier, R.N., Bone-Graft Substitutes: Facts, Fictions, and Applications. *The Journal of Bone and Joint Surgery*, 2001. 83-A(Supplement 2, Part 2): p. 98-103.
56. Gupta, K., Kumar, M., An overview on Chitin and Chitosan Applications with an Emphasis on Controlled Drug Release Formulations. *J.M.S. Reviews in Macromolecular Chemistry and Physics*, 2000. C40(4): p. 273-308.
57. Heux, L., Brugnerotto, J., Desbrieres, J., Versali, M.F., Rinaudo, M., Solid State NMR for Determination of Degree of Acetylation of Chitin and Chitosan. *Biomacromolecules*, 2000. 1: p. 746-751.

58. Hing, K.A., Bone repair in the twenty-first century: biology, chemistry or engineering? *Philosophical transactions. Series A, Mathematical, Physical, and Engineering Sciences*, 2004. 362(1825): p. 2821-50.
59. Hing, K.A., Annaz, B., Saeed, S., Revell, P.A., Buckland, T., Microporosity enhances bioactivity of synthetic bone graft substitutes. *Journal of Materials Science: Materials in Medicine*, 2005. 16: p. 467-475.
60. Hirai, A., Odani, H., Nakajima, A., Determination of degree of deacetylation of chitosan by ^1H NMR spectroscopy. *Polymer Bulletin*, 1991. 26: p. 87-94.
61. Hoemann, C.D., Sun, J., Legare, A., McKee, M.D., Ranger, P., Buschmann, M.D., A Thermosensitive Polysaccharide Gel for Cell Delivery in Cartilage Repair, in 47th Annual Meeting of the Orthopaedic Research Society. 2001: San Francisco, CA.
62. Hoemann, C.D., Hurtig, M., Sun, J., Rossomacha, E., Shive, M.S., McKee, M.D., Chevrier, A., Buschmann, M.D., Improved Cartilage Repair with Cargel®: An Injectable Chitosan Device, in 50th Annual Meeting of the Orthopaedic Research Society. 2004: San Francisco, CA.
63. Hollinger, J.O., Brekke, J., Gruskin, E., Lee, D., Role of Bone Substitutes. *Clinical Orthopaedics and Related Research*, 1996. 324: p. 55-65.
64. Hollister, S.J. BME/ME 456 Biomechanics (Bone Structure). 5/18/05 cited; Available from: <http://www.engin.umich.edu/class/bme456/bonestructure/bonestructure.htm>.
65. Hsu, S., Whu, S.W., Tsai, C., Wu, Y., Chen, H., Hsieh, K., Chitosan as Scaffold Materials: Effects of Molecular Weight and Degree of Deacetylation. *Journal of Polymer Research*, 2004. 11: p. 141-147.
66. Hu, Q., Li, B., Wang, M., Shen, J., Preparation and characterization of biodegradable chitosan/hydroxyapatite nanocomposite rods via in situ hybridization: a potential material as internal fixation of bone fracture. *Biomaterials*, 2004. 25: p. 779-785.
67. Inoue, Y., NMR determination of the degree of acetylation, in Chitin Handbook, M. Muzzarelli, Peters, M., Editor. 1997. p. 133-136.
68. Ito, M., Hidaka, Y., A chitosan-bonded hydroxyapatite bone filling material, in Chitin Handbook, R.A.A. Muzzarelli, Peter, M.G., Editor. 1997. p. 373-382.

69. Itoh, S., Matsuda, A., Kobayashi, H., Ichinose, S., Shinomiya, K., Tanaka, J., Effects of a Laminin Peptide (YIGSR) Immobilized on Crab-Tendon Chitosan Tubes on Nerve Regeneration. *Journal of Biomedical Material Research, Part B*, 2005. 73(2): p. 375-382.
70. Iwasaki, N., Yamane, S., Majima, T., Kasahara, Y., Minami, A., Harada, K., Nonaka, S., Maekawa, N., Tamura, H., Tokura, S., Shiono, M., Monde, K., Nishimura, S., Feasibility of Polysaccharide Hybrid Materials for Scaffolds in Cartilage Tissue Engineering: Evaluation of Chondrocyte Adhesion to Polyion Complex Fibers Prepared from Alginate and Chitosan. *Biomacromolecules*, 2004. 5: p. 828-833.
71. J. Karlsen, O.S., Excipient properties of chitosan. *Manufacturing chemist*, 1991. 62: p. 18-19.
72. Jiang, T., Pilane, C., Laurencin, C., Fabrication of Novel Porous Chitosan Matrices as Scaffolds for Bone Tissue Engineering. *Materials Research Society Symposium*, 2005. 845: p. 187-192.
73. Johnson, R., Lewis, T., Lampecht, E., *In vivo* tissue response to implanted chitosan glutamate, in *Advances in Chitin and Chitosan*, C. Brine, Sandford, P., Zikakis, J., Editor. 1992. p. 3-8.
74. Jumaa, M., Furkert, F.H., Müller, B.W., A new lipid emulsion formulation with high antimicrobial efficacy using chitosan. *European Journal of Pharmaceutics and Biopharmaceutics*, 2002. 53: p. 115-123.
75. Kato, Y., Onishi, H., Machida, Y., Application of Chitin and Chitosan Derivatives in the Pharmaceutical Field. *Current Pharmaceutical Biotechnology*, 2003. 4: p. 303-309.
76. Kawakami, T., Antoh, M., Hasegawa, H., Yamagishi, T., Ito, M., Eda, S., Experimental study on osteoconductive properties of a chitosan-bonded hydroxyapatite self-hardening paste. *Biomaterials*, 1992. 13(11): p. 759-763.
77. Khan, T.A., Peh, K.K., Ch'ng, H.S., Reporting degree of deacetylation values of chitosan: the influence of analytical methods. *Journal of Pharmaceutical Sciences*, 2002. 5(3): p. 205-212.
78. Khor, E., Lim, L.Y., Implantable applications of chitin and chitosan. *Biomaterials*, 2003. 24: p. 2339-2349.
79. Kim, S.J., Shin, S.R., Kim, S.I., Thermal Characterizations of Chitosan and Polyacrylonitrile Semi-Interpenetrating Polymer Networks. *High Performance Polymers*, 2002. 14: p. 309-316.

80. Kind, G.M., Bines, S.D., Staren, E.D., Templeton, A.J., Economou, S.G., Chitosan: Evaluation of a New Haemostatic Agent. *Current Surgery*, 1990. 47(1): p. 37-39.
81. Kittur, F., Prashanth, K., Sankar, K., Tharanathan, R., Characterization of chitin, chitosan, and their carboxymethyl derivatives by differential scanning calorimetry. *Carbohydrate Polymers*, 2002. 49: p. 185-193.
82. Klokkevold, P.R., Vandemark, L., Kenney, E.B., Bernard, G.W., Osteogenesis enhanced by chitosan (poly-N-acetylglucosaminoglycan) *in vitro*. *Journal of Periodontology*, 1996. 67(11): p. 1170-1175.
83. Kumar, M., Muzzarelli, R., Muzzarelli, C., Sashiwa, H., Domb, A., Chitosan Chemistry and Pharmaceutical Perspectives. *Chemistry Review*, 2004. 104: p. 6017-6084.
84. Kumar, M.N.V.R., A review of chitin and chitosan applications. *Reactive and Functional Polymers*, 2000. 46: p. 1-27.
85. Kurita, K., β -Chitin and Reactivity Characteristics, in Applications of Chitin and Chitosan, M.F.A. Goosen, Editor. 1997. p. 79-87.
86. Laurencin, C.T., Khan, Y. Bone Graft Substitute Materials. 5/18/05 cited; Available from: www.emedicine.com/orthoped/topic611.htm.
87. Laurencin, C.T., Khan, Y., El-Amin, S.F., Bone Graft Substitutes. *Expert Review of Medical Devices*, 2006. 3(1): p. 49-57.
88. Lavertu, M., Xia, Z., Serreqi, A., Berrada, M., Rodrigues, A., Wang, D., Buschmann, M., Gupta, A., A validated ^1H NMR method for the determination of the degree of deacetylation of chitosan. *Journal of Pharmaceutical and Biomedical Analysis*, 2003. 32: p. 1149-1158.
89. Li, H., Miyahara, T., Tezuka, Y., Watanabe, M., Nemoto, N., Seto, H., Kadota, S., The effect of low molecular weight chitosan on bone resorption *in vitro* and *in vivo*. *Phytomedicine*, 1999. 6(5): p. 305-310.
90. Li, Q., Dunn, E.T., Grandmason, E.W., Goosen, M.F.A., ed. Applications and Properties of Chitosan. Applications of Chitin and Chitosan, ed. M.F.A. Goosen. 1992, Technomic Publishing Company, Inc.: Lancaster. p. 3-29.
91. Li, X., Feng, Q., Jiao, Y., Cui, F., Collagen-based scaffolds reinforced by chitosan fibers for bone tissue engineering. *Polymer International*, 2005. 54: p. 1034-1040.

92. Li, Z., Ramay, H.R., Hauch, K.D. Xiao, D., Zhang, M., Chitosan-alginate hybrid scaffolds for bone tissue engineering. *Biomaterials*, 2005. 26: p. 3919-3928.
93. Lian, Q., Samuels, R., Process-Structure-Properties of Chitosan. *ANTEC*, 1996: p. 1709-1713.
94. Logeart-Avramoglou, D., Anagnostou, F., Bizios, R., Petite, H., Engineering bone: challenges and obstacles. *Journal of Cellular and Molecular Medicine*, 2005. 9(1): p. 72-84.
95. M. Terbojevich, R.A.A.M., Chitosan, in Handbook of Hydrocolloids, G.O.P.a.P.A. Williams, Editor. 2000.
96. Malette, W.G., Quigley Jr., H.J., Adickes, E.D., Chitosan Effect in Vascular Surgery, Tissue Culture and Tissue Regeneration, in Chitin in Nature and Technology, C.J. R. Muzzarelli, G. Gooday, Editor. 1986, Plenum. p. 435-442.
97. Mallapragada, S., Narasimhan, B., Handbook of Biodegradable Polymeric Materials and their Applications. Vol. 1 & 2. 2006.
98. Marks Jr., S.C., Odgren, P.R., Structure and Development of the Skeleton, in Principles of Bone Biology, J.P. Bilezikian, Raisz, L.G., Rodan, G.A., Editor. 2002. p. 3-15.
99. Mauney, J., Sjostrom, S., Blumberg, J., Horan, R., O'Leary, J., Vunjak-Novakovic, G., Volloch, V., Kaplan, D., Mechanical Stimulation Promotes Osteogenic Differentiation of Human Bone Marrow Stromal Cells on 3-D Partially Demineralized Bone Scaffolds *In vitro*. *Calcified Tissue International*, 2004. 74: p. 458-468.
100. McAuliffe, J.A., Bone Graft Substitutes. *Journal of Hand Therapy*, 2003. 16(2): p. 180-187.
101. McCord, M., Spence, M., Hudson, S. A chitosan composite material for bone replacement. in Proceedings of the First Joint BMES/EMBS Conference. 1999. Atlanta, GA.
102. Mi, F., Wu, Y., Shyu, S., Schoung, J., Huang, Y., Tsai, Y., Hao, J., Control of wound infections using a bilayer chitosan wound dressing with sustainable antibiotic delivery. *Journal of Biomedical Materials Research*, 2002. 59(3): p. 438-449.
103. Moore, W.R., Graves, S.E., Bain, G.I., Synthetic Bone Graft Substitutes. *Australia and New Zealand Journal of Surgery*, 2001. 71: p. 354-361.

104. Mukherjee, D., Method for producing chitin or chitosan, U.S.P. Office, Editor. 2001, Board of Supervisors of Louisiana State University and Agricultural and Mechanical College, Baton Rouge, Louisiana: USA.
105. Mukherjee, D.P., Tunkle, A.S., Roberts, R.A., Clavenna, A., Rogers, S., Smith, D., An Animal Evaluation of a Paste of Chitosan Glutamate and Hydroxyapatite as a Synthetic Bone Graft Material. *Journal of Biomedical Material Research, Part B*, 2003. 67B: p. 603-609.
106. Muzzarelli, R., Medical Applications, in Chitin. 1978, Pergamon Press. p. 255-265.
107. Muzzarelli, R., Baldassarre, V., Conti, F., Ferrara, P., Biagini, G., Biological activity of chitosan: ultrastructural study. *Biomaterials*, 1988. 9: p. 247-253.
108. Muzzarelli, R.A.A., Colorimetric Determination of Chitosan. *Analytical Biochemistry*, 1998. 260: p. 255-257.
109. Nagahata, M., Nakaoka, R., Teramoto, A., Abe, K., Tsuchiya, T., The response of normal human osteoblasts to anionic polysaccharide polyelectrolyte complexes. *Biomaterials*, 2005. 26: p. 5138-5144.
110. NiMhurchu, C., Poppitt, S., McGill, A., Leahy, F., Bennett, D., Lin, R., Ormrod, D., Ward, L., Strik, C., Rodgers, A., Effect of chitosan on body-weight is clinically negligible. *International Journal of Obesity*, 2004. 28: p. 1149-1156.
111. No, H., Meyers, S., Preparation and characterization of chitin and chitosan - A review. *Journal of Aquatic Food Product Technology*, 1995. 4(2): p. 27-52.
112. No, H., Park, N., Lee, S., Meyers, S., Antibacterial activity of chitosans and chitosan oligomers with different molecular weights. *International Journal of Food Microbiology*, 2002. 74: p. 65-72.
113. No, H.K., Meyers, S.P., Lee, K.S., Isolation and Characterization of Chitin from Crawfish Shell Waste. *Journal of Agricultural and Food Chemistry*, 1989. 37(3): p. 575-579.
114. No, H.K., Meyers, S.P., Preparation of chitin and chitosan, in Chitin Handbook, R.A.A. Muzzarelli, Peter, M.G., Editor. 1997. p. 475-489.
115. No, H.K., Lee, S.H., Park, N.Y., Meyers, S.P., Comparison of Physicochemical, Binding, and Antibacterial Properties of Chitosans Prepared without and with Deproteinization Process. *Journal of Agricultural and Food Chemistry*, 2003. 51: p. 7659-7663.

116. Ogawa, K., Yui, T., Okuyama, K., Three D structures of chitosan. *International Journal of Biological Macromolecules*, 2004. 34: p. 1-8.
117. Okamoto, Y., Kawakami, K., Miyatake, K., Morimoto, M., Shigemasa, Y., Minami, S., Analgesic Effects of chitin and chitosan. *Carbohydrate Polymers*, 2002. 49: p. 249-252.
118. Okamoto, Y., Yano, R., Miyatake, K., Tomohiro, I., Shigemasa, Y., Minami, S., Effects of chitin and chitosan on blood coagulation. *Carbohydrate Polymers*, 2003. 53: p. 337-342.
119. Okamura, Y., Nomura, A., Minami, S., Okamoto, Y., Effects of chitin/chitosan and their oligomers/monomers on release of type I collagenase from fibroblasts. *Biomacromolecules*, 2005. 6(5): p. 2382-2384.
120. P. VandeVord, H.M., S. DeSilva, L. Mayton, B. Wu, P. Wooley, Evaluation of the biocompatibility of a chitosan scaffold in mice. *Journal of Biomedical Materials Research*, 2002. 59: p. 585-590.
121. Pal, A., Rawat, N., Pal, S., Characterization of Hydroxyapatite based composites for bone repair. Engineering in Medicine and Biology Society, 1995 and 14th Conference of the Biomedical Engineering Society of India. An International meeting, Proceedings of the First Regional Conference., IEEE, 1995: p. 4/5-4/6.
122. Pan, J., Bao, Z., Li, J., Zhang, L., Wu, C., Yu, Y., Chitosan-Based Scaffolds for Hepatocyte Culture. *Key Engineering Materials*, 2005. 288/289: p. 91-94.
123. Parikh, S.N., Bone graft substitutes: past, present, future. *Journal of Postgraduate Medicine*, 2002. 48(2): p. 142-148.
124. Patel, M., Matthew, H., DeSilva, S., Wu, B., Wooley, P. Functional evaluation of chitosan nerve guides for peripheral nerve regeneration in the rat animal model. in 51st Annual Meeting of the Orthopaedic Research Society. 2005. Washington D.C.
125. Peltier, L.F., Bickel, E.Y., Lillo, R., Thien, M.S., The use of Plaster of Paris to fill defects in bone. *Annals of Surgery*, 1957. 146(1): p. 61-69.
126. Peltier, L.F., The use of plaster of Paris to fill large defects in bone. *The American Journal of Surgery*, 1959. 97(3): p. 311-315.
127. Prashanth, K., Kittur, F., Tharanathan, R., Solid state structure of chitosan prepared under different N-deacetylating conditions. *Carbohydrate Polymers*, 2002. 50: p. 27-33.

128. Prasitsilp, M., Jenwithisuk, R., Kongsuwan, K., Damrongchai, N., Watts, P., Cellular responses to chitosan *in vitro*: The importance of deacetylation. *Journal of Materials Science: Materials in Medicine*, 2000. 11: p. 773-778.
129. Rabea, E.I., Badawy, M.E.T., Stevens, C.V., Smagghe, G., Steurbaut, W., Chitosan as Antimicrobial Agent: Applications and Mode of Action. *Biomacromolecules*, 2003. 4(6): p. 1457-1465.
130. Rao, S.B., Sharma, C.P., Use of chitosan as a biomaterial: Studies on its safety and haemostatic potential. *Journal of Biomaterials Research*, 1997. 34: p. 21-28.
131. Ratto, J., Hatakeyama, T., Differential scanning calorimetry investigation of phase transitions in water/chitosan systems. *Polymer*, 1995. 36(15): p. 2915-2919.
132. Raymond, L., Morin, F., Marchessault, R., Degree of deacetylation of chitosan using conductometric titration and solid-state NMR. *Carbohydrate Research*, 1993. 246: p. 331-336.
133. Reddi, A.H., Wientroub, S., Muthukumar, N., Biologic Principals of Bone Induction. *The Orthopaedic Clinics of North America*, 1987. 18(2): p. 207-212.
134. Rinaudo, M., Milas, M., Desbrieres, J., Characterization and Solution Properties of Chitosan and Chitosan Derivatives, in Applications of Chitin and Chitosan, M.F.A. Goosen, Editor. 1997, Technomic. p. 89-102.
135. Roberts, G., Structure of Chitin and Chitosan, in Chitin Chemistry. 1992. p. 1-53.
136. Romoren, K., Aaberge, A., Smistad, G., Thu, B.J., Evensen, O., Long-Term Stability of Chitosan-Based Polyplexes. *Pharmaceutical Research*, 2004. 21(12): p. 2340-2346.
137. Rush, S., Bone Graft Substitutes: Osteobiologics. *Clinics in Podiatric Medicine and Surgery*, 2005. 22: p. 619-630.
138. S. Tokura, I.S., J. Murata, and T. Makabe, Inhibition of tumor induced angiogenesis by sulfated chitin derivatives, in Advances in Chitin and Chitosan, P.S. C. Brine, and J. Zikakis, Editor. 1992. p. 87-95.
139. Saraswathy, G., Sastry, T., Pal, S., Sreenu, M., Kumar, R., A new bio-inorganic composite as bone grafting material: *in vivo* study. *Trends in Biomaterials and Artificial Organs*, 2004. 17(2): p. 37-42.

140. Sashiwa, H., Kawaski, N., Nakayama, A., Muraki, E., Yamamoto, N., Aiba, S., Chemical Modification of Chitosan. Synthesis of Water-Soluble Chitosan Derivates by Simple Acetylation. *Biomacromolecules*, 2002. 3: p. 1126-1128.
141. Schmitz, J., Hollinger, J., The Critical Size Defect as an Experimental Model for Craniomandibulofacial Nonunions. *Clinical Orthopaedics and Related Research*, 1986. 205: p. 299-308.
142. Seol, Y., Lee, J., Park, Y., Lee, Y., Ku, Y., Rhyu, I., Lee, S., Han, S., Chung, C., Chitosan sponges as tissue engineering scaffolds for bone formation. *Biotechnology Letters*, 2004. 26: p. 1037-1041.
143. Service, R., Tissue Engineers build new bone. *Science*, 2000. 289(5484): p. 1498-1501.
144. Shahidi, F., Abuzaytoun, R., Chitin, Chitosan, and Co-products: Chemistry, Production, Applications, and Health Effects. *Advances in Food and Nutrition Research*, 2005. 49: p. 93-135.
145. Shi, Z., Neoh, K., Kang, E., Wang, W., Antibacterial and mechanical properties of bone cement impregnated with chitosan nanoparticles. *Biomaterials*, 2006. 27: p. 2440-2449.
146. Singla, A.K., Chawla, M., Chitosan: some pharmaceutical and biological aspects - an update. *Journal of Pharmacy and Pharmacology*, 2001. 53(8): p. 1047-1067.
147. Society, N.A.S. Bone Graft Alternatives. 5/18/05 cited; Available from: www.spine.org/articles/bone_graft.cfm.
148. Sorlier, P., Denuziere, A., Viton, C., Domard, A., Relation between the Degree of Acetylation and the Electrostatic Properties of Chitin and Chitosan. *Biomacromolecules*, 2001. 2: p. 765-772.
149. Sorlier, P., Viton, C., Domard, A., Relation between Solution Properties and Degree of Acetylation of Chitosan: Role of Aging. *Biomacromolecules*, 2002. 3: p. 1336-1342.
150. Spence, M.L., McCord, M.G., A Novel Composite for Bone Replacement. *IEEE*, 1997: p. 257-259.
151. Strocchi, R., Orsini, G., Iezzi, G., Scarano, A., Rubini, C., Pecora, G., Piattelli, A., Bone Regeneration with Calcium Sulfate: Evidence for increased Angiogenesis in Rabbits. *Journal of Oral Implantology*, 2002. 28(6): p. 273-278.

152. Synowiecki, J., Al-Khateeb, N. A., Production, Properties, and Some New Applications of Chitin and Its Derivatives. *Critical Reviews in Food Science and Nutrition*, 2003. 43(2): p. 145-171.
153. Tan, W., Krishnaraj, R., Desai, T. Influence of chitosan on cell viability and proliferation in 3-D collagen gels. in 22nd Annual International Conference of the IEEE. 2000. Chicago, IL.
154. Tancred, D.C., Carr, A.J., McCormak, B.A.O., Development of a new synthetic bone graft. *Journal of Materials Science: Materials in Medicine*, 1998. 9(12): p. 819-823.
155. Teitelbaum, S.L., Bone Resorption by Osteoclasts. *Science*, 2000. 289(5484): p. 1504-1509.
156. Turner, C., Owan, I., Alvey, T., Hulman, J., Hock, J., Recruitment and proliferative responses of osteoblasts after mechanical loading *in vivo* determined using sustained release Bromodeoxyuridine. *Bone*, 1998. 22(5): p. 463-469.
157. Ueno, H., Mori, T., Fujinaga, T., Topical formulations and wound applications of chitosan. *Advanced Drug Delivery Reviews*, 2001. 52: p. 105-115.
158. Vert, M., Biopolymers and Artificial Biopolymers in Biomedical Applications, an Overview, in *Biorelated Polymers - Sustainable Polymer Science & Technology*, H.G. E. Chiellini, G. Braunegg, J. Burchert, P. Gatenholm, M. van der Zee, Editor. 2001.
159. Wu, A., Bough, W. A study of variables in the chitosan manufacturing process in relation to molecular-weight distribution, chemical characteristics and waste-treatment effectiveness. in *Proceedings of the First International Conference on Chitin/Chitosan*. 1978. Boston, MA.
160. Xie, W., Xu, P., Liu, Q., Antioxidant Activity of Water-Soluble Chitosan Derivatives. *Bioorganic & Medicinal Chemistry Letters*, 2001. 11: p. 1699-1701.
161. Xu, H.H.K., Simon Jr., C.G., Fast setting calcium phosphate-chitosan scaffold: mechanical properties and biocompatibility. *Biomaterials*, 2005. 26: p. 1337-1348.
162. Yilmaz, E., Chitosan: A Versatile Biomaterial, in *Biomaterials: from molecules to engineered tissues*. 2004. p. 59-68.
163. Zhang, H., Oh, M., Allen, C., Kumacheva, E., Monodisperse Chitosan Nanoparticles for Mucosal Drug Delivery. *Biomacromolecules*, 2004. 5: p. 2461-2468.

164. Zhang, L., Ao, Q., Wang, A., Lu, G., Kong, L., Gong, Y., Zhao, N., Zhang, X., A sandwich tubular scaffold derived from chitosan for blood vessel tissue engineering. *Journal of Biomedical Materials Research Part A*, 2006. 77A: p. 277-284.
165. Zhong, Y., Li, J., Gong, Y., Zhao, N., Zhang, X., Feasibility of using chitosan in nerve repair. *Tsingua Science and Technology*, 2000. 5(4): p. 432-435.
166. Jarvinen, T.L.N., Kannus, P., Sievanen, H., Jolma, P., Heinonen, A., Jarvinen, M., Randomized controlled study of effects of sudden impact loading on rat femur. *Journal of Bone and Mineral Research*, 1998. 13(9): p. 1475-1482.
167. Umemura, Y., Ishiko, T., Yamauchi, T., Kurono, M., Mashiko, S., Five jumps per day increase bone mass and breaking force in rats. *Journal of Bone and Mineral Research*, 1997. 12(9): p. 1480-1485.